AD NUMBER

AD901957

LIMITATION CHANGES

TO:

Approved for public release; distribution is unlimited.

FROM:

Distribution authorized to U.S. Gov't. agencies only; Test and Evaluation; APR 1972. Other requests shall be referred to Aeronautical Systems Div., Wright-Patterson AFB, OH 45433.

AUTHORITY

AFFDL ltr, 12 Nov 1973

FTC-TD-71-9

ANALYSIS OF THE APPROACH, FLARE AND LANDING CHARACTERISTICS OF THE X-24A LIFTING BODY

DAVID F. RICHARDSON
Aerospace Research Engineer

NTIS DISCLAIMER

- This document has been reproduced from the very best copy that was furnished by the Source Agency. Although NTIS realizes that parts of this document may be illegible, it is being released in order to make available as much information as possible.

FOREWORD

This technology document presents an analysis of the approach. flare and landing characteristics of the X-24A lifting reentry research vehicle. The X-24A made 28 landings on Rogers Dry Lake at Edwards Air Force Base between 17 April 1969 and 4 June 1971. This test program was conducted jointly with the NASA Flight Research Center (FRC). References 1 through 8 are related documents which have been or will be published.

The author wishes to acknowledge the efforts of Mr. Richard R. Larson of NASA FRC who gathered the touchdown accuracy and landing rollout data, and Mr. Robert G. Hoey of the AFFTC who provided the F-104A idle power performance data. Acknowledgement is also extended to Mr. John A. Manke of NASA FRC and Major Cecil W. Powell, who gave piloting comments and assistance in preparing this document.

The participation of AFFTC personnel in this program was authorized by Project Directive 69-38. The assigned Program Structure was 680A.

Foreign announcement and dissemination by the Defense Documentation Center are not authorized because of technology restrictions of the U.S. Export Control Acts as implemented by AFR 400-10.

Prepared by:

David F. Richardson

DAVID F. RICHARDSON
Aerospace Research Engineer

Reviewed and approved by:
30 JUNE 1972

James W. Wood

JAMES W. WOOD
Colonel, USAF
Commander, 6510th Test Wing

Robert M. White

ROBERT M. WHITE
Brigadier General, USAF
Commander

ABSTRACT

This report presents the results of the X-24A lifting body flight test program pertaining to the approach, flare and landing. The approach and flare were flown with clean configurations (landing gear up), having maximum lift-to-drag ratios (L/D)'s between 2.95 and 4.30. The landing configuration (gear down) had a maximum L/D value of 2.65. The landing approach pattern was a 180-degree, unpowered, left-hand, circling approach followed by a short wings-level, high energy final approach at airspeeds ranging from 267 to 318 KCAS, terminating with a flare to near level flight near the ground, and a deceleration to landing. The landing gear was extended near the completion of the flare in close proximity to the ground. The landings were at airspeeds between 168 and 205 KCAS at sink rates of less than 5 feet per second and within 2,000 feet of the intended landing point. An effective speed brake function was generated on the X-24A by using the flap bias feature. This was essential to the accomplishment of accurate landings. Visibility and handling qualities of the X-24A in the final approach and landing configuration were excellent; however, lateral upsets in turbulence were disconcerting to the pilot especially near the ground. The trim change due to landing gear deployment was also somewhat objectionable to the pilots. Differential braking and rudder/aileron deflection were sufficient for ground steering of the X-24A after touchdown for conditions of zero crosswind, but were inadequate for light to moderate crosswinds. This program obtained results similar to those of earlier lifting body programs and of routine X-15 operations indicating that the unpowered visual approach and landing was relatively easy for the project test pilots after extensive F-104A low L/D practice prior to the X-24A flights.

table of contents

list of illustrations

list of tables

list of abbreviations and symbols

Item	Definition	Units
A_f	acceleration factor	dimensionless
AGL	above ground level	- - -
$\bar{c}$	vehicle reference length (23 ft)	ft
C_D	drag coefficient	dimensionless
cg	longitudinal center of gravity	pct $\bar{c}$
C_L	lift coefficient	dimensionless
C_{L_α}	lift curve slope	per deg
D	drag force	lb
g	acceleration of gravity	ft per sec^2
h	tapeline altitude	ft
$\dot{h}$	tapeline rate of climb (+) or sink (-)	ft per sec
ILS	instrument landing system	- - -
KCAS	knots calibrated airspeed	kt
KIAS	knots indicated airspeed	kt
L	lift force	lb
L/D	lift-to-drag ratio	dimensionless
L/D_{eff}	effective lift-to-drag ratio [L/(D-T)]	dimensionless
m	mass	slugs
MSL	mean sea level	- - -
NASA	National Aeronautics and Space Administration	- - -
n_{x_b}	body axis longitudinal acceleration	g's
n_{z_b}	body axis normal acceleration	g's
n_{z_s}	stability axis normal acceleration	g's
PCM	pulse code modulation	- - -

Item	Definition	Units
PILOT	Piloted Low Speed Test	- - -
PIO	pilot-induced oscillation	- - -
PRIME	Precision Recovery Including Maneuvering Entry	- - -
q	dynamic pressure	lb per ft^2
R	turn radius	ft
R/D	rate of descent	ft per sec
RMS	root mean square	- - -
S	vehicle reference planform area (160 ft^2)	ft^2
SAS	stability augmentation system	- - -
SPS	samples per second	- - -
T	thrust	lb
V_c	calibrated airspeed	kt
V_e	equivalent airspeed	kt
V_t	true airspeed	kt
W	weight	lb
α	true angle of attack	deg
$\dot{\alpha}$	rate of change of angle of attack	deg per sec
γ	flightpath angle	deg
γ_g	glide slope angle	deg
Δ	prefix meaning increment	- - -
δe_L	lower flap deflection	deg
δe_U	upper flap deflection	deg
δL_B	lower flap bias position	deg
δR_B	rudder bias position	deg
δSB	speed brake position	deg
δU_B	upper flap bias position	deg
θ	pitch angle	deg
ρ_{SL}	standard sea level density	slug per ft^3
ϕ	roll (bank) angle	deg

Subscripts

c	corrected	- - -
eff	effective	- - -

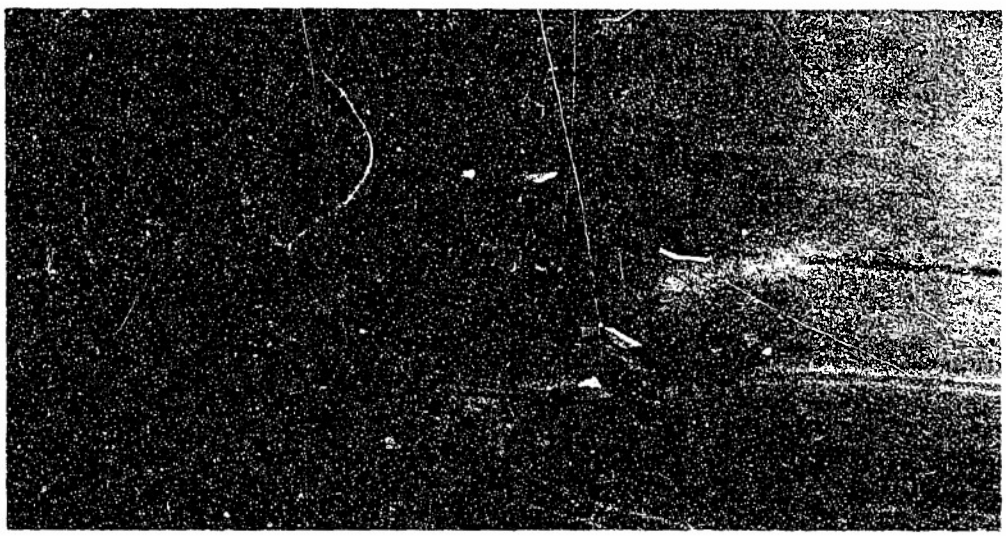

INTRODUCTION

The X-24A project was the second flight test project to use the SV-5 lifting body reentry configuration. The first project, called PRIME (Precision Recovery Including Maneuvering Entry) used three subscale unmanned SV-5's which were boosted to orbital speeds on Atlas boosters. This program provided data, and a feasibility demonstration of the SV-5 configuration in the technical areas of aerodynamics, stability, control, heat protection, and maneuverability covering the speed range from orbital velocity to Mach 2.0.

The purpose of the second project, the X-24A project, called PILOT (Piloted Low Speed Test), was to investigate maneuverable lifting body flight from the low supersonic speed range to touchdown. One of the main X-24A project objectives was to gather data on and to prove that the SV-5 configuration could be maneuvered to a safe horizontal unpowered landing at a pre-selected landing site. Twenty-eight successful X-24A landings accomplished this objective. This report analyzes the X-24A unpowered approach and landing characteristics from approximately 20,000 feet mean sea level (MSL) down through the flare, touchdown, and ground rollout. Pertinent pilot comments are included within the discussion.

VEHICLE DESCRIPTION

The X-24A vehicle (figures 1 and 2) was a blunt-nosed, wingless lifting body vehicle. The aft end had a large base area and three vertical fins. The outboard fins supported the two upper and the two lower rudders. The upper rudders were used for directional trim and control. The four rudder surfaces could be biased inboard or outboard for improved handling characteristics at the subsonic or supersonic airspeeds, respectively. On the aft end were located the two upper and the two lower flaps which were used for pitch and roll control. When either lower flap reached

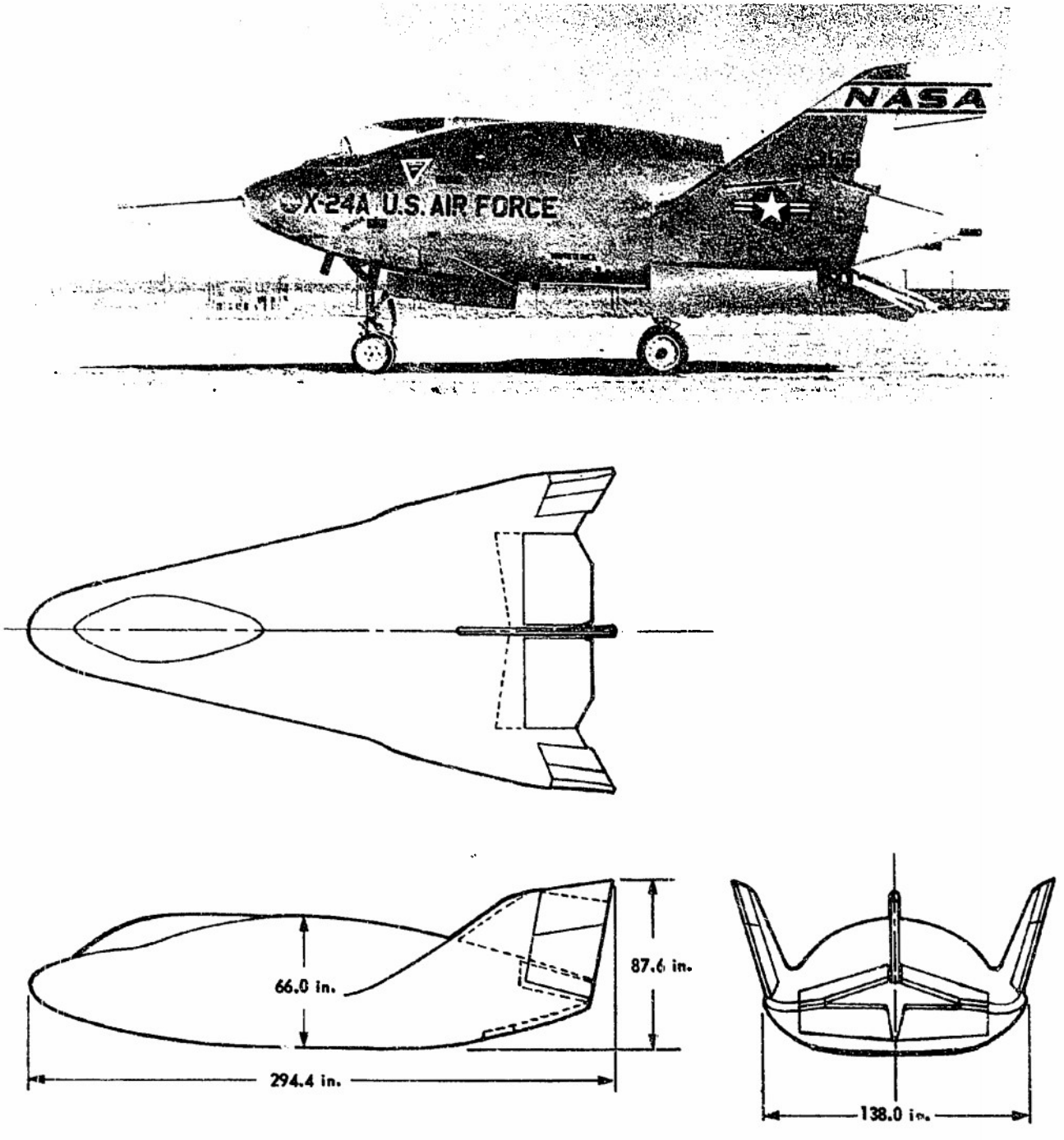

Figure 1 X-24A Lifting Body Vehicle

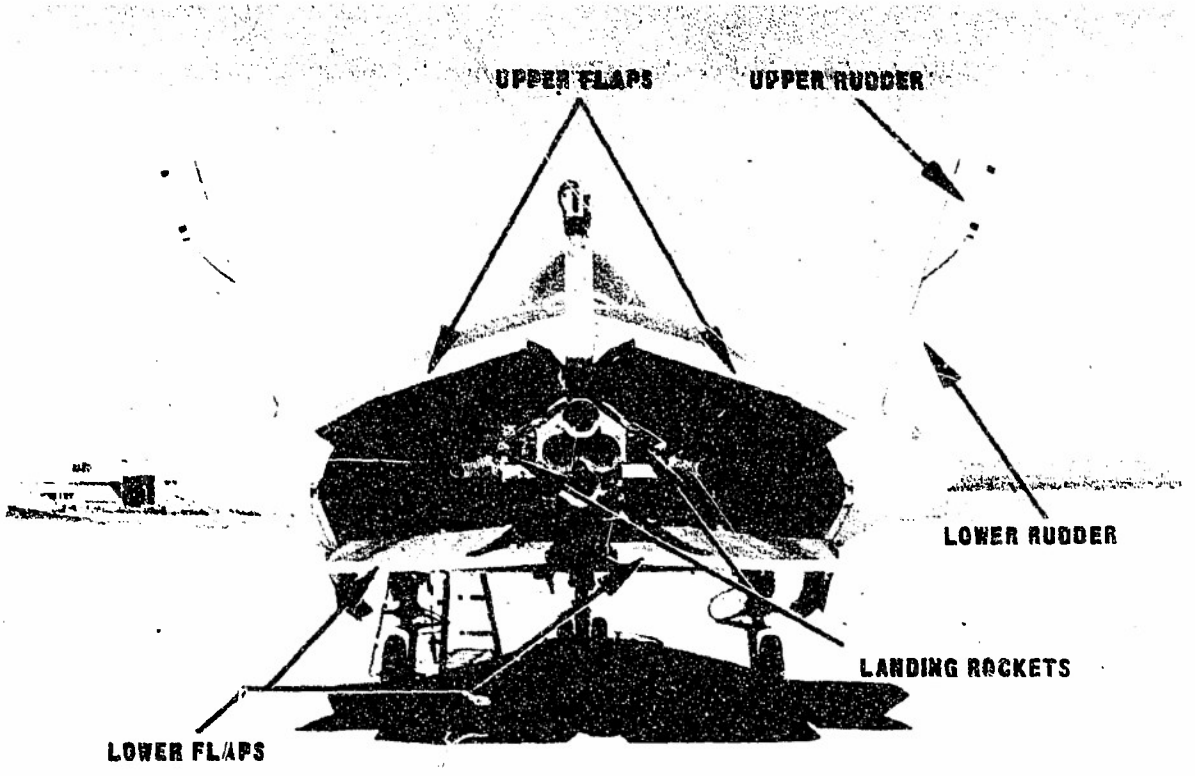

Figure 2 X-24A Lifting Body Vehicle - Aft End

the fully closed position (zero degrees), pitch and roll inputs were transferred through a clapper mechanism to the corresponding upper flap. Both pairs of upper and lower flaps could be deflected symmetrically (biased) independent of pilot control input. The rudder bias was programmed as a function of upper flap bias position. The flap bias feature was used as a speed brake. The cockpit contained typical aircraft instruments, stick and rudder pedals, zero -zero ejection seat, and a jettisonable bubble canopy. The landing gear system was a conventional tricycle arrangement with a quick acting pneumatic deployment system. In addition to the primary propulsion system (XLR-11 rocket engine) with 8,480 pounds of vacuum thrust, the vehicle was equipped with two 500-pound thrust hydrogen peroxide rocket engines which were available to the pilot to extend his glide during the landing approach if required. Reference 1 contains a more extensive description of the X-24A. The subsystems pertinent to the approach and landing task are discussed in appendix I and in reference 2.

TEST TECHNIQUE

The X-24A was launched from an NB-52 mother ship at an altitude of 40,000 to 47,000 feet MSL. On 10 flights, the entire flight was a preplanned glide flight from launch to touchdown. On 18 flights, the first portion of each flight was powered, in which case the vehicle accelerated to a preplanned Mach number and altitude using the primary propulsion system. On the powered flights the vehicle entered a gliding flight phase at rocket engine shutdown. After launch on both the glide and powered flights, various stability and performance data gathering maneuvers were executed. During this phase, the pilot's attention was primarily directed to data maneuvers and he was relying heavily on the ground controller for navigation information. These ground calls, based on real time radar data in the control room, consisted of vehicle position relative to the preplanned ground track and altitude profile. These ground calls were to guide the pilot to a low key point. Low key is defined as the point where the final 180-degree turn was initiated and was considered the dividing point between data maneuvers and the landing maneuver. From low key the pilot performed, without ground controller assistance, an unpowered visual gliding approach to the preselected runway where an unpowered visual flare and landing were completed.

The approach and flare were accomplished with the landing gear retracted. The landing gear was not extended until flare completion since the low gear-down lift-to-drag ratio (maximum L/D of 2.65) and the gear-down limit airspeed (300 KCAS) would have made visual flares and landings quite marginal (reference 9) if the entire approach and landing had been flown with the gear extended.

Various parameters (appendix I) were telemetered to the ground for later examination to determine the vehicle characteristics and pilot technique during the approach, flare and landing. Bank angle (ϕ) and radar space positioning data were used to determine the time and location of the low key points. The bank angle data were used to determine the altitude at which the pilot had rolled out on the final approach. The point at which the pilot had started the flare was determined by examining the angle of attack (α), longitudinal stick position, normal acceleration (n_{z_b}) and pitch angle (θ) data. Gear extension and touchdown were determined from the landing gear strut position data.

For most of the flights, the pilots were asked to perform landings at a predetermined point on a designated runway with the stipulation that flight safety should in no way be compromised to achieve this objective. On four flights (17 to 20), the pilots were requested to maintain a desired final approach airspeed and forego the accuracy landings. The pilots were also requested not to use the flap bias feature as a speed brake for the first seven flights.

The desired approach and landing configuration (flaps and rudder bias settings, stability augmentation system (SAS) gains, etc.) were selected during the planning phase of each flight using a fixed base six-degree-of-freedom simulator. Before each flight the pilots practiced unpowered approaches to the primary runway and to the alternate runways using an inflight performance simulator. This simulator was an F-104 aircraft in high drag configurations which provided L/D's and airspeeds similar to those of the X-24A (appendix V).

TEST CONDITIONS

Tables I, II and III present a listing of the vehicle landing weights and pilots, together with the conditions existing during the initial and final approaches, at flare initiation, gear extension, flare completion, and touchdown for each flight. These tabulations form the nucleus of this report and will be referred to frequently in subsequent sections.

The X-24A flight test program had three test pilots (A, B and C in table III). Table IV presents a summary of the lifting body piloting experience of each of these pilots.

Vehicle gross weights at touchdown ranged from a low of 6,157 pounds to a high of 7,023 pounds. The average touchdown weight was 6,387 pounds, which corresponded to a planform loading of 39.4 pounds per square foot.

All the landings reported herein were made on marked, 300-foot wide, runways on the hard surface of Rogers Dry Lake at Edwards Air Force Base, California. All of the flights terminated on the planned runway except for flight 3 in which an alternate runway was used due to an inadvertent early launch. Figure 3 is an aerial drawing of Rogers Dry Lake showing the marked lakebed runways. Nineteen landings were made to runway 18 in figure 3. Seven landings were performed to runway 33. One landing was made to runway 15 and the one early launch flight landed on runway 17.

During the course of the X-24A flight test program there were three distinct subsonic configuration modes used during the approaches and landings.

1. Configuration Mode 1 - Flights 1 to 7, pitch and roll control with lower flaps, upper flap bias set at -18 to -23 degrees depending on the flight.

2. Configuration Mode 2 (figure 4) - Flights 8 to 18 and 21 to 28, pitch and roll control with lower flaps, upper flap bias at -13 degrees until gear extension at which time control crossed over from the lower to the upper flaps and the actual landing was performed using the upper flaps (figure 5). This configuration was the standard subsonic approach and landing configuration for the X-24A.

3. Configuration Mode 3 - Flights 19 and 20, lower flaps fully closed (zero degrees), pitch and roll control with the upper flaps which varied between -8 and -12 degrees during the approach.

These configuration modes will be referred to throughout this document.

Table I

INITIAL APPROACH PARAMETERS

Flight No.	Conditions at Preplanned Low Key		Conditions at Actual Low Key		Time From Actual Low Key to Rollout on Final (sec)	Configuration After Close-Up		Average Speed Brake Used (deg)	Altitudes Where Speed Brake Used		Altitude Lost During Turn (ft)	Turn Rate at 15,000 ft MSL (deg/1000 ft)	Average Bank Angle During Turn (deg)
	Altitude (ft MSL)	Airspeed (KCAS)	Altitude (ft MSL)	Airspeed (KCAS)		δU_B (deg)	δR_B (deg)		Out (ft MSL)	In (ft MSL)			
1	21,000	180	21,420	229	67	-21	-10	N.A.[a]	---	---	16,440	11.7	44
2	20,000	210	19,940	228	67	-21	-10	N.A.	---	---	15,540	13.7	46
3	19,000	215	21,130	214	69	-21	-10	N.A.	---	---	14,400	19.8	45
4	20,000	190	22,710	212	70	-20	-10	N.A.	---	---	18,280	9.2	44
5	20,000	215	21,970	209	81	-18	-10	N.A.	---	---	17,590	8.2	40
6	20,000	215	21,990	193	80	-21	-10	N.A.	---	---	15,600	----	40
7	18,000	210	19,400	205	53	-12	-10	N.A.	---	---	11,400	20.0	44
8	18,000	190	19,800	206	61	-15	-10	-19	12,400	8,500	13,450	18.0	40
9	18,000	190	19,540	208	61	-13	-10	-19 -20	26,800 16,200	21,400 9,200	12,880	17.5	40
10	18,000	205	18,040	206	62	-14	-10	-22	15,100	7,000	11,630	12.2	37
11	18,000	200	19,910	231	70	-13	-10	N.U.[b]	---	---	11,660	11.5	34
12	18,000	215	21,310	206	83	-13	-10	-19	16,300	9,400	17,130	11.0	34
13	18,000	225	21,380	231	65	-13	-10	-23	19,800	11,800	13,260	12.0	37
14	18,000	225	22,420	230	71	-13	-10	-27	16,600	9,100	14,780	18.0	40
15	18,000	200	19,900	217	66	-14	-10	-18	11,800	8,200	14,410	9.0	38
16	18,000	200	21,230	239	64	-12	-10	-21	14,900	11,300	12,490	12.8	42
17	18,000	200	19,070	220	50	-13	-10	-20	16,100	10,900	11,030	14.0	46
18	18,000	200	18,080	246	67	-12	-10	N.U.	---	---	11,260	14.0	35
19	18,000	200	20,510	196	83	Var	-10	N.A.	---	---	15,000	16.0	31
20	18,000	200	21,160	202	87	Var	-10	N.A.	---	---	16,030	9.5	30
21	18,000	200	18,630	237	65	-15	-9	-23 -16	15,600 7,700	10,600 5,900	13,710	14.1	44
22	18,000	200	18,320	202	64	-13	-10	-24	7,800	3,800	11,550	11.2	36
23	18,000	200	17,300	232	55	-13	-10	N.U.	---	---	10,100	13.7	41
24	18,000	200	18,590	200	63	-13	-10	-25	19,100	13,800	12,970	----	42
25	18,000	200	18,320	230	54	-13	-10	-19	5,700	4,200	10,860	14.0	43
26	18,000	200	18,020	244	61	-13	-10	N.U.	---	---	13,720	10.5	41
27	18,000	200	19,350	211	56	-13	-10	-21	7,200	4,300	10,570	----	46
28	18,000	200	20,060	223	55	-13	-10	-23	9,800	4,600	11,240	----	48

[a]None available

[b]None used

Table II

FINAL APPROACH PARAMETERS

Flight No.	Rollout Altitude (ft AGL)	Rollout Airspeed (KCAS)	Time Speed Brakes Used (sec)	Time on Final (sec)	Upper Flap Bias (deg)	Rudder Bias (deg)	Average L/D	Average Airspeed (KCAS)	Average Flightpath Angle (deg)	Glide Slope at 4,500 ft MSL (deg)
1	2,700	297	---	5.0	-21	-10	2.24	294	-21.9	-21.6
2	2,120	289	---	3.8	-21	-10	2.18	285	-22.5	-17.5
3	4,460	272	---	11.8	-21	-10	2.25	267	-21.9	-24.5
4	2,170	279	---	2.2	-20	-10	2.23	277	-22.1	-22.0
5	2,110	280	---	3.0	-18	-10	2.55	278	-19.5	-19.3
6	4,130	290	---	9.6	-21	-10	2.15	294	-22.6	---
7	5,730	300	---	19.2	-20	-10	1.96	290	-24.5	-21.9
8	4,080	297	---	17.6	-13	-10	2.86	298	-17.3	-18.5
9	4,390	297	---	19.0	-13	-10	2.71	293	-18.2	-18.4
10	4,140	282	---	18.0	-13	-10	3.27	297	-15.3	---
11	5,980	303	---	22.6	-13	-10	2.61	310	-18.6	-19.4
12	1,910	311	---	5.5	-13	-10	2.97	308	-16.6	-18.0
13	5,840	308	---	24.0	-13	-10	2.68	314	-18.2	-16.5
14	5,370	280	---	24.0	-13	-10	3.00	291	-16.6	-16.4
15	3,210	311	---	17.8	-13	-10	3.28	305	-15.1	-15.3
16	6,470	302	---	23.0	-12	-10	2.72	313	-17.9	-20.3
17	5,770	286	---	32.4	-12	-10	3.24	280	-15.5	-17.0
18	4,550	281	---	20.5	-12	-10	3.44	278	-14.7	-16.5
19	3,240	295	---	11.0	var	-10	3.10	297	-16.0	-15.0
20	2,660	299	---	8.8	var	-10	3.15	297	-15.8	-16.4
21	2,050	308	--	4.0	-13	-10	2.65	305	-18.5	-19.3
22	4,500	303	14	15.0	-15/-24*	-9/-6*	1.85	303	-25.9	-22.6
23	4,930	291	---	16.8	-13	-10	3.30	296	-15.0	-18.3
24	3,360	308	---	10.0	-13	-10	3.07	311	-16.0	---
25	5,180	296	7	16.0	-13/-19*	-10/-7*	2.87	305	-17.1	-19.6
26	2,030	318	---	1.0	-13	-10	3.06	318	-16.0	-21.0
27	6,510	291	14	23.5	-13/-21*	-10/-7*	2.48	302	-19.6	-20.1
28	6,440	303	17	18.7	-13/-23*	-10/-6*	2.07	304	-23.0	-21.9

*First value = δU_B before and after application of speed brakes. The second value = δU_B during speed brake application.

Table III

FLARE AND LANDING PARAMETERS

Flight No.	Pilot	Runway	Landing Gross Weight (lb)	Gear Up $c.g._i$ (pct $\bar{c}$)	Flare Initiation $\dot{h}$ (fps)	Flare Initiation V_c (KCAS)	Flare Initiation Altitude (ft AGL)	Flare Initiation δ_{U_B} (deg)	Flare Initiation δ_{e_L} (deg)	Flare Initiation δ_{R_B} (deg)	Landing Rockets "ON" Altitude (ft AGL)	Flare Completion V_c (KCAS)	Gear Extension V_c (KCAS)	Gear Extension Altitude (ft)	Touchdown V_c (KCAS)	Touchdown α (deg)	Touchdown $\dot{h}$ (fps)
1 [a,c]	A	18	6,161	57.86	-176.2	290.3	1,850	-21	var	-10	1,300	240.5	237.9	50	194.4	12.43	---
2[a]	A	18	6,263	58.06	-138.5	280.4	1,600	-21	↓	-10	600	227.3	220.2	50	183.3	15.70	---
3[a,b]	A	17	6,170	57.83	-195.3	268.7	2,080	-21	↓	-10	1,600	233.3	232.5	60	174.2	13.81	---
4	A	18	6,435	58.46	-182.6	273.8	1,800	-20	↓	-10	None	222.0	221.2	--	174.6	15.37	---
5	A	18	6,295	57.64	-158.4	277.8	1,650	-23	↓	-10	Used	216.0	192.5	--	167.6	16.53	---
6[c]	B	18	6,299	57.61	---	288.8	1,860	-21	↓	-10	↓	228.3	223.2	--	179.0	13.61	-2.0
7	A	18	6,299	57.62	-183.5	286.0	1,800	-20	↓	-10	↓	234.4	229.4	--	173.0	15.45	---
8	A	18	6,299	57.62	-142.9	305.0	1,030	-12	↓	-10	↓	264.7	244.4	40	171.8	14.45	---
9	A	18	6,461	57.35	-153.0	292.5	1,200	-13	↓	-10	↓	256.7	248.5	50	182.3	12.05	---
10	A	18	6,580	56.39	---	296.0	850	-13	↓	-10	↓	261.8	261.8	80	175.3	14.11	---
11	B	18	6,393	56.69	-174.4	314.0	1,350	-13	↓	-10	↓	267.9	271.0	60	195.6	9.17	---
12	A	18	6,462	56.55	-142.5	302.0	1,060	-13	↓	-10	↓	259.0	271.9	90	178.0	13.22	---
13	B	18	6,395	56.61	-156.9	316.9	1,290	-13	↓	-10	↓	270.0	267.9	60	188.6	10.14	---
14	B	18	6,391	56.60	-140.4	290.9	1,230	-13	↓	-10	↓	243.5	254.6	100	187.4	13.00	---
15[c]	A	18	7,003	56.11	-106.0	293.0	720	-13	↓	-10	↓	239.4	257.8	80	174.3	15.60	---
16	B	18	6,417	56.68	-180.3	314.5	1,500	-12	↓	-10	↓	268.8	264.3	50	198.6	9.88	-1.7
17[k]	A	19	6,396	56.96	-126.0	275.6	1,040	-12	↓	-10	↓	241.4	230.3	50	169.7	13.79	-1.0
18[k]	B	19	6,594	56.70	-134.1	279.	1,600	-12	var	-10	↓	245.3	242.2	90	180.0	14.09	-4.6
19[c,k]	B	18	6,337	57.27	-138.2	296.7	1,500	var	0	-10	↓	242.7	260.1	115	175.0	12.12	-2.3
20[k]	A	18	6,284	57.46	-148.4	295.7	1,500	var	↓	-10	↓	252.7	236.3	40	169.4	13.48	-2.9
21	B	23	6,231	57.35	-132.8	305.0	1,350	-13	↓	-10	↓	236.7	256.9	90	189.4	9.97	-3.5
22[c]	C	19	6,336	57.68	-188.7	311.1	1,400	-13	↓	-10	↓	255.7	257.0	50	191.2	10.33	-2.5
23	B	23	6,566	56.44	-161.4	317.5	1,850	-13	↓	-10	↓	242.5	266.0	130	184.1	12.71	---
24	C	13	6,261	57.37	---	304.1	1,200	-13	↓	-10	↓	242.1	245.5	60	195.5	9.97	0
25	B	23	6,596	56.23	-175.7	308.4	1,700	-13	↓	-10	↓	259.7	252.5	75	190.6	11.16	-2.5
26	C	19	6,224	57.16	-189.8	317.2	1,750	-13	↓	-10	↓	259.7	266.	60	204.8	8.79	-2.0
27	B	23	6,247	56.62	-[illegible]	301.1	1,500	-13	↓	-10	None	---	263.1	--	198.8	11.90	---
28	B	23	6,[illegible]	56.89	-[illegible]	310.3	1,870	-13	var	-10	Used	---	261.	--	200.1	10.35	---

Table III (Concluded)

Flight No.	Surface Wind Speed (kt)	Surface Wind Direction (deg true)	Runway Crosswind Speed (kt)	Long. Distance From Intended Touchdown (ft)	Lateral Distance From Intended Touchdown[j] (ft)	Landing Roll Distance (ft)	Time Flare Initiation to Touchdown (sec)	Time End of Flare to Touchdown (sec)	Time Gear Extension to Touchdown (sec)	Time Landing Rockets "ON" to Touchdown (sec)
1	calm[f]			---	---	7,920	27.3	8.8	8.3	24.4
2	calm			-317	208 (L)	7,220	28.5	9.3	7.3	19.9
3	calm			---	---	7,530	31.1	10.9	10.8	28.3
4	calm			-2,057	100 (R)	9,980	23.6	6.9	6.8	None Used
5	calm			-70	30 (L)	6,450	24.5	7.8	3.7	
6	calm			-758	1 (L)	7,520	23.1	6.7	5.9	
7	calm			2,668	154 (R)	5,860	26.0	8.8	7.9	
8	calm			4,185	38 (L)	6,556	26.8	14.7	10.3	
9	calm			199	6 (L)	5,774	23.6	10.4	9.0	
10	15	030	2.9	3,780	170 (R)	6,428	23.3	12.5	12.5	
11	calm			382	37 (R)	9,371	23.4	8.8	9.3	
12	calm			-197	37 (L)	6,135	23.3	11.2	12.4	
13	5	144	4.1	1,100	8 (R)	7,593	25.5	10.3	10.1	
14	calm			-640	1 (R)	10,940[g]	24.0	8.5	10.1	
15	10	229	5.0	-301	28 (L)	5,930	23.5	9.7	12.1	
16	calm			1,796	19 (R)	9,451	25.4	9.0	8.8	
17	calm			2,819	15 (L)	7,038	25.6	12.0	9.0	
18	5	291	5.0	2,885	14 (R)	7,351[h]	28.3	9.8	9.1	
19	15	060	9.9	1,053	35 (R)	7,765	28.9	9.1	11.4	
20	7	219	2.4	3,863	12 (L)	6,231	31.2	14.4	10.2	
21	calm			385	0	6,206[h]	23.4	6.4	9.0	
22	calm			123	100 (R)	5,858	23.0	8.4	8.6	
23	6	270	5.9	-1,115	0	6,359[h]	28.5	7.7	10.4	
24	10	290	8.5	633	0	8,711	22.6	6.5	6.9	
25	calm			-167	0	8,586	28.7	10.1	8.9	
26	calm			-511	0	8,255[h]	24.8	7.2	7.6	
27	calm			203	0	7,571[h]	22.6	--	8.0	
28	calm			1,329	0	7,263[h]	25.6	--	7.6	None Used

[a]Landing rockets used, off at touchdown.
[b]Inadvertent launch, alternate runway used.
[c]Pilot checkout flight.
[d]Heavyweight landing.
[e]Highest crosswind pilot would want to land in.
[f]"Calm" is variable zero to four knots.
[g]Landing rockets used during landing roll.
[h]Speed brakes opened during landing roll.
[i]Gear increment cg = -.72 pct.
[j]L and R denote left and right, respectively.
[k]Touchdown accuracy was not a primary task.

Table IV

PILOTING EXPERIENCE IN LIFTING BODY VEHICLES

Pilot	Experience in Lifting Bodies Prior to the X-24A	X-24A Experience
	Number of Landings	
A	15	13
B	10	12
C	0	3

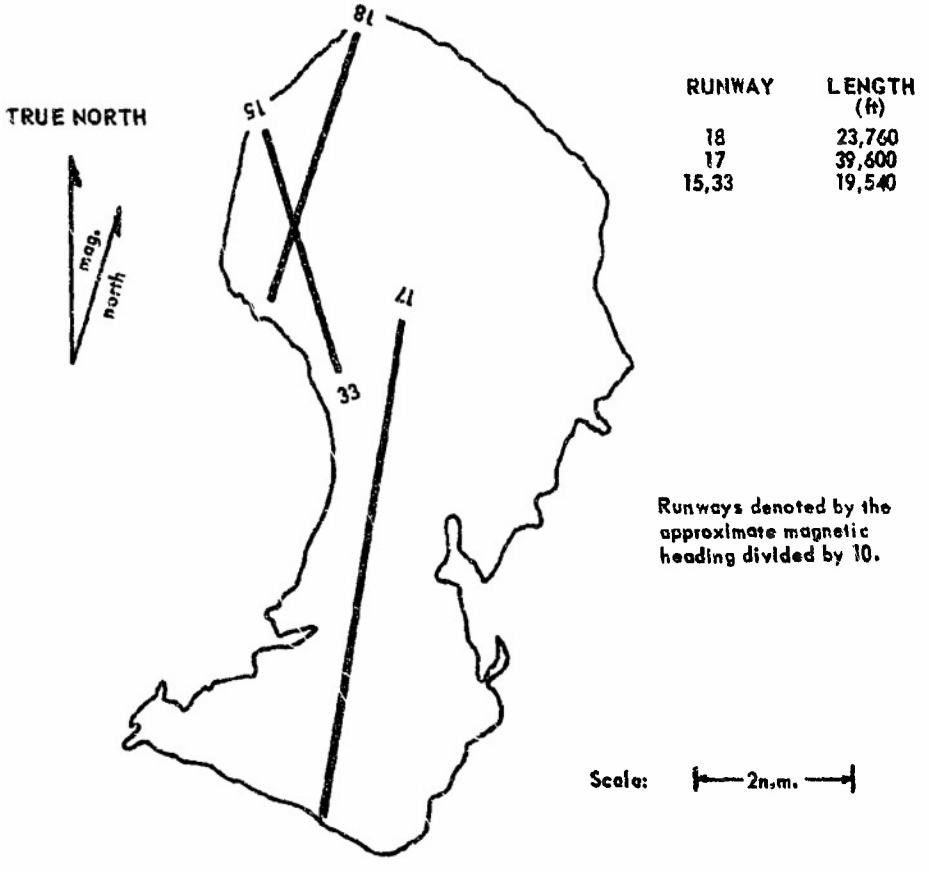

Figure 3 Rogers Dry Lakebed

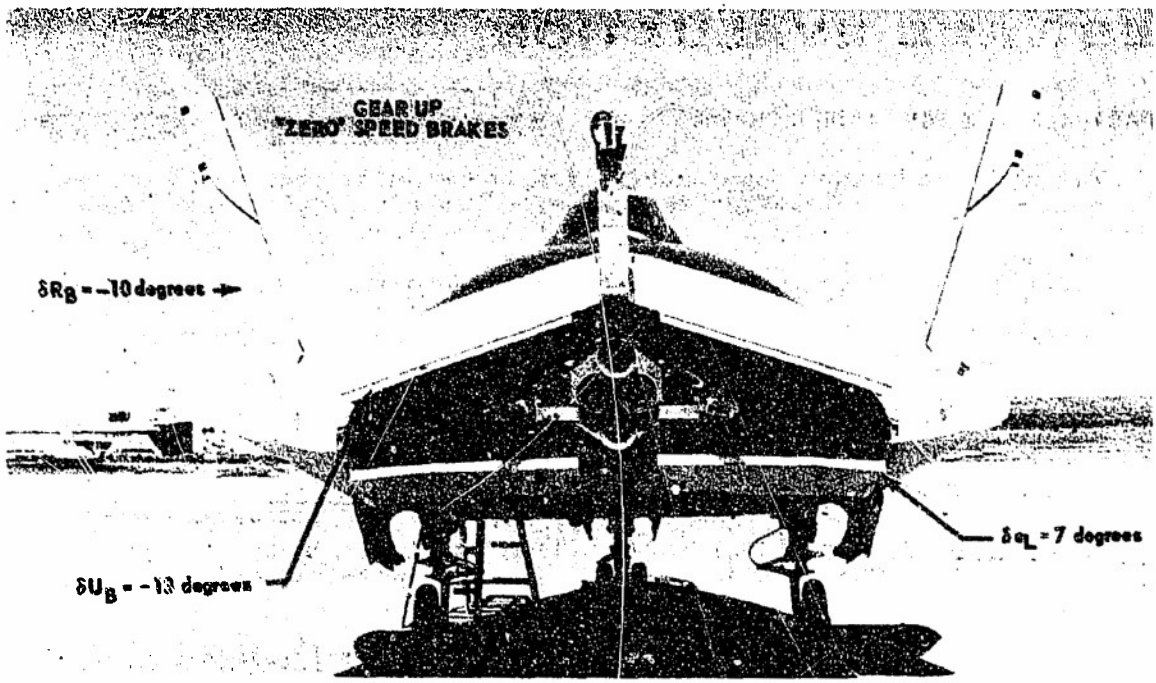

Figure 4 Approach Configuration Mode Two

Figure 5 Landing Configuration Modes Two and Three

TEST AND EVALUATION

APPROACH, FLARE AND LANDING PHASES

The unpowered visual approach, flare and landing were divided into four phases for analysis (figures 6 and 7). In actual practice, these phases were blended together by the pilot in a slightly different manner on each individual flight. For this reason, caution must be exercised in generalizing the statistical values included herein.

I. Initial Approach Phase - A 180-degree circling unpowered turn starting at a low key point between 18,000 and 21,000 feet MSL.

II. Final Approach Phase - A constant airspeed, gliding approach on the runway heading with bank angle less than ±10 degrees.

III. Landing Flare Phase - A wings level, angle of attack increase at elevated load factor producing a transition from the steep final approach glide angle (γ_g) to a shallow deceleration-to-touchdown glide angle. The landing gear was extended near the end of the flare.

IV. Deceleration Phase - Deceleration along a shallow glide angle to the point of touchdown.

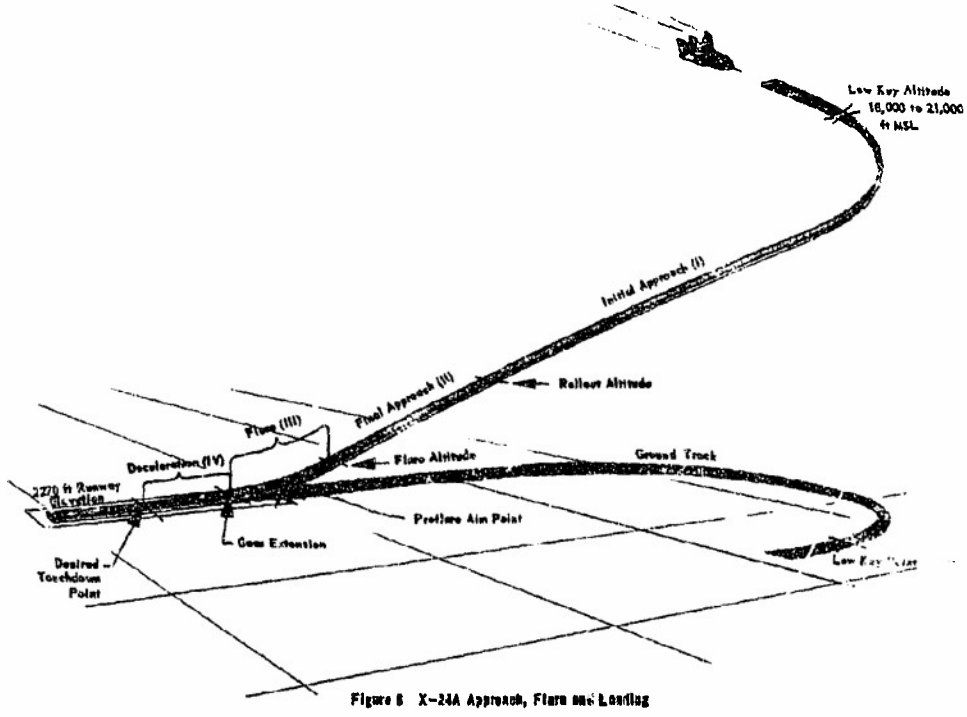

Figure 6 X-24A Approach, Flare and Landing

Figure 8 presents a sequence of photos taken with a camera aimed through the nose of the X-24A. This sequence starts halfway through the initial approach and terminates at touchdown.

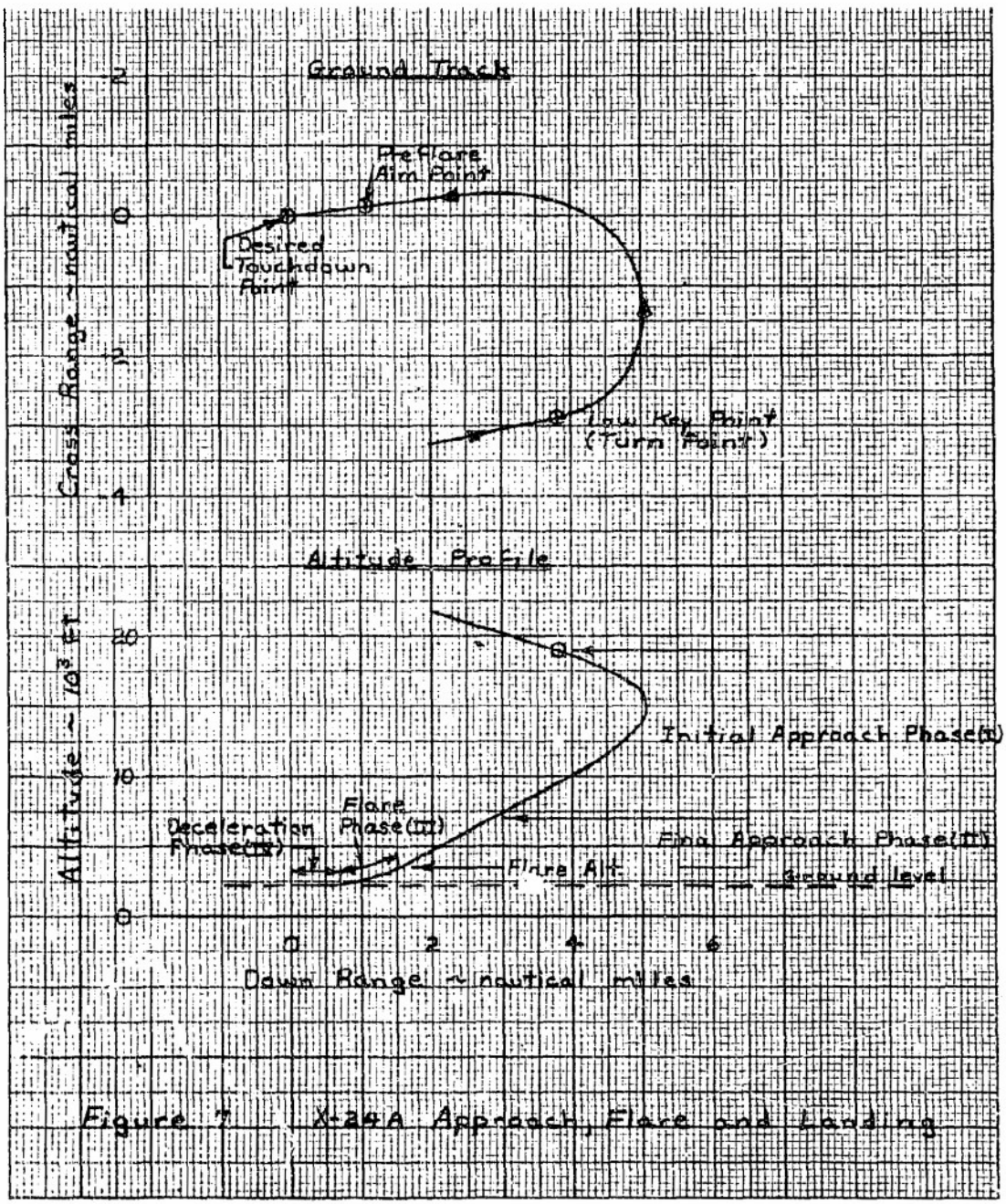

Figure 7 X-24A Approach, Flare and Landing

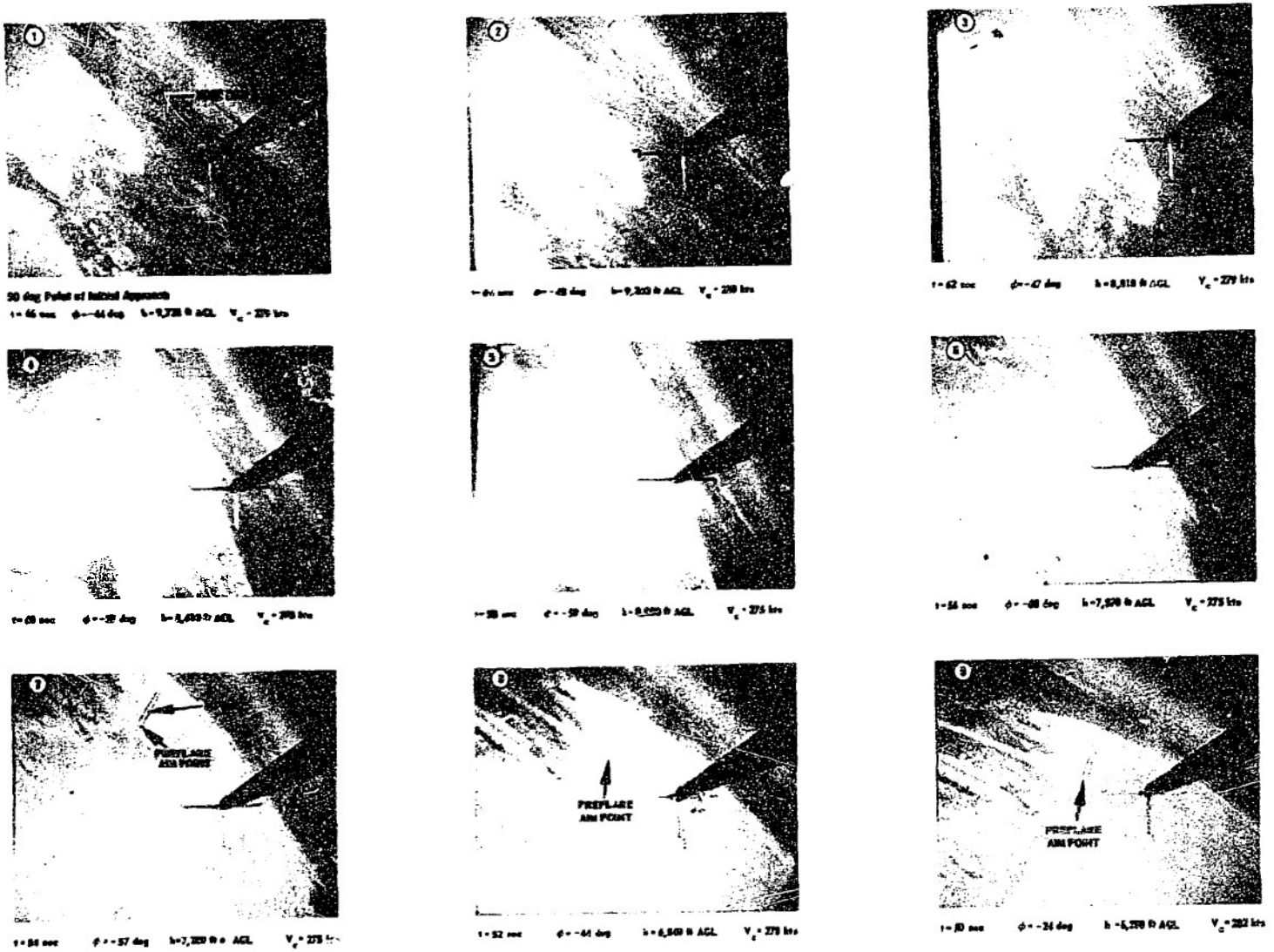

Figure 8 X-24A Approach, Flare and Landing

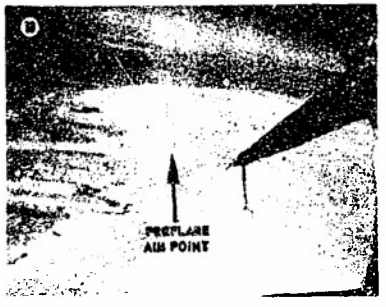

t = 48 sec ϕ = −20 deg   h = 5,970 ft AGL V_c = 287 kts

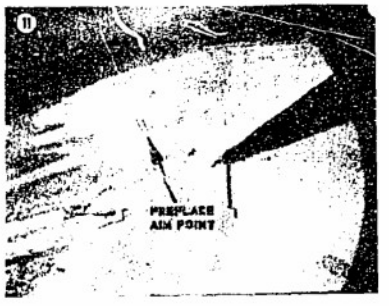

t = 46 sec   h = 5,500 ft AGL V_c = 292 kts

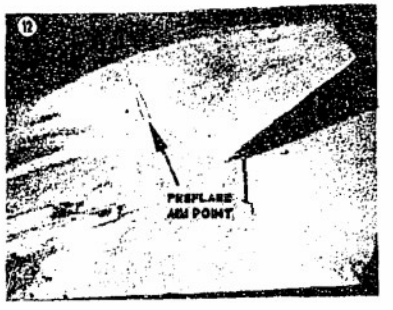

ROLLOUT ON FINAL
t = 44 sec   h = 5,180 ft AGL V_c = 296 kts

t = 42 sec   h = 4,750 ft AGL V_c = 299 kts

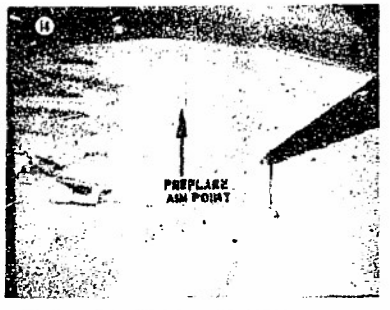

t = 40 sec   h = 4,300 ft AGL V_c = 301 kts

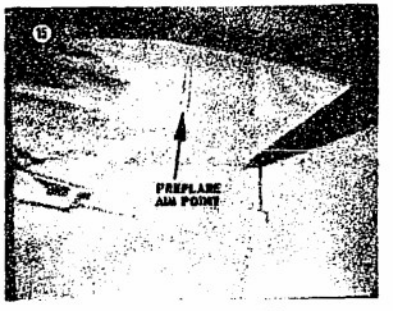

t = 38 sec   h = 3,860 ft AGL V_c = 304 kts

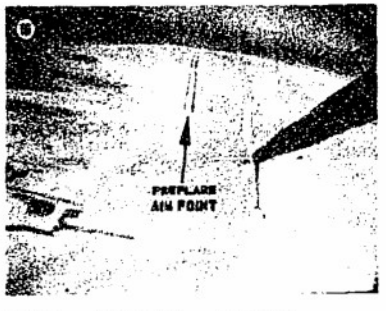

t = 36 sec   h = 3,400 ft AGL V_c = 305 kts

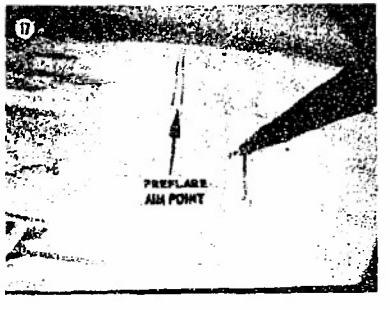

t = 34 sec   h = 2,960 ft AGL V_c = 306 kts

t = 32 sec   h = 2,540 ft AGL V_c = 307 kts

Figure 8 (continued)

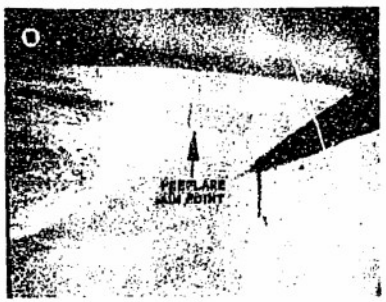

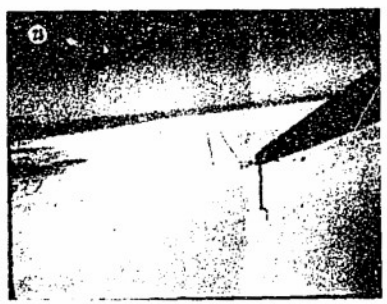

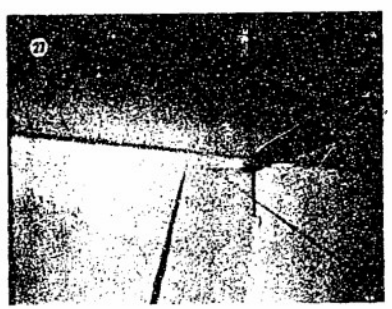

Figure 8 (continued)

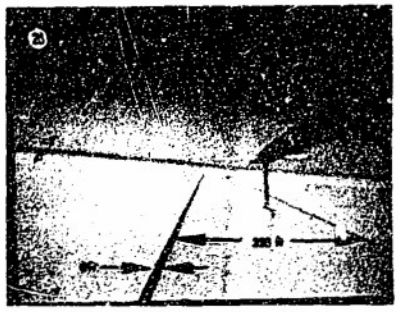

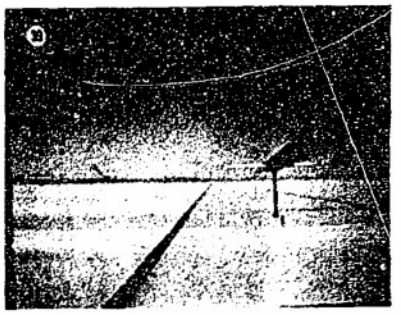

Gear Extension

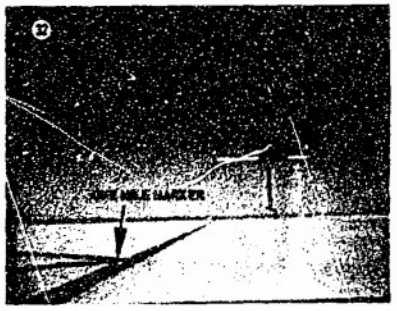

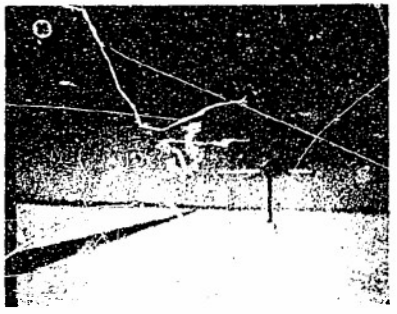

The marked runway is 200 feet wide.
The left and right runway marker strips are 6 feet wide.

Figure 8 (concluded)

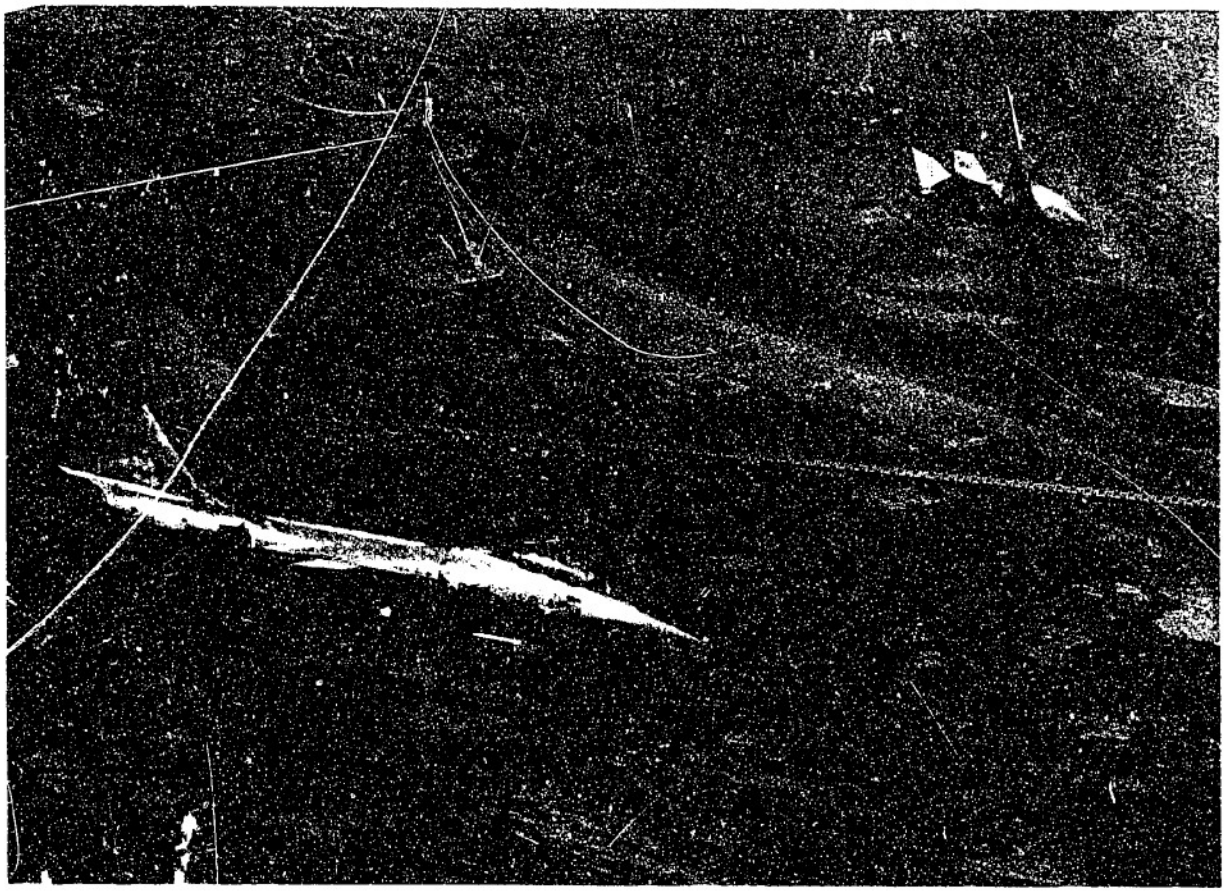

Initial Approach

The basic pattern used during the X-24A program was a 180-degree, unpowered, left-hand, circling approach beginning at a low key point. The advantages of this pattern over other possible patterns for the X-24A were:

1. The variation of bank angle, airspeed and speed brake deflection provided for a broad energy management capability.
2. A 270- or 360-degree overhead pattern (X-15 pattern) would have devoted too much valuable flight time to the landing pattern and thus compromised the amount of research data gathered per flight.
3. A straight-in approach would be more difficult from a pilot's judegement standpoint. It would be more difficult to judge glide angle from the distances and altitudes associated with this type of approach. Also, a straight-in approach would have substantially reduced any energy management capability through bank angle modulation.

There were two low key points: the preplanned low key and the actual low key. The preplanned low key point was the turn initiation point for the X-24A landing approach with no wind. It was initially determined by the pilots during their training when using the inflight performance simulator aircraft and the fixed base X-24A simulator. The preplanned low key point was located 2.8 to 3.4 nautical miles to the side of, and 1.6 to 2.4 nautical miles downwind from the end of the runway (figures 6 and 7). There was an altitude associated with this point to aid the pilot in assessing his energy. This altitude was 19,000 to 21,000 feet MSL for configuration mode 1 and 18,000 feet for configuration modes 2 and 3; however, there was a comfortable altitude window of at least 5,000 feet (+4,000, -1,000 feet) associated with the preplanned low key point. This point was changed several times during the early X-24A flights as the pilot re-examined his evaluation of the pattern and as different approach configurations were tested.

The actual low key point was the point at which the pilot actually initiated the turn on each X-24A flight.

Because of the type of research mission flown in which the pilot was performing data maneuvers down to the low key point and in some cases beyond it, verbal guidance from a ground controller was necessary to the pilot. The help that the pilot received from the ground controller was an assessment of how far he was above or below the preplanned altitude profile or left or right of the preplanned ground track[1] and how far he was from the preplanned low key point. Based on this information the pilot could judge his flight conditions, terminate data maneuvers and reconfigure from the transonic configuration[2] to the subsonic configuration

[1]The preplanned altitude profile and ground track was determined prior to each flight through the use of a fixed base X-24A simulator.

[2]The transonic configuration was with -30 to -40 degrees upper flap bias position and was used at Mach numbers above 0.5.

(either modes 1, 2 or 3) prior to reaching low key. A continuous assessment of total energy was made by the pilot based on known winds and ground controller guidance information. This information plus a visual assessment was used to determine the actual low key point (see the section titled Effects of Winds and Turbulence in the Approach Pattern and Flare). Once the turn was started, the pilot received no energy management advice from the ground controller. The pilot used his own experience and judgement to fly the pattern. The ground controller was available to remind the pilot of any specific events to be performed during the approach. The chase aircraft pilots observed their airspeeds and power settings at various times in the pattern when they were stabilized alongside the X-24A. These observations were useful later in improving the inflight performance simulation of the X-24A.

The piloting task during the initial approach phase was to position the vehicle on an imaginary glide slope intercepting a preflare aim point on the ground and accelerate to the desired final approach (preflare) airspeed. (An instrument landing system (ILS) was not used with the X-24A.) The pilots generally planned to have excess energy approaching the low key point. They modulated this energy during the initial approach to arrive on the desired glide slope either by airspeed and/or bank angle modulation or they remained at approximately the same airspeed and used the flap bias feature for speed brakes (appendix III). The pilots had an intermediate altitude window of between 12,000 and 15,000 feet MSL at the 90-degree point of the pattern, and they used this to aid them with their energy management. Figure 9 shows the X-24A at approximately the 90-degree point. Also refer to figure 8 (frames t = 66 to 46).

Figure 9 X-24A at the 90-Degree Point of the Initial Approach

For the initial approach phase, the pilots tried to arrive at the low key point with an airspeed between 190 and 230 KIAS and then allowed it to increase during the turn while striving to have at least 250 KIAS at the 90-degree point and the desired final approach speed at rollout on final. The pilots decreased the angle of attack as they rolled out on final to maintain the final approach airspeed.

Final Approach

The desired final approach (figure 6) was a wings level, constant-indicated-airspeed, gliding approach of short duration lined up with the runway. Refer to figure 8 (frames t = 44 to 30). The pilot was not trying to rollout on final at any specific altitude, but rather was trying to position the vehicle on an imaginary glide slope which intercepted the preflare aim point[3]. The pilots were striving to establish a final approach airspeed of 300 KIAS, which was more than adequate for a flare. However, the airspeed was allowed to vary somewhat in order to establish a glide angle which would intercept the desired aim point. This permitted the pilot to arrive at a flare initiation point with sufficient energy to accomplish the flare and with excess airspeed after flare to allow for some margin for error.

Landing Flare

The transitional maneuver between the steep final approach glide angle and the shallow deceleration glide angle was a wings level angle of attack increase to an elevated load factor. Refer to figure 8 (frames t = 28 to 10). The pertinent characteristics (altitude and airspeed lost and the timing) of this flare maneuver were predicted prior to the first flight through the use of the X-24A fixed base simulator and the inflight performance simulator using F-104 aircraft.

During the actual X-24A flights, the pilots stated that their primary cue for flare initiation was altitude. However, they indicated that the determination of flare initiation was also a combination of pilot experience and the interrelation of several factors including sink rate, airspeed, altitude, and their position relative to the desired aim point. The pilots made corrections to the desired final approach glide slope/aim point right up to what they considered their flare initiation point. Therefore, it was often difficult to differentiate between these corrections, which produced "g" excursions, and what the pilots considered their actual flare maneuver although technically these glide slope corrections usually resulted in a partial flare maneuver.

A flare initiation airspeed of 300 KIAS was suggested to the pilot; however, simulator studies indicated that flares could be initiated at airspeeds as low as 250 KIAS. On four flights this target airspeed was 270 KIAS.

For postflight data analysis, the flare initiation point was determined by examination of the normal acceleration, angle of attack, pitch angle and stick position data. The flare completion point was arbitrarily considered to be the point at which the flare initiation sink rate had been arrested to 20 feet per second as determined by the radar altimeter.

[3]For the X-24A, this preflare aim point was 1-1/4 miles short of the intended touchdown point.

Deceleration

At or near flare completion, the pilot extended the landing gear and the vehicle decelerated along a shallow glide angle (less than three degrees) to the point of touchdown. Refer to figure 8 (frames t = 8 to 0). The length of time of this phase was very important because it allowed for some margin for error in the flare maneuver. It also gave the pilot time to recover from the gear transient and to adjust the sink rate to a very low value prior to touchdown. The amount of time that the pilot had during the deceleration phase was obviously a function of the gear down performance and the touchdown airspeed, but more importantly, was related to the energy at flare initiation (airspeed and glide angle) and the flare technique used (high or low load factor).

The chase aircraft pilot performed several functions during this time period: (1) advised the X-24A pilot of his distance above the ground, (2) reminded him to extend the landing gear, (3) reminded him to be aware of the gear transient and (4) confirmed that the gear was down.

FLIGHT TEST RESULTS

X-24A Performance

Figure 10 presents the L/D versus equivalent airspeed for the three landing gear up approach configuration modes and the landing gear down touchdown configuration. These data are the flight data as presented in reference 4. All of the gear-up data were obtained from push-over/pull-up maneuvers and the gear down data were obtained during the deceleration between gear extension and touchdown. The data in figure 10 were corrected to a planform loading of 39.3 pounds per square foot which corresponds to a gross weight of 6,360 pounds. All of the X-24A approaches were made at Mach numbers of 0.55 and less.

There are certain characteristics of these L/D curves which are important to test results. The positive slope of this L/D curve (higher airspeeds to the left of maximum L/D) was commonly referred to as the "front side" and was the speed stable flight regime. When operating on the front side, lowering the nose would increase the airspeed and decrease the L/D, producing a steeper flightpath angle. Raising the nose would reduce the airspeed and increase the L/D, producing a shallower flightpath angle. The vehicle would also be speed stable while flying along a particular flightpath angle, i.e., excess speed along a given flightpath angle would produce excess drag resulting in a deceleration to the desired speed. The degree of speed stability would increase with the steepness of the L/D curve. Flying on the front side of the L/D curve was a natural task for the pilot and all X-24A approaches were made in that regime.

The negative slope portion of the L/D curve (lower speeds to the right of maximum L/D) was designated the "back side" and was characterised by speed instability. Lowering the nose would increase the airspeed but (unlike the case on the front side) the L/D increased with increasing airspeed and consequently would result in a shallower flightpath angle. It would have been an unnatural task for the pilot to conduct the energy management task on this portion of the L/D curve. No X-24A approaches were made on the back side of the L/D curve.

Configuration
Symbol
Gear
Flaps
Mach
Lift vs. Drag
Figure 10 - X-24A Configuration
23

Figure 11 illustrates the L/D during a typical X-24A landing flare. The approach and flare initiation airspeed of approximately 300 knots placed the approach conditions well down the speed stable front side of the L/D curve. During the flare maneuver, the normal acceleration and lift coefficient (C_L) increased and the flare was accomplished at L/D values approaching the maximum. As the flare was completed and the normal acceleration decreased, the C_L again dropped down the front side of the L/D curve. The pilot lowered the landing gear while the vehicle decelerated and glided essentially parallel to the ground. The C_L gradually increased during the deceleration, and touchdown occurred near the point of maximum L/D.

The X-24A was not built with independent surfaces for speed brake usage. Figure 12 presents the effect of using the flap bias feature as a speed brake. Speed brake was the combined effect of the upper flap bias position, rudder bias position, and the trim lower flap deflection. Speed brake is expressed in terms of the upper flap bias position where δU_B = -13 degrees is considered zero speed brakes. This figure illustrates that the use of the flap bias control system feature provided a very effective speed brake function (refer to appendix III).

Approaches

Initial Approach Phase

Figure 13 shows the spread of the patterns flown to runway 18 from flights 8 to 20. The envelope of the pattern radar data is indicated as the shaded area. This figure illustrates the wide flexibility available with this type of pattern. In general, the pilots reached the low key point with excess energy to compensate for uncertain wind conditions and possible misjudgement of distance. The excess energy was then expended through the use of maneuvering flight and/or speed brakes during the pattern.

Figures 14 and 15 illustrate the size of the energy footprint at low key that evolved during the X-24A flight test program. This footprint was 1.3 nautical miles square and 5,000 feet deep. The scatter in the data was expected since the preplanned low key point was a non-wind-corrected point and the pilot, who was correcting for wind, was not necessarily trying to reach this exact point.

A summary of the speed brake usage is presented in figure 16. This summary does not include flights 1 to 7, 19, and 20, in which the pilots were asked not to use the speed brakes (appendix III). On 79 percent of the flights in which speed brakes were available, they were used at some time during the pattern as indicated on figure 16. Most of the usage was below 15,000 feet MSL at an airspeed between 240 to 280 KCAS which indicated that the pilot had passed through the 90-degree point of the pattern and was converging on the preflare aim point. This figure also illustrates that when speed brakes were used the upper flap bias was deflected from the normal -13 degrees position to an average position of between -18 and -24 degrees. Figure 17 is configuration mode 2 with speed brakes (-25 degrees of upper flap bias).

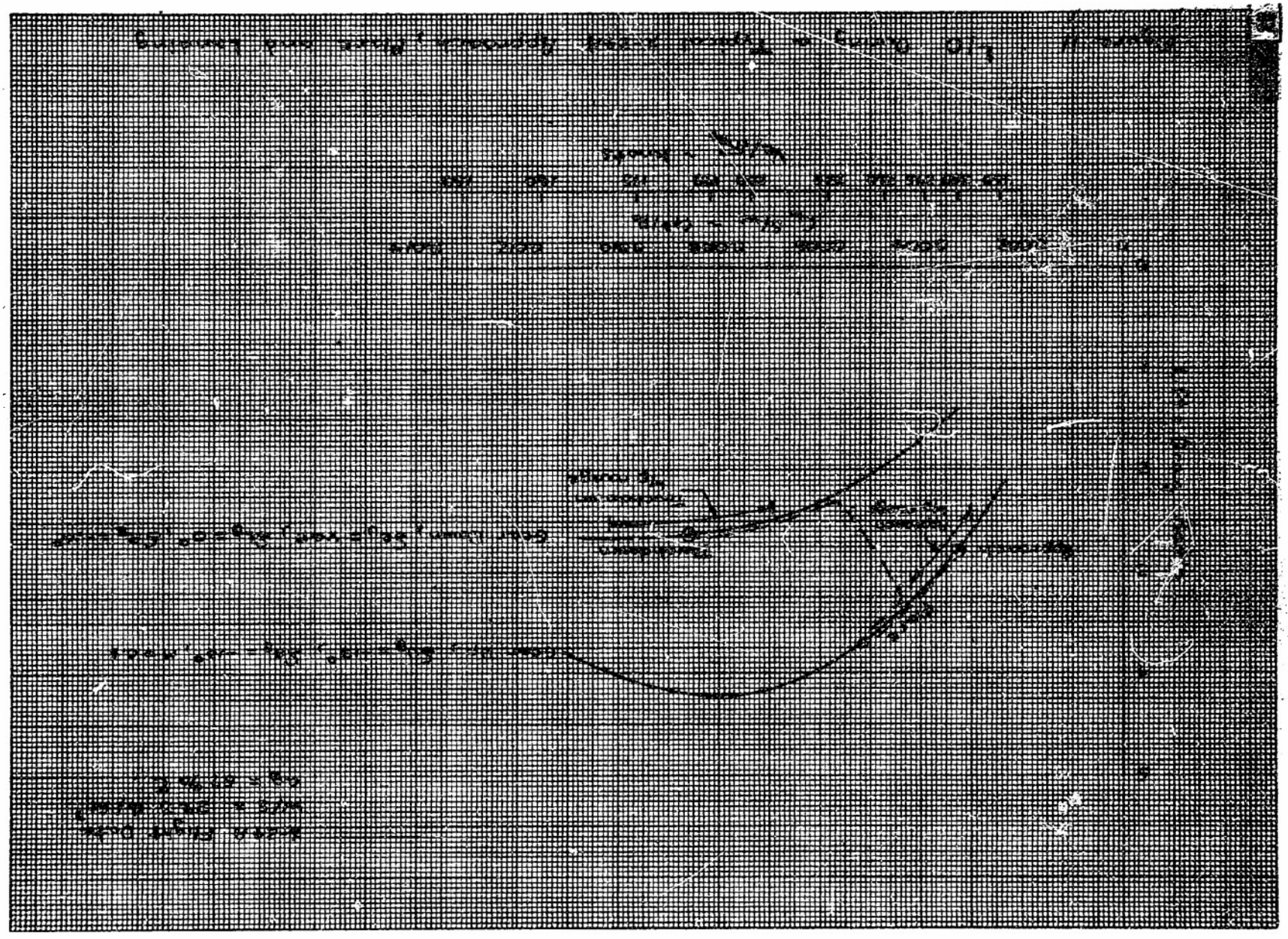

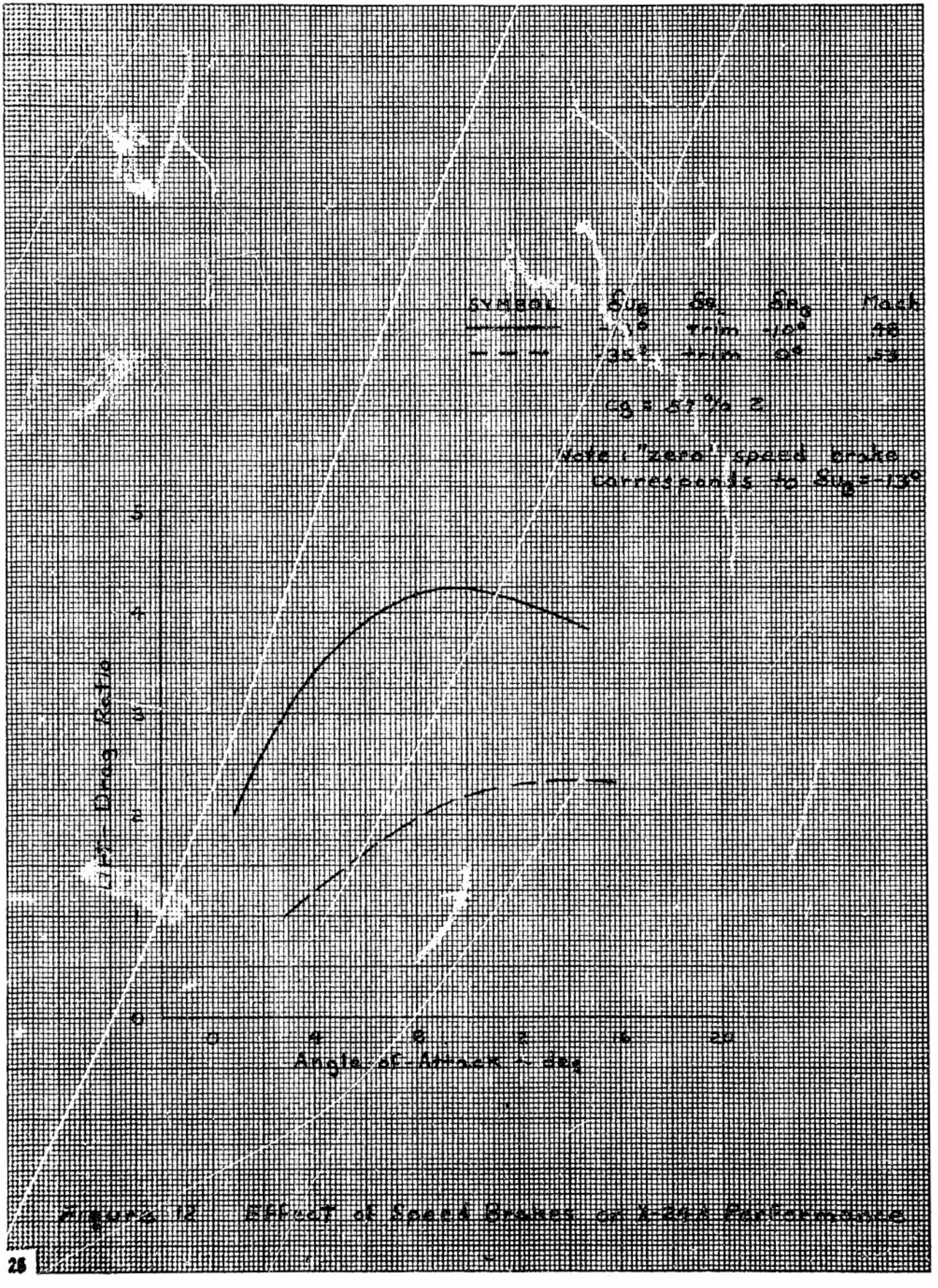

Figure 12 Effect of Speed Brakes on X-24A Performance

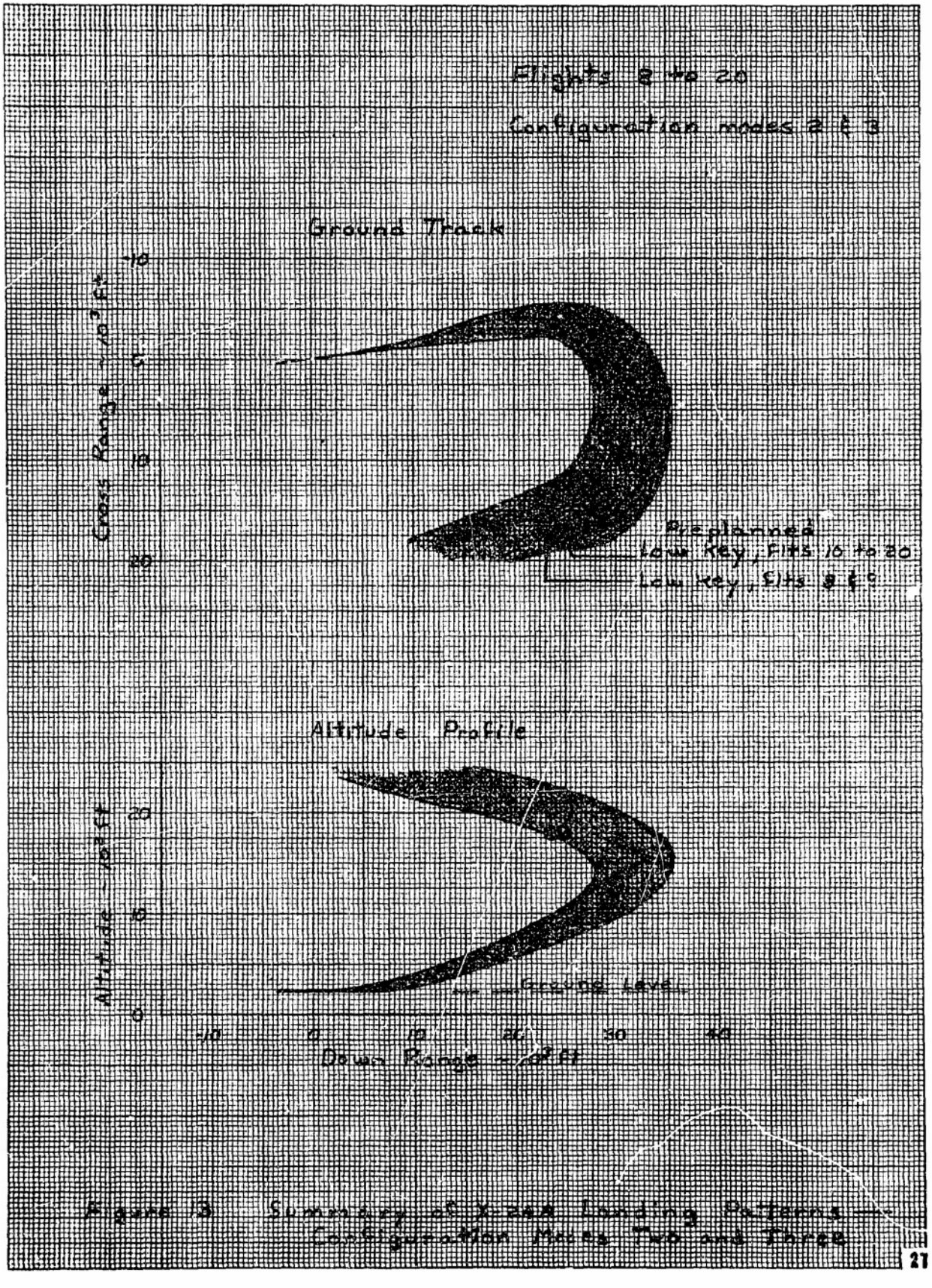

Figure 13 Summary of X-24A Landing Patterns — Configuration Modes Two and Three

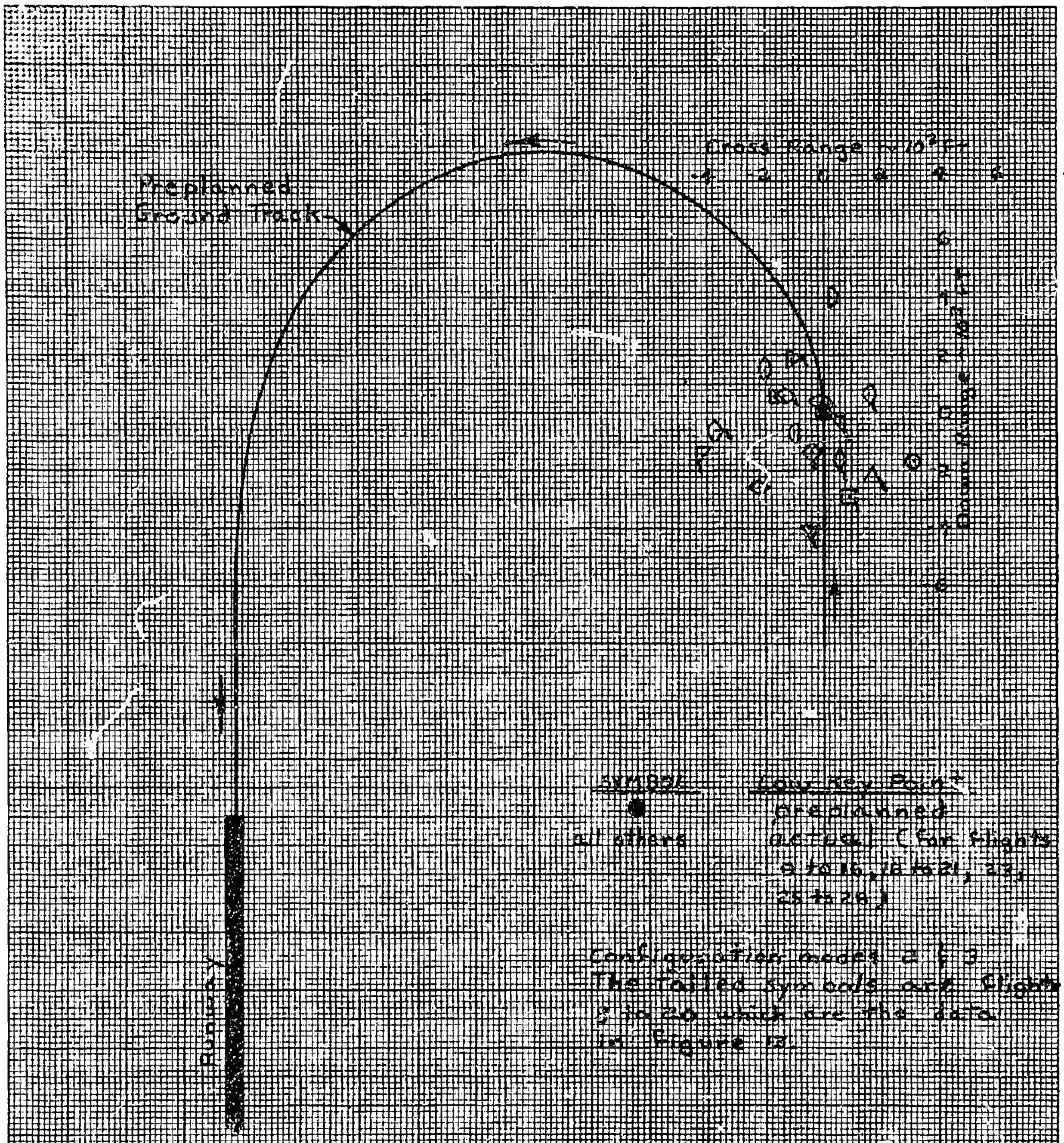

Figure 14 Comparison of the Actual Low Key Points to the Preplanned Low Key Point

Figure 8 Energy at the Altitude Low Key Point

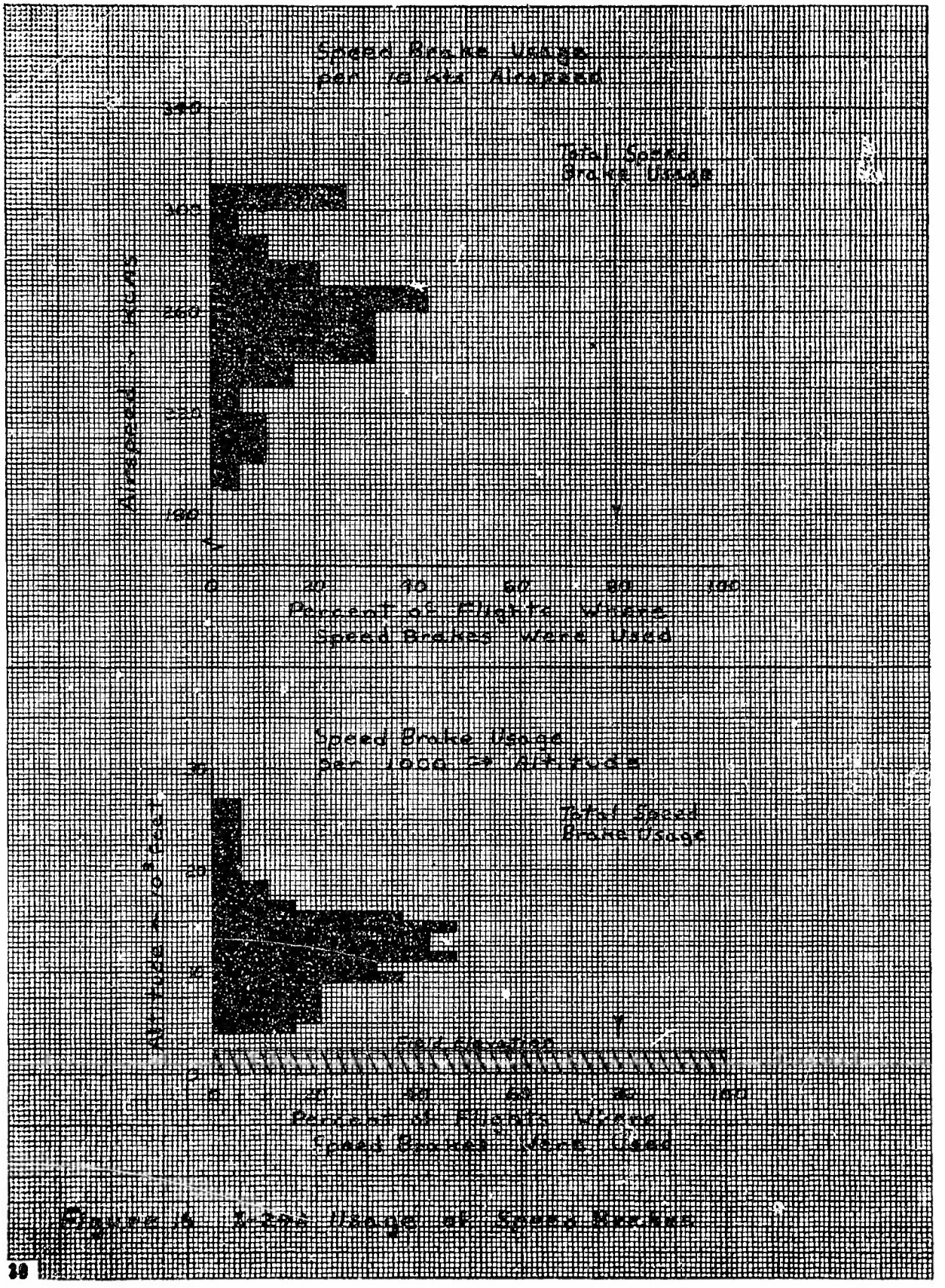

Figure 16. B-2HA Usage of Speed Brakes

Figure 15 X-24A Usage of Speed Brakes (concluded)

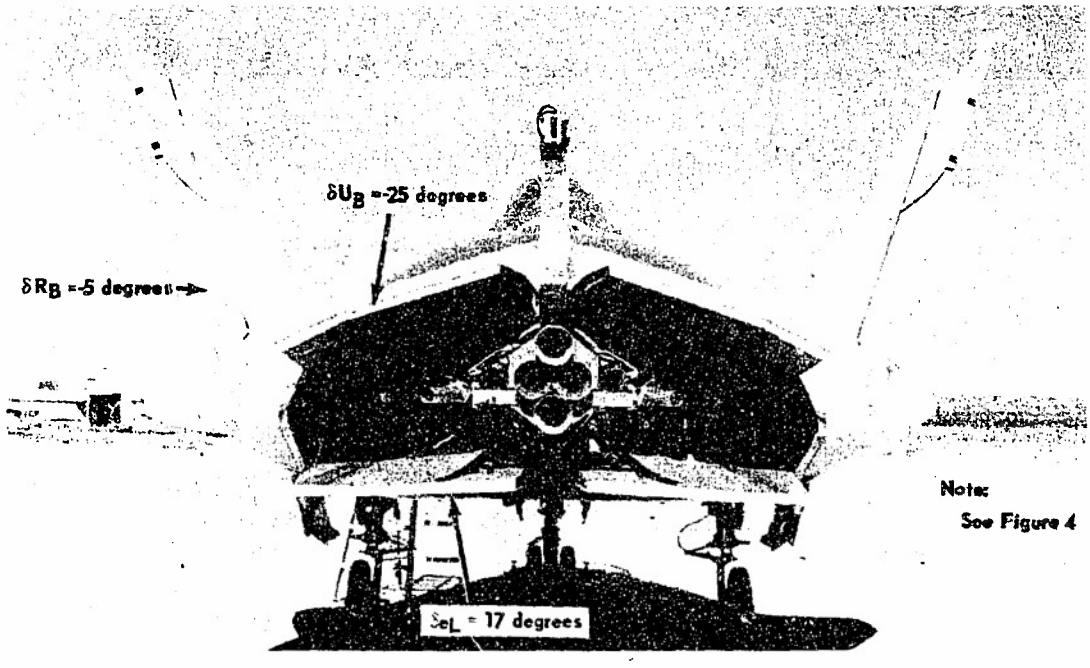

Figure 17 Speed Brakes in Configuration Mode Two

Figure 18 shows the effect of vehicle configuration on the landing pattern. In both cases, the winds at altitude were low (average value of 12 to 15 knots). The patterns started at the same altitude, and the flight with the lower lift-drag ratio used a higher bank angle and started laterally closer to the touchdown point since the turn rate is directly proportional to the L/D and bank angle, and the turn radius is inversely proportional to the turn rate (appendix II).

Figure 19 illustrates the glide slope, airspeed, bank angle, and sink rate encountered during a typical approach in configuration modes 1 and 2 (configuration mode 3 was very similar to mode 2).

Table I shows that the overall average bank angle used with configuration mode 1 was 44 degrees, and for modes 2 and 3 it was 39 degrees. The average altitude lost during the turn was 16,300 feet for configuration mode 1 and 12,700 feet for configuration modes 2 and 3. The flight time from the actual low key point to rollout on the final approach ranged between 50 to 87 seconds. This time was a function of the bank angle (figure 20), configuration and airspeed (figures 2 and 3, appendix III) and certainly the wind.

Pilots commented that the 180-degree circling approach pattern was a very comfortable pattern. It was easy to pick up the airspeed during the turn. At rollout on final, he had to reduce the angle of attack to pick up or hold the desired airspeed of 300 knots. Bank angles as high as 60 degrees were used on occasion in the turns without undue concern. Pilots commented that the pilot task when flying the initial approach in the X-24A was like flying a similar approach in an F-104 aircraft.

THIS PAGE LEFT BLANK FOR PRESENTATION PURPOSES

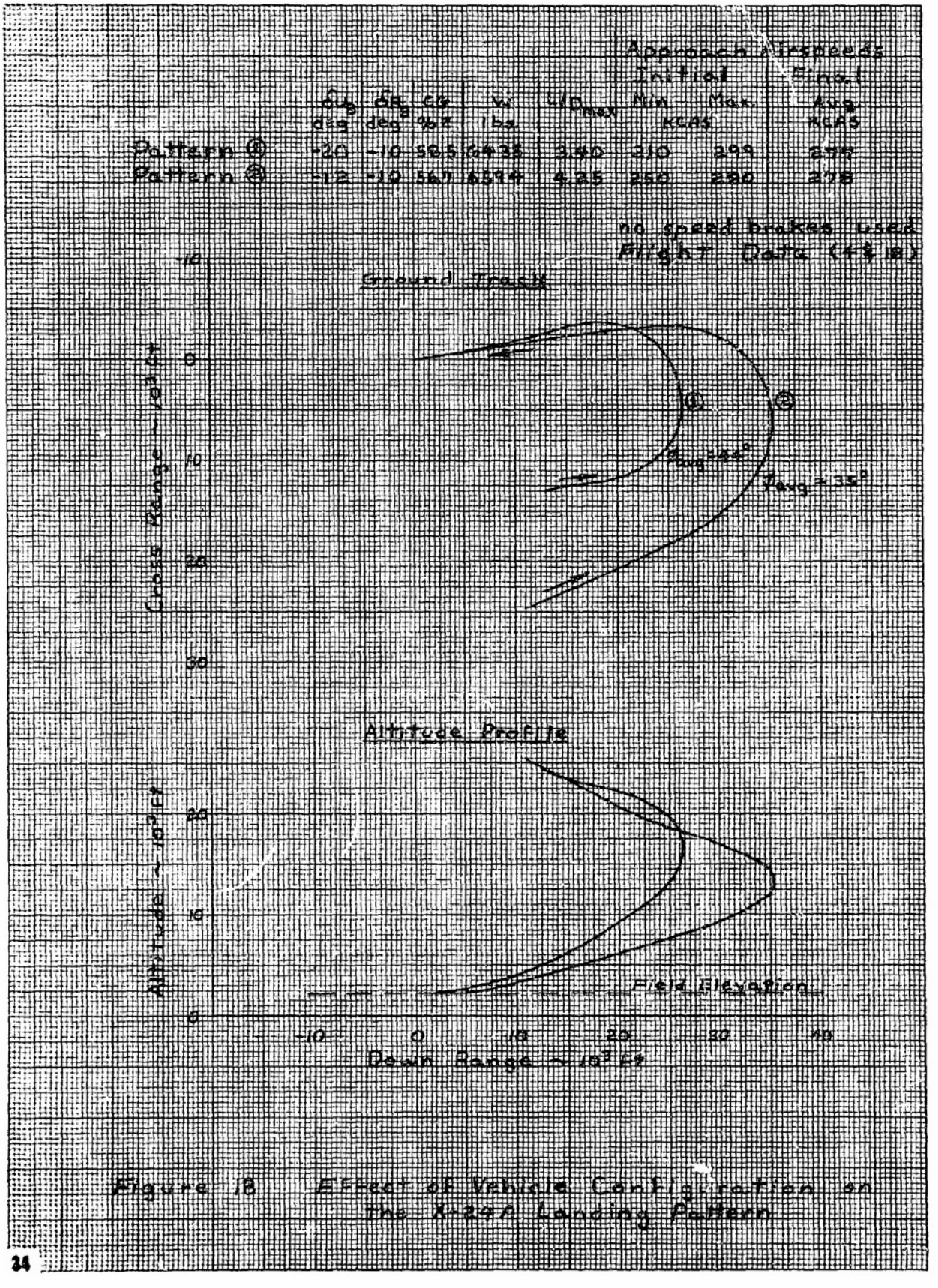

Figure 18 Effect of Vehicle Configuration on the X-24A Landing Pattern

Figure 19 Effect of Configuration on the Flight Parameters of the Final and Final Approach Phases

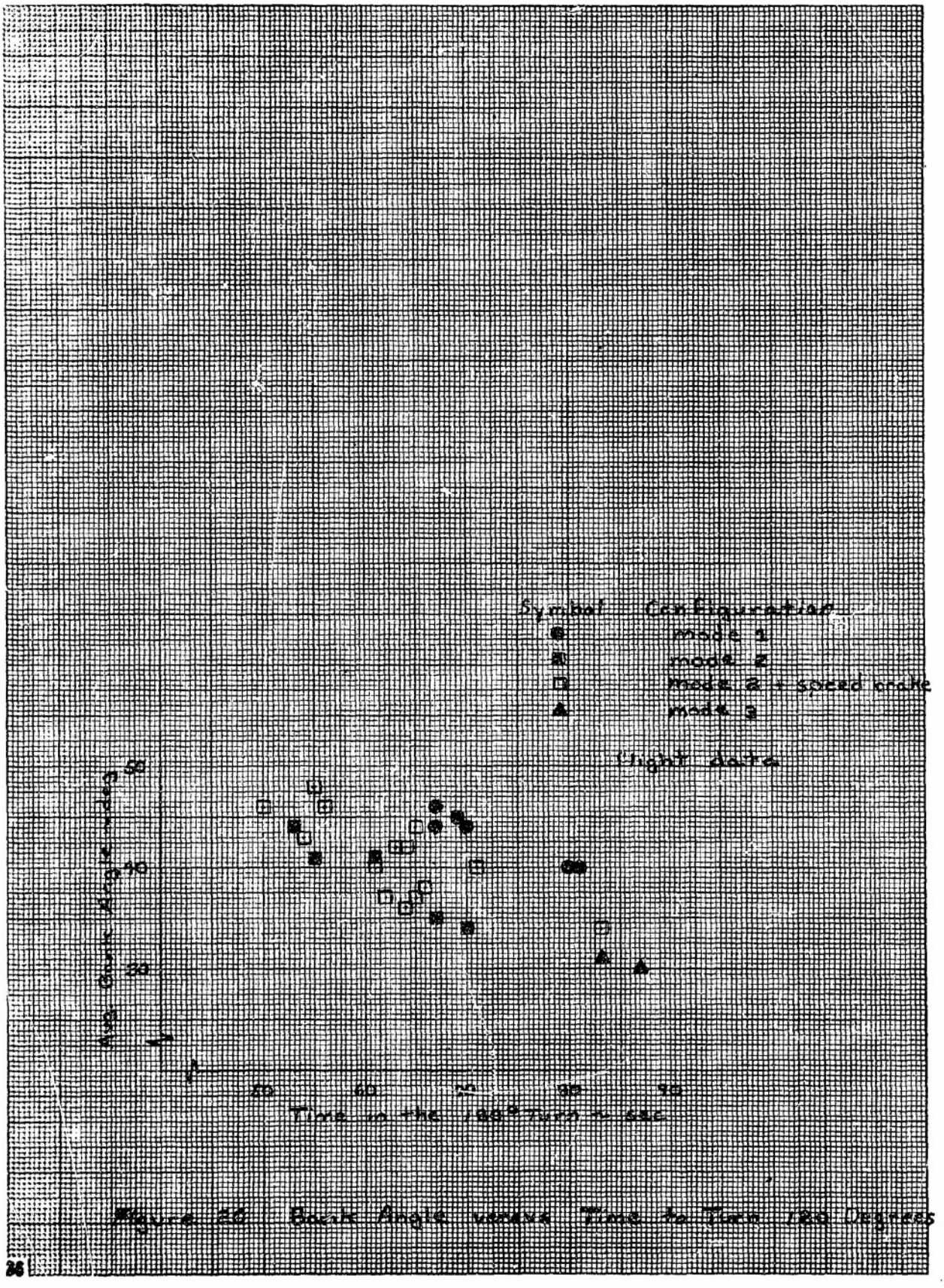

Figure 20. Bank Angle versus Time to Turn 180 Degrees

Final Approach Phase

The altitude at rollout on final varied between 1,910 and 6,510 feet AGL with an average of 3,350 feet for configuration mode 1 and 4,420 feet for configuration modes 2 and 3 (table II). The time on final, defined as the time from the attainment of wings level flight (ϕ <$\pm$10 degrees) to flare initiation varied between 1.0 and 32.4 seconds depending on the airspeed and pilot technique. The average time on final was 7.8 seconds for configuration mode 1 and 16.6 seconds for modes 2 and 3. Although some of these times were short, one must remember that there still remained 22 to 30 seconds of wings level flight in the flare and deceleration prior to touchdown.

The ranges of average final approach airspeeds, flightpath angles, and L/D's without speed brakes are shown in table V along with the glide slope at 4,500 feet MSL. An average airspeed can be computed, because as illustrated in tables II and III, the airspeed varied little between rollout-on-final and flare initiation.

Table V

SUMMARY OF FINAL APPROACH PARAMETERS

Configuration Mode	Airspeed (KCAS)	Flightpath Angle (deg)	Glide Slope @ 4500 ft MSL (deg)	L/D
1	294 to 267	-24.6 to -19.5	-24.5 to -17.5	1.96 to 2.55
2	318 to 278	-18.6 to -14.7	-21.0 to -15.3	2.61 to 3.44
3	297	-16	-16.4 to -15	3.13

The flightpath angle was a parameter associated with the air mass in which the vehicle was flying and was calculated from the L/D. The glide slope was the angle of glide path that terminated on the ground at a fixed point and was calculated from radar data. The piloting task associated with final approach was primarily related to establishing the vehicle on an imaginary glide slope terminating at the aim point.

Figure 21 illustrates that all of the final approaches were made well down the speed-stable front side of the L/D curve. The L/D data points in figure 21 were calculated using flight data from actual approaches and the equations from appendix II. The lines on this figure were obtained from pushover-pullup data maneuvers (reference 4).

The final approach airspeeds of the first few flights (configuration mode 1) were generally less than for the balance of the program. This was the result of low angle of attack handling qualities problems rather than energy management considerations and is discussed in depth in reference 5.

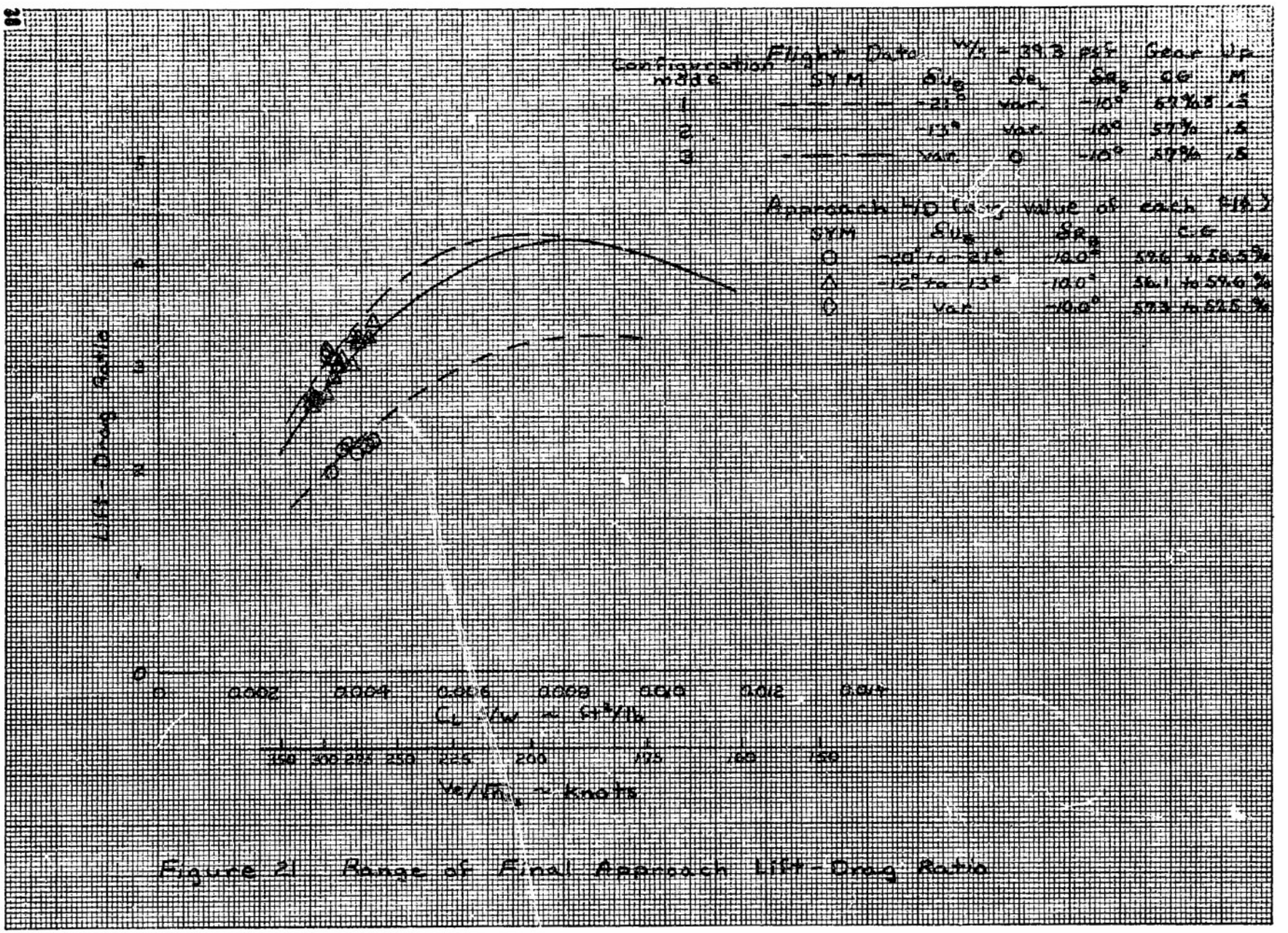

Figure 21 Range of Final Approach Lift - Drag Ratio

Two flights (numbers 17 and 18) were flown in configuration mode 2 using 270 knots as the approach airspeed in preparation for the 270 KIAS upper flap approaches (configuration mode 3). The maximum approach L/D (3.44) in the X-24A program occurred on one of these two flights. This high value of L/D coupled with the low airspeed accounted for the pilot comment that the approach was very flat and he had plenty of time on final. The times on final for these two flights were 32.4 and 20.5 seconds, respectively, as compared to an average of 16.3 seconds for the 300-knot approaches.

Upper Flap Approaches

The maximum subsonic performance potential of the X-24A configuration was achieved with the lower flaps stowed while controlling the vehicle with the upper flaps in pitch and roll (configuration mode 3). Two landings were performed in this configuration to demonstrate the approach and landing capability. Wind tunnel and flight data, reference 6, showed that roll effectiveness with the upper flaps was about twice that of the lower flaps and the pitch effectiveness was increased by a factor of 1.5. Because of the increased sensitivity and the resulting potential longitudinal pilot-induced oscillation (PIO) problem when flying at an airspeed of 300 KIAS with the upper flaps, a final approach airspeed of 270 KIAS was selected.

The two upper flap approaches (configuration mode 3) were flown on flights 19 and 20. These approaches were planned for a 270-KIAS final approach with the pilot option to explore the pitch and roll control sensitivity at higher airspeeds. The average approach airspeed for these flights was 287 KIAS because the pilots did explore the pitch and roll sensitivity at the higher airspeed.

The mechanization of the flight control system was such that the flap bias feature could not be used as a speed brake while controlling the vehicle with the upper flaps. The lack of the speed brake capability made it difficult for the pilots to adjust their aim and touchdown points for accurate landings. The pilots felt that the added energy management provided by the flap bias "speed brake" feature far overshadowed any performance or handling qualities improvements observed during the upper flap approaches, thus the mode 2 configuration was used for all subsequent X-24A landings.

Flare and Landing

Figures 22 to 30 present, in terms of flare initiation airspeed, a summary of various flare parameters, including time from flare initiation to touchdown, gear extension airspeed, flare initiation altitude, and airspeed lost during the flare. It was interesting to note that the time to touchdown (figures 22 and 23) appeared to be independent of the airspeed at flare initiation. This is further confirmed by examining figures 24 and 25 where it is shown that when the flare initiation airspeed was high the gear extension airspeed and the touchdown airspeed were also high. The time for flare was dependent upon the normal acceleration used during the flare (figure 26) and this accounts for most of the scatter in the data of figure 23. Figures 22 and 23 also show the time from gear extension to touchdown. Note, however, that this was the time from pilot

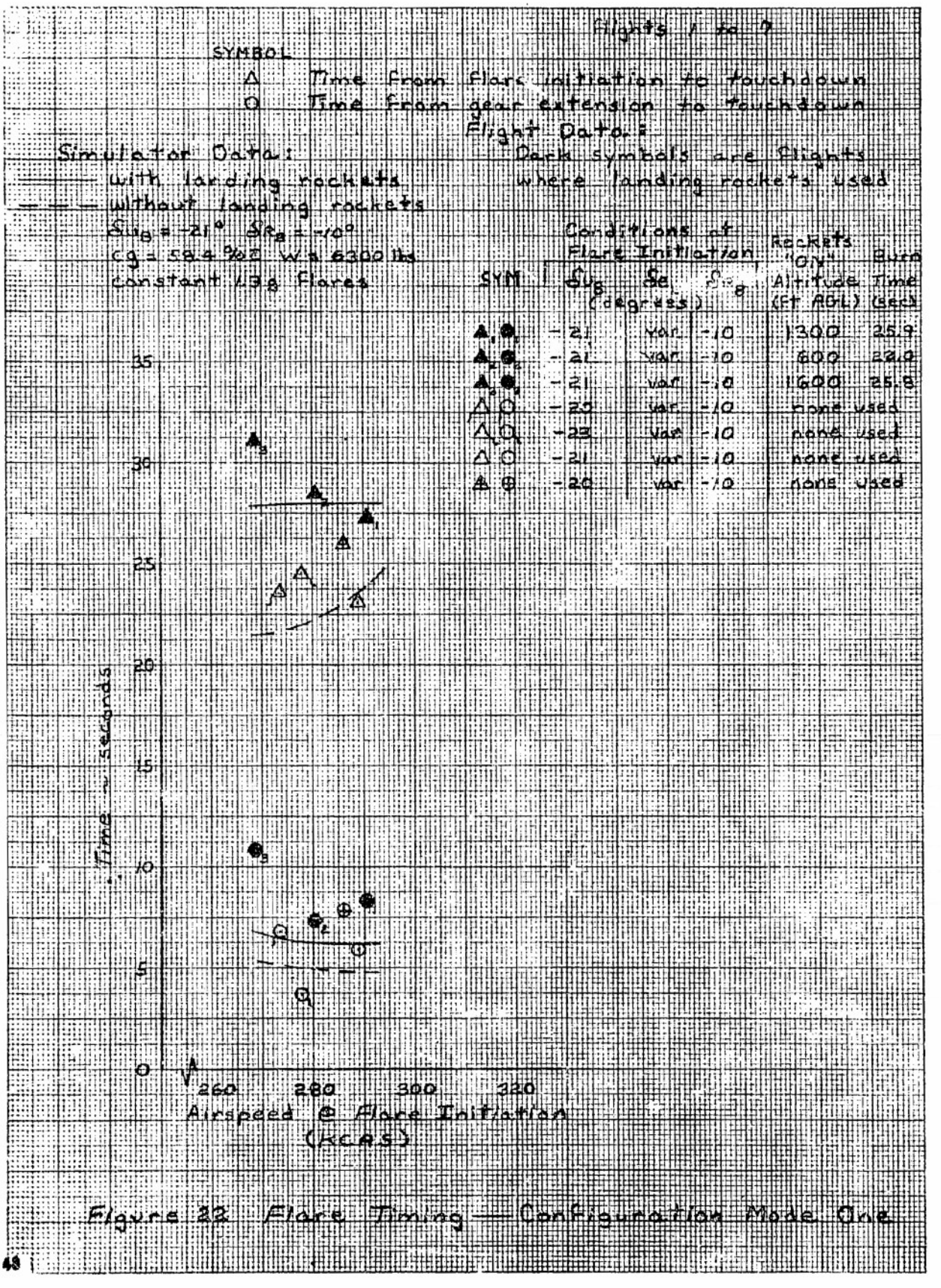

Figure 22 Flare Timing — Configuration Mode One

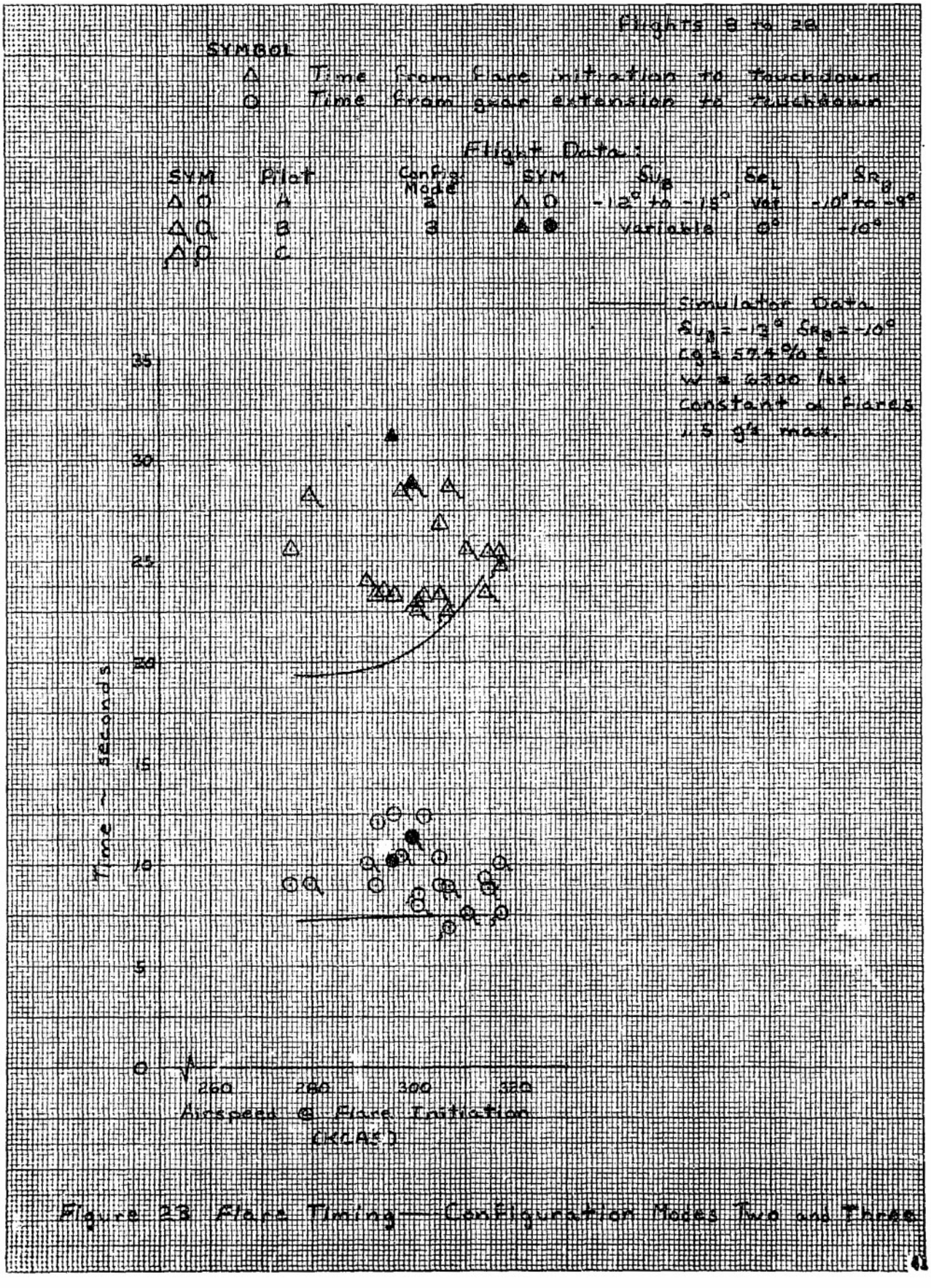

Figure 23 Flare Timing—Configuration Modes Two and Three

Airspeed @ Gear Extension (KCAS)
Gear Speed Limit
Airspeed @ Touchdown (KCAS)
Fine speed limit
Coarse speed limit
Conditions @ Flare Initiation
SYM
Clients
Airspeeds at Gear Extension and Touchdown
Configuration Made One

Figure 24

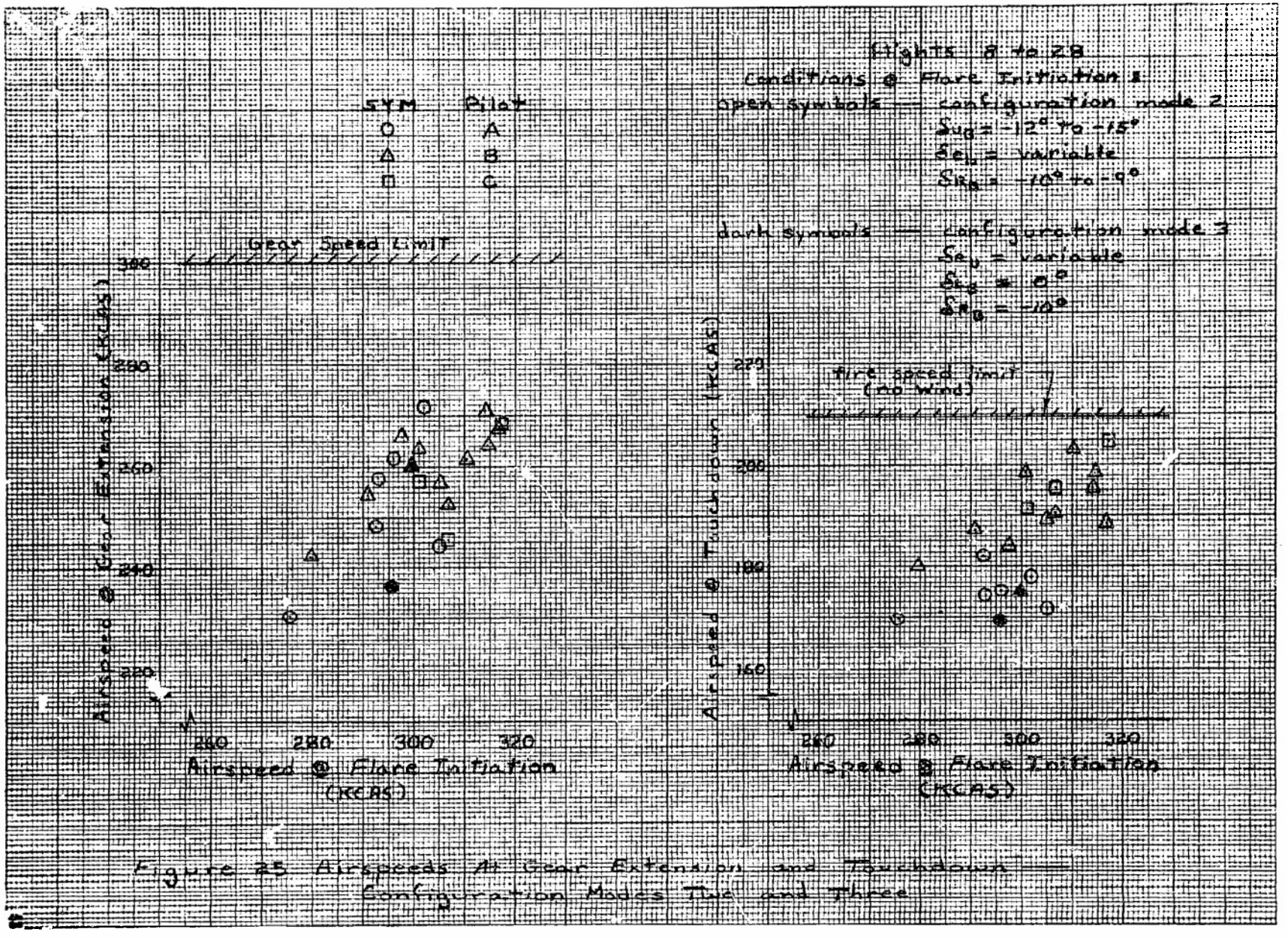

Figure 25 Airspeeds At Gear Extension and Touchdown — Configuration Modes Two and Three

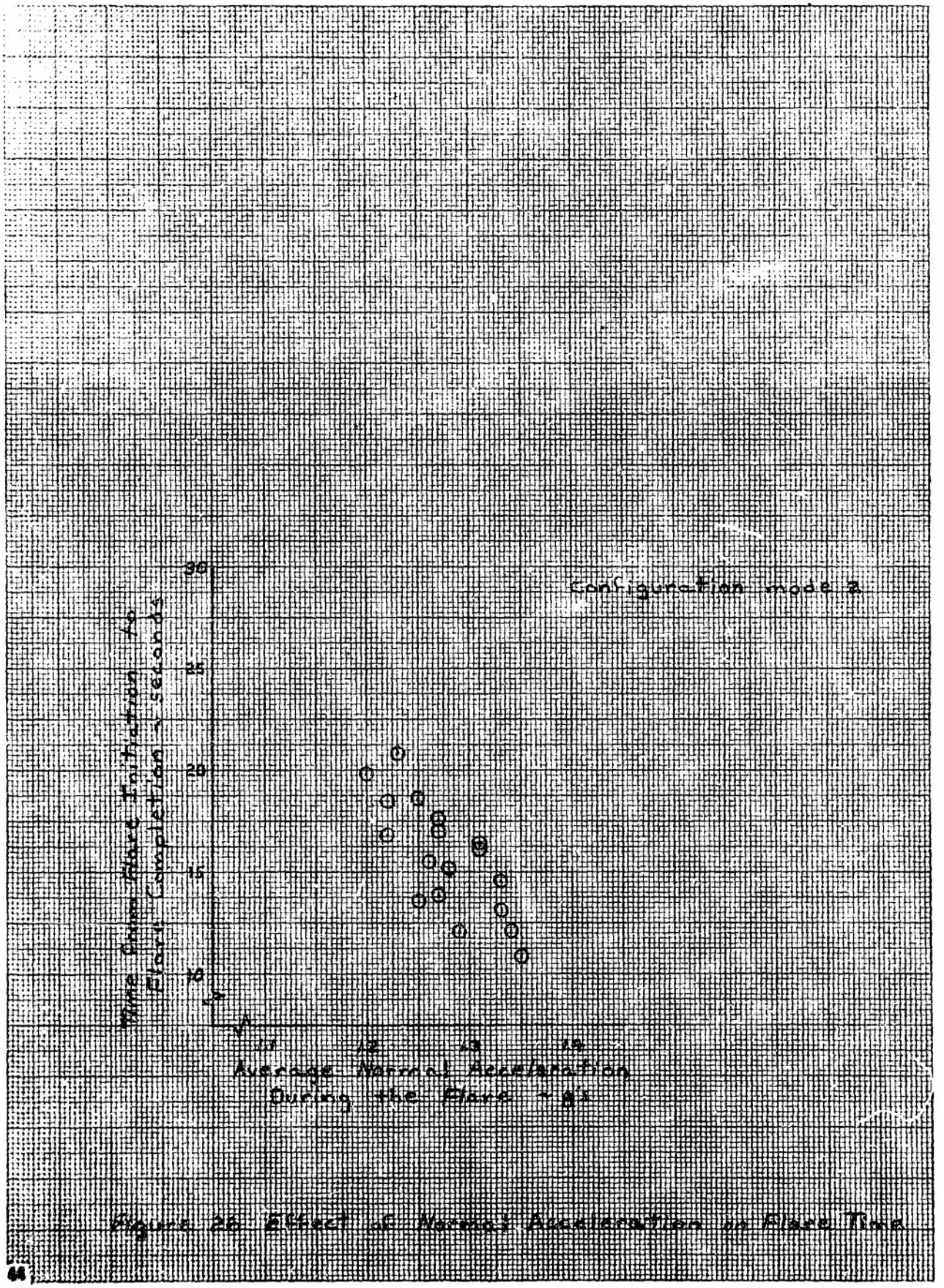

Figure 26 Effect of Normal Acceleration on Flare Time

action (pulled gear handle) to touchdown. To get the time from gear-down-and-locked to touchdown, one must subtract the gear extension time of 1.2 to 1.5 seconds.

Figures 27 and 28 show the flare initiation altitude and figures 29 and 30 are the airspeed lost during the flare where the end of flare was defined as the point at which the sink rate was arrested to 20 feet per second. These parameters generally increased with flare initiation airspeed, as might be expected.

The pilots indicated that their primary cue for flare initiation was altitude. They used an indicated altitude of 800 to 1,200 feet AGL, which was 300 feet below the actual altitude of 1,100 to 1,500 feet AGL due to the position error (lag error was insignificant). Most of the data in figure 28 fell within this altitude band. However, the pilots also indicated that the determination of their flare initiation point was a combination of pilot experience and the interrelation of several factors including sink rate, airspeed, altitude and position relative to the desired preflare aim point.

The flare timing and the flare altitude as determined from an X-24A fixed base simulator study (appendix V) are compared with flight data in figures 22, 23, 27, and 28. In general, the data compared well; however, the simulator flare timing was 2 to 3 seconds shorter than the flight data. The reason for this was that the predicted gear-down drag data were 10 to 20 percent higher than the flight data (reference 4).

Figure 31 summarizes the flare altitude versus the time from flare initiation to touchdown. Also shown on this figure are some boundaries (dashed lines) from reference 10. This reference contains an initial attempt at defining the minimum and maximum requirements for flare and landing of a lifting reentry vehicle. Reference 10 divides the flare timing requirements into two segments: (1) the minimum time from flare initiation to flare completion and (2) the minimum and maximum float time. However, the pilots, who have flown the X-24A and other low to medium L/D lifting body vehicles, feel that it is more meaningful to consider the total time from flare initiation to touchdown rather than considering the time from flare initiation to flare completion and the float time separately. Therefore, the two boundaries from reference 10 have been combined to give the boundaries (dashed lines) presented in figure 31. These boundaries are for class IV lifting reentry vehicles with level 2 flying qualities, where level 2 was defined in reference 10 as "Flying qualities adequate to accomplish the mission flight phase, but some increase in pilot workload or degradation in mission effectiveness, or both, exists." Class IV was defined as: "Light to medium weight, medium to high cross range based on hypersonic $(L/D)_{max}$ and normal load factor."

The total time from flare initiation to touchdown was considered because the primary piloting task associated with the flare is to adjust the sink rate to an acceptable touchdown value, this does not necessarily require any minimum level attitude float time as required by reference 10. In the case of the X-24A, the sink rate did not reach a value of five feet per second (essentially a level attitude) until three to seven seconds prior to touchdown. This was of no concern to the X-24A pilots, in fact, they commented that they were impressed with the way the vehicle handled near the ground. The pilots were more concerned about having

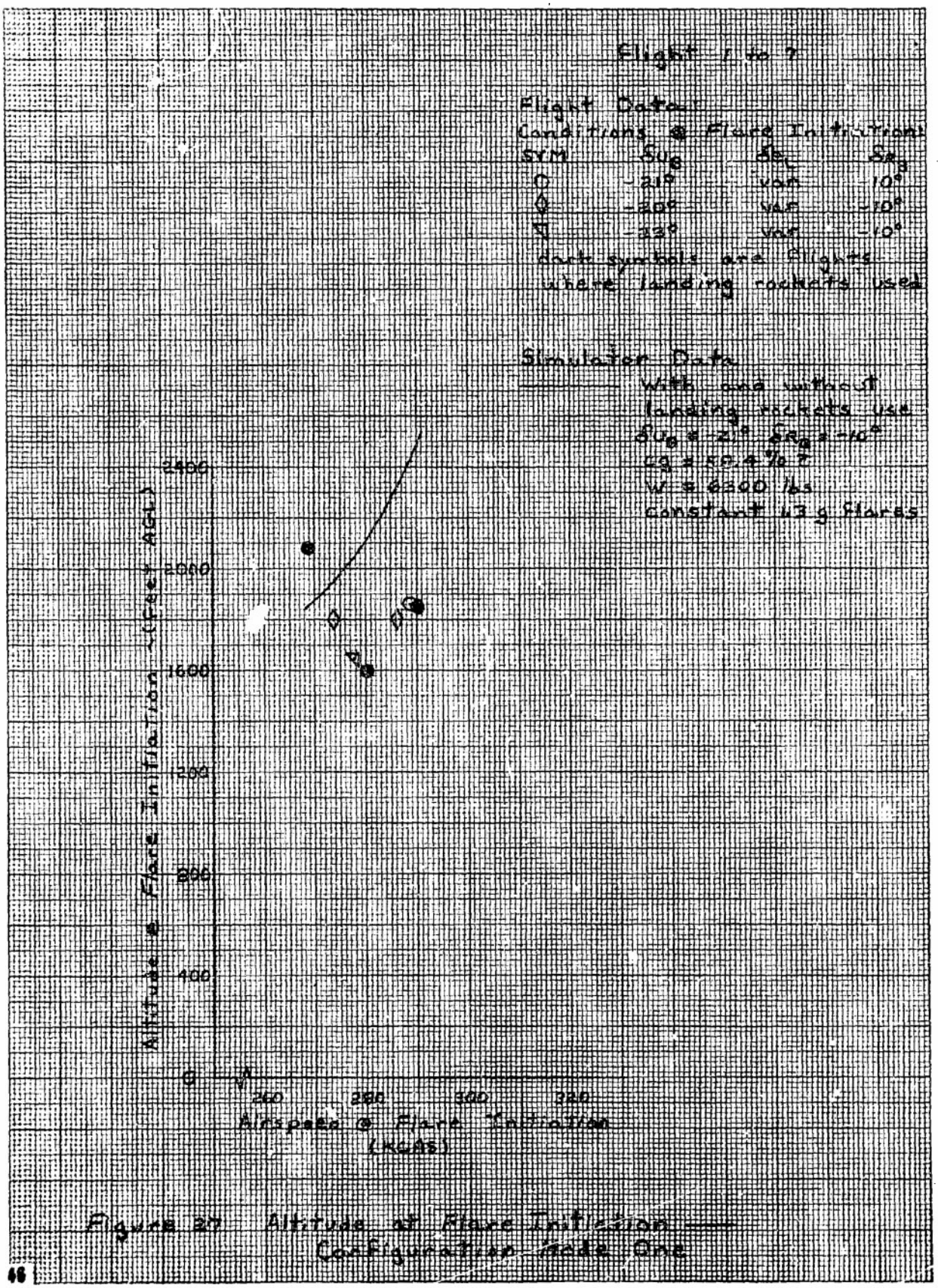

Figure 27 Altitude at Flare Initiation — Configuration Code One

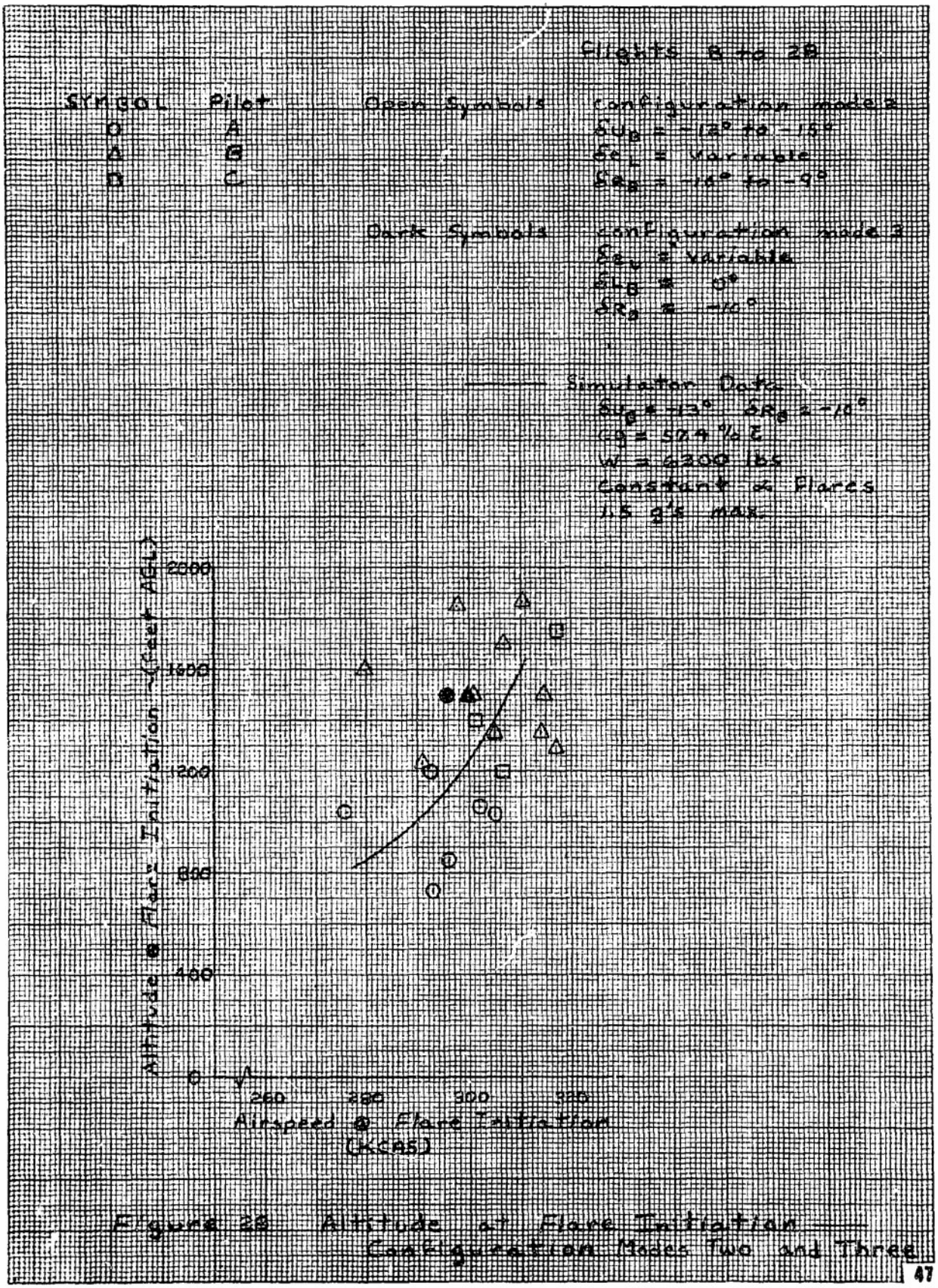

Figure 28 Altitude at Flare Initiation — Configuration Modes Two and Three

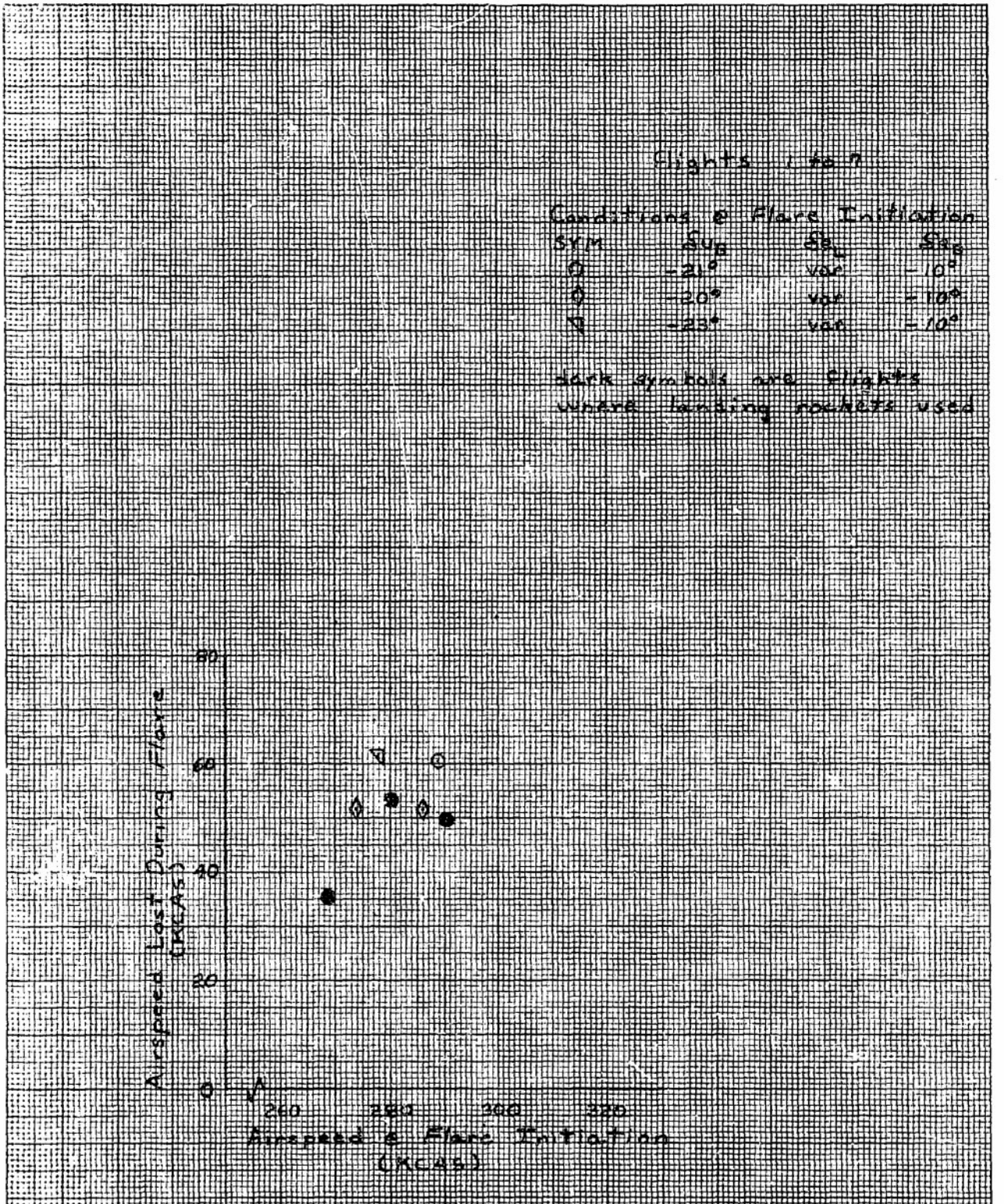

Figure 29 Airspeed Lost During The Flare Configuration Mode One

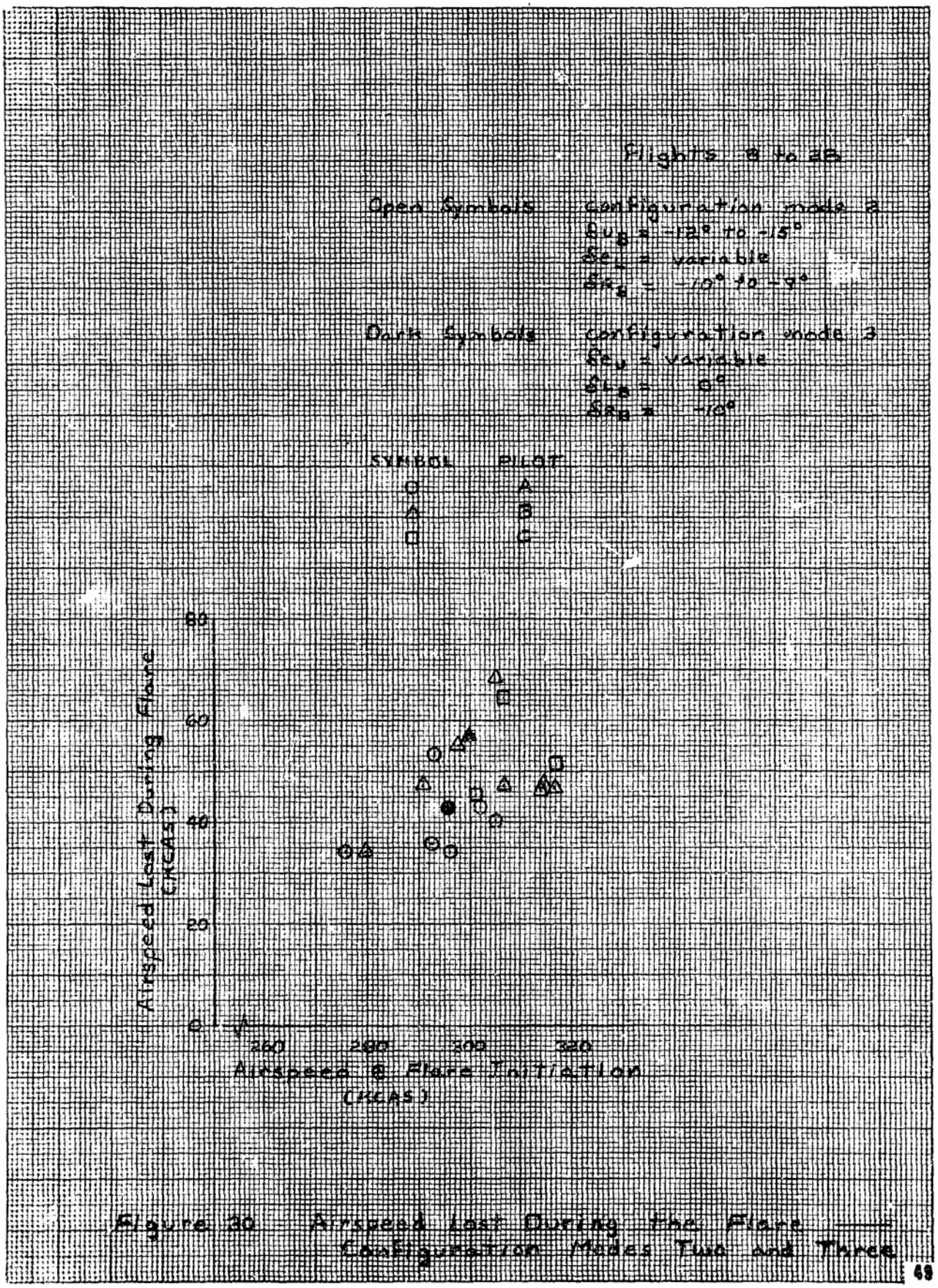

Figure 30 Airspeed Lost During the Flare — Configuration Modes Two and Three

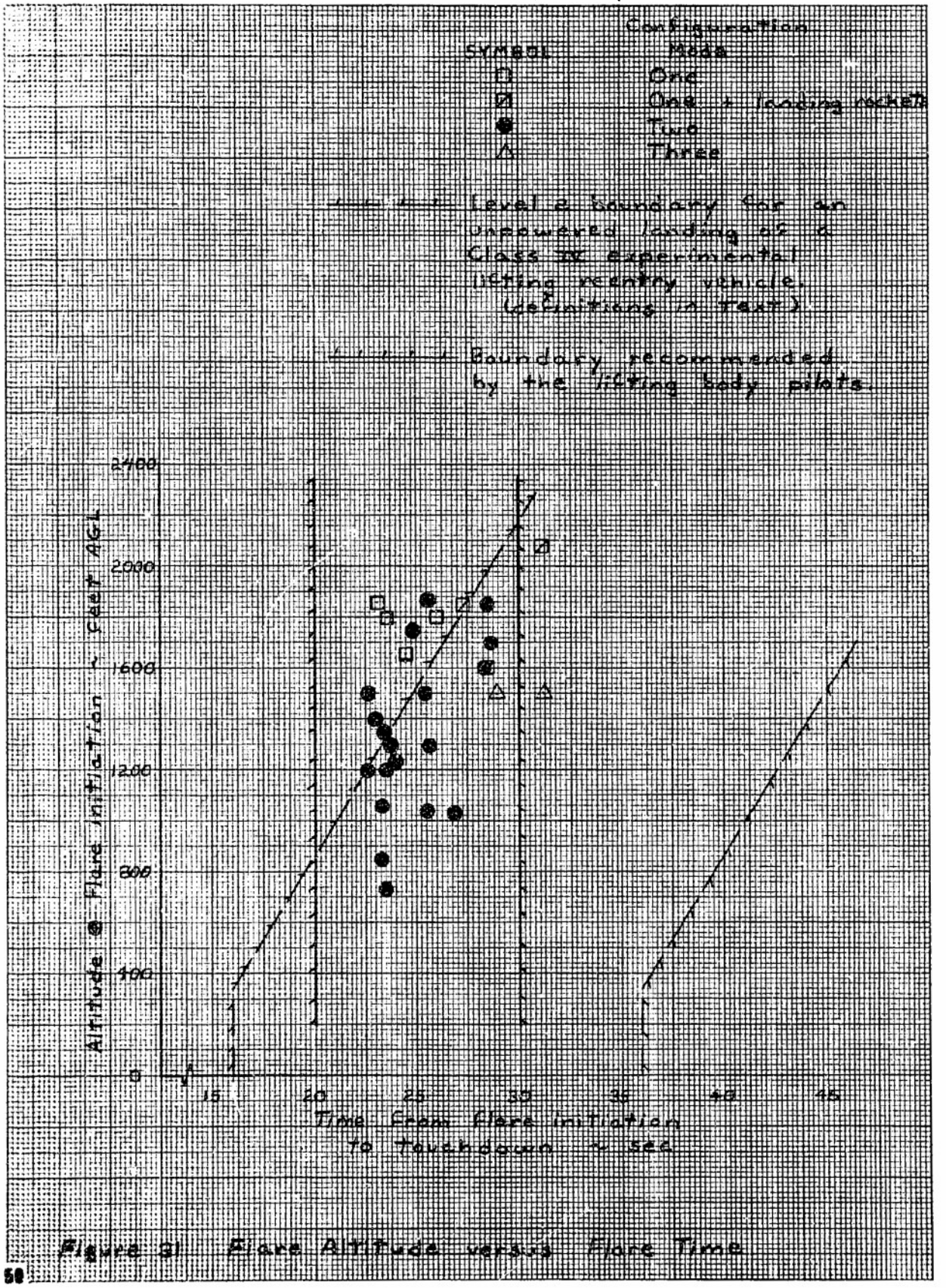

Figure 31 Flare Altitude versus Flare Time

adequate total time from flare initiation to touchdown and energy to accomplish the tasks of arresting the sink rate, extending the landing gear, recovering from the gear trim change, and adjusting the sink rate to an acceptable value prior to touchdown. These factors established a minimum time from flare initiation to touchdown. A maximum time was dictated by the fact that it is more difficult to judge the touchdown point as the flare time increases. The X-24A pilots who have flown in other lifting body vehicles suggest that a total time from flare initiation to touchdown of 20 seconds minimum to 30 seconds maximum is adequate with 24 seconds as an optimum for a medium L/D lifting body vehicle. These minimum and maximum values are considered independent of the flare altitude and are plotted as the solid line boundaries in figure 31.

The distance traveled after flare initiation was determined to a large extent by the energy at flare initiation (figure 32). That is to say that the touchdown point was largely determined by the airspeed and altitude at flare initiation. This distance was also a small inverse function of the average flare normal acceleration and touchdown airspeed and a weak function of flightpath angle at flare initiation. The winds would certainly affect this distance also.

Figures 33 and 34 show that the true angle of attack at touchdown, generally increased with decreasing touchdown airspeed, as expected. In general the touchdown angles of attack varied from 12 to 16 degrees in configuration mode 1 and from 9 to 15 degrees in configuration modes 2 and 3. Also shown for reference in these figures is the angle of attack for 1 g trimmed flight as predicted by the wind tunnel tests. Further discussion of the wind tunnel and flight gear-down data is contained in the section titled Landing Gear Characteristics.

Figure 35 was the sink rate at touchdown as recorded by the Honeywell radar altimeter (appendix I). (There were only a few flights in which this quantity was valid. The unit usually did not operate, or the data were not accurately readable.) This parameter appeared to be independent of touchdown airspeed and was usually less than four feet per second. Figure 35 also contains a touchdown limit boundary as defined by the landing gear/carry-through structural limits and the tire limits.

All the flare parameters: flare initiation airspeed, gear extension airspeed, touchdown airspeed, normal acceleration, and flightpath angle are complexly interrelated as to their effect on the flare altitude, distance traveled, flare timing, and airspeed lost during the flare. This interrelation accounts for the data scatter of figures 22 to 34.

Although the flightpath angle at flare initiation varied between -15 and -25 degrees, depending on the configuration, the pilots commented that the flares were quite comfortable to perform. The high airspeeds associated with these steep approaches provided ample "g" capability for the flare and sufficient float time after flare completion/gear extension to provide for some margin for error. As the flare initiation airspeed decreased, the determination of the flare initiation altitude became more critical because less time remained after flare completion for corrections.

The pilots felt that the X-24A had a very mild flare compared to that of the other lifting body vehicles, and it seemed to flare more quickly especially in configuration modes 2 and 3. In these configurations

the pilots commented that the vehicle seemed to flare itself, there was no conscious flare maneuver, but rather just a slight easing back on the stick. One of the reasons for these comments can be seen by comparing the lift curve slope (C_{L_α}) of the three lifting body vehicles: the X-24A had a C_{L_α} of 0.024 per degree (reference 4) and the M2-F2 and HL-10 had C_{L_α}'s of 0.019 and 0.021 per degree, respectively (references 11 and 12). That is, the "g" available from a small α change in the X-24A was greater than that for the other two lifting bodies.

In summary, a typical X-24A flare in configuration mode 1 without the use of the landing rockets was initiated at an airspeed of 282 KCAS and an altitude of 1,820 feet AGL. The airspeed lost was 54.6 knots and the landing gear was extended at an airspeed of 224 KCAS at 6.8 seconds before touchdown. Touchdown was at 175 KCAS and an angle of attack of 14.8 degrees, 24 seconds after flare initiation. A typical X-24A flare in configuration mode 2 was initiated at an airspeed of 301 KCAS and an altitude of 1,350 feet AGL. The airspeed lost was 47 knots and the gear was extended at 256 KCAS at 9.6 seconds before touchdown. Touchdown was at 186 KCAS and an angle of attack of 11.9 degrees, 24.8 seconds after flare initiation.

There were no appreciable differences between the flares in configuration modes 2 and 3 other than that the time from flare initiation to touchdown was 30 seconds for mode 3 versus 24.8 seconds for mode 2. This was due partially to the fact that the average normal acceleration (table VI) used during the flares in configuration mode 3 (flights 19 and 20) was less than that used with mode 2. Also, the L/D for configuration mode 3 was one-quarter of an L/D greater than for mode 2.

The lower flare initiation airspeeds of configuration mode 1 were a result of the low angle-of-attack handling qualities problem on those flights. The lower flare initiation airspeed combined with the larger airspeed loss during flare for configuration mode 1 resulted in lower gear extension speeds than for configuration mode 2 landings. The same comments hold true for the differences in average touchdown airspeeds for configuration modes 1 and 2.

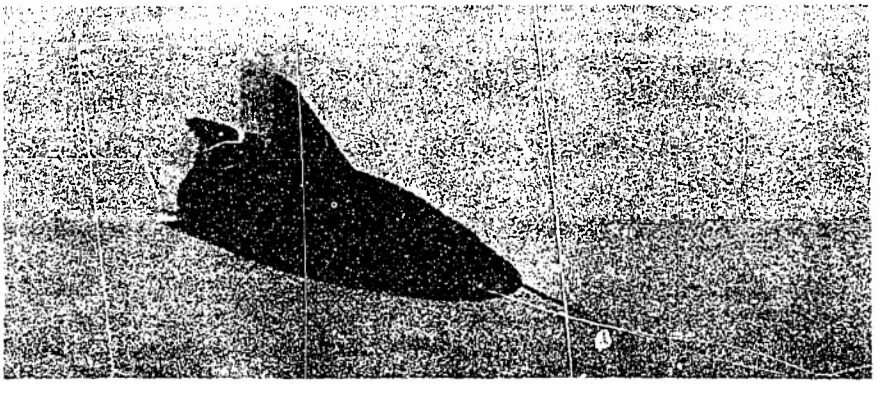

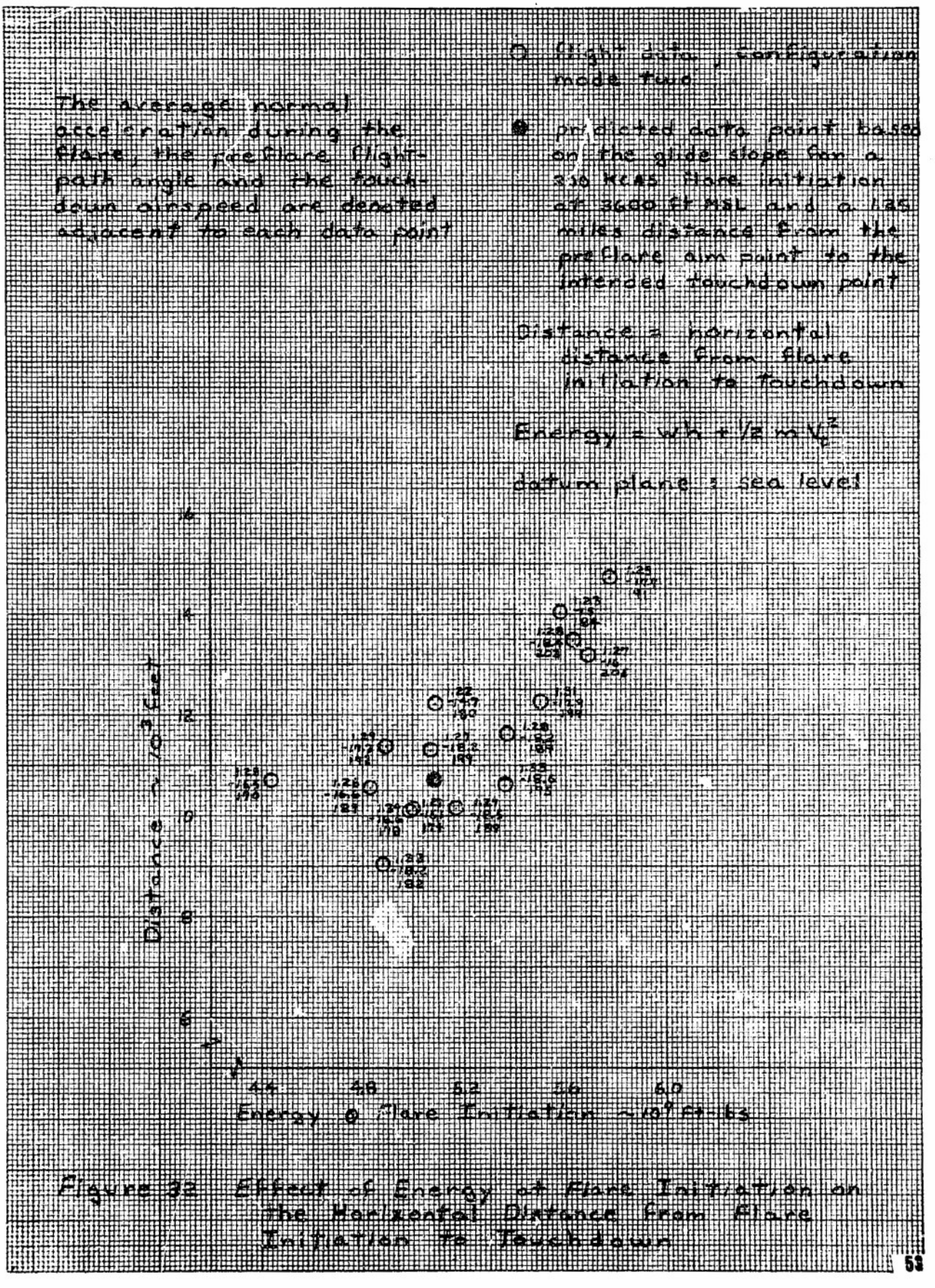

Figure 32 Effect of Energy at Flare Initiation on the Horizontal Distance from Flare Initiation to Touchdown

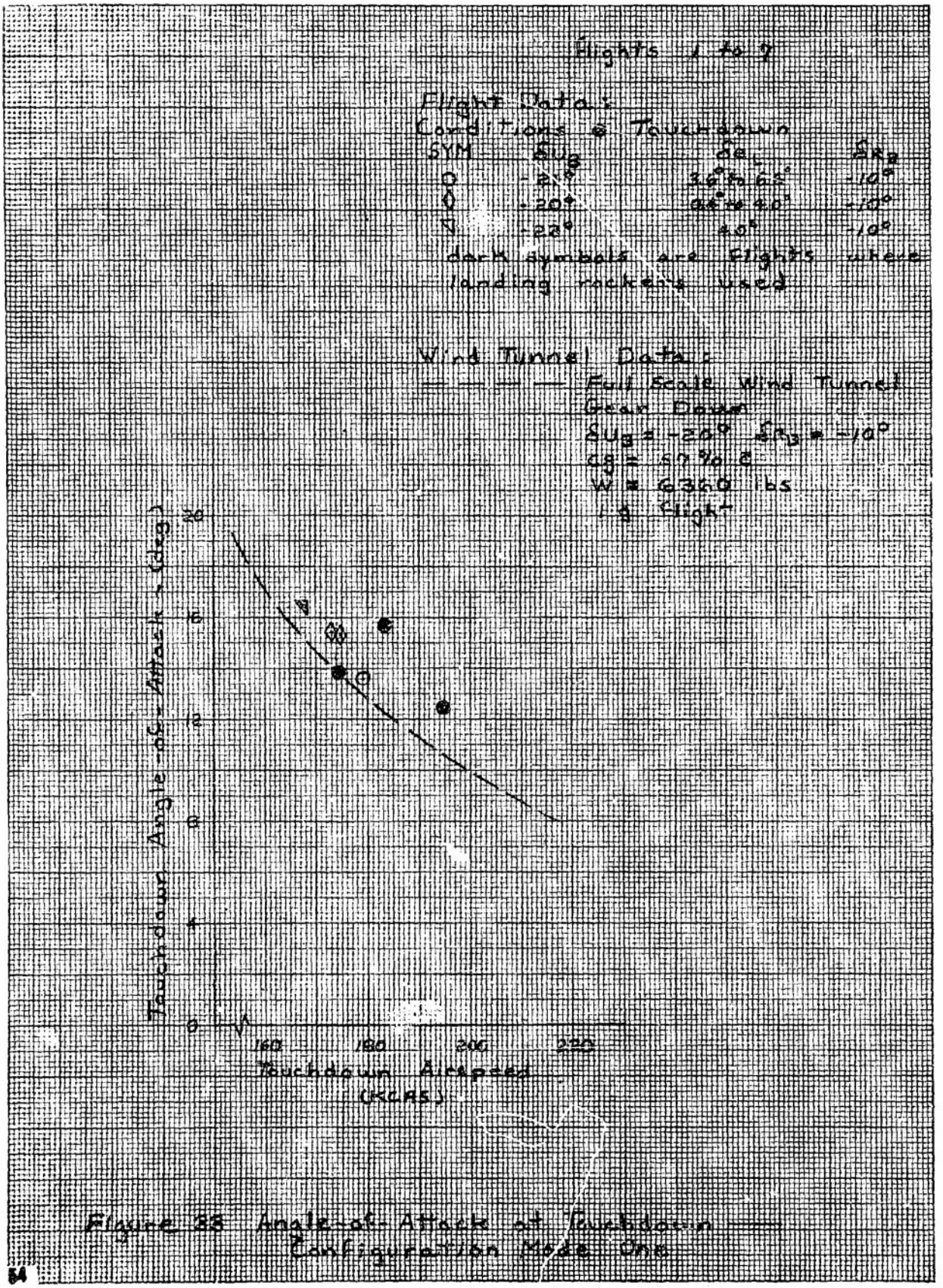

Figure 38 Angle-of-Attack at Touchdown — Configuration Mode One

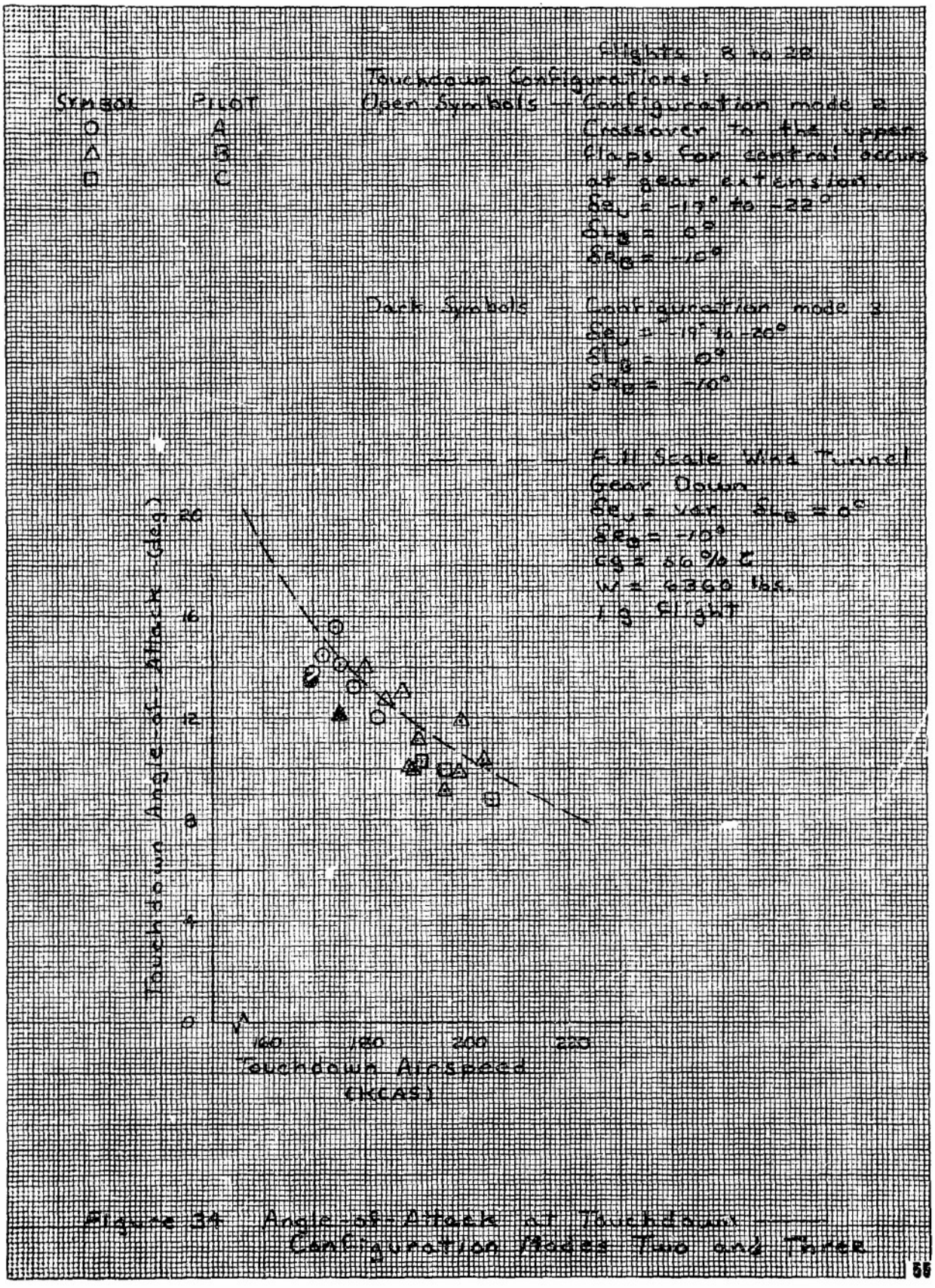

Figure 34 Angle-of-Attack at Touchdown — Configuration Modes Two and Three

Figure 25. Touchdown Sink Rate

Flare Technique

All of the X-24A landings were reviewed in an attempt to isolate a repeatable pattern in the piloting technique being used. This information will be useful in establishing the flare characteristics of future lifting reentry vehicles. During the X-24A program the flare maneuvers could be divided into two basic flare techniques:

1. A constant n_{z_b} or a constant-rate-of-change-in-angle-of-attack ($\dot{\alpha}$) flare.

2. A constant-angle-of-attack flare.

Referring to table VI, it is significant to note that the constant n_{z_b} flare was generally associated with the lower L/D configurations of mode 1. The constant α flare was generally associated with the higher L/D configurations of modes 2 and 3.

Table VI

FLARE TECHNIQUE

Flight No.	Type of Flare Maneuver	Upper Flap During Flare (deg)	Maximum Normal Acceleration During Flare (g's)	Average Normal Acceleration During Flare (g's)
1	constant n_{z_b}, $\dot{\alpha}$	-21	1.40*	1.30
2	constant n_{z_b}, $\dot{\alpha}$	-21	1.42	1.20
3	constant α	-21	1.45	1.23
4	constant n_{z_b}, $\dot{\alpha}$	-20	1.40	1.30
5	constant n_{z_b}, $\dot{\alpha}$	-23	1.35	1.25
6	combination of constant α and n_{z_b}	-21	1.49	1.33
7	constant n_{z_b}, $\dot{\alpha}$	-20	1.33	1.25
8	constant α	-12	1.43	1.29
9	constant α	-13	1.50	1.31
10	constant α	-13	1.50	1.35
11	constant α	-13	1.60	1.33
12	combination of constant n_{z_b} and α	-13	1.60	1.34
13	constant α	-13	1.48	1.28
14	constant α	-13	1.35	1.26
15	constant α	-13	1.38	1.27
16	constant α	-12	1.50	1.31
17	constant α	-12	1.40	1.25
18	constant n_{z_b}, $\dot{\alpha}$	-12	1.30	1.22
19	constant α (2 steps)	var	1.45	1.20
20	constant α (2 steps)	var	1.40	1.22
21	constant α	-13	1.40	1.27
22	constant α	-15	1.60	1.33
23	constant α (2 steps)	-13	1.25	1.23
24	constant α	-13	1.47	1.31
25	constant α	-13	1.35	1.25
26	constant α	-13	1.40	1.27
27	constant α	-13	1.55	1.27
28	constant α (2 steps)	-13	1.45	1.28

*Minimum one second duration.

Figure 36 is a time history of a constant n_{z_b} flare in configuration mode 1. In this type of flare maneuver, the pilot continued to pull back on the stick throughout the flare as the speed decreased, resulting in a constant $\dot{\alpha}$ while n_{z_b} remained approximately constant. The average values of n_{z_b} used during this type of X-24A flare were from 1.20 to 1.30 g's.

Figure 37 is a time history of a constant α flare in configuration mode 2. For this type of flare maneuver the pilot pulled rapidly to some initial value of normal acceleration and then held the stick relatively fixed (constant α) while allowing the normal acceleration to bleed off as airspeed decreased. The values of the maximum normal acceleration obtained during these X-24A flares were from 1.3 to 1.6 g's.

Figure 38 is a time history of a constant α flare in configuration mode 3. The two flares performed with this configuration were both constant α flares, but there were two distinct α steps.

It should be pointed out that the X-24A flares were not programmed maneuvers. The pilots did what they intuitively felt was necessary to break the descent and bring the vehicle to a safe horizontal landing.

The three X-24A pilots used the same basic flare techniques; however, as shown in figures 23, 25, 28, 30, and 34, pilot A started his flares at a lower altitude and airspeed than the other pilots. Also, he landed at slower speeds, hence, the touchdown angles of attack for his flights were higher than the average, and the time from gear extension to touchdown was longer.

THIS PAGE LEFT BLANK FOR PRESENTATION PURPOSES

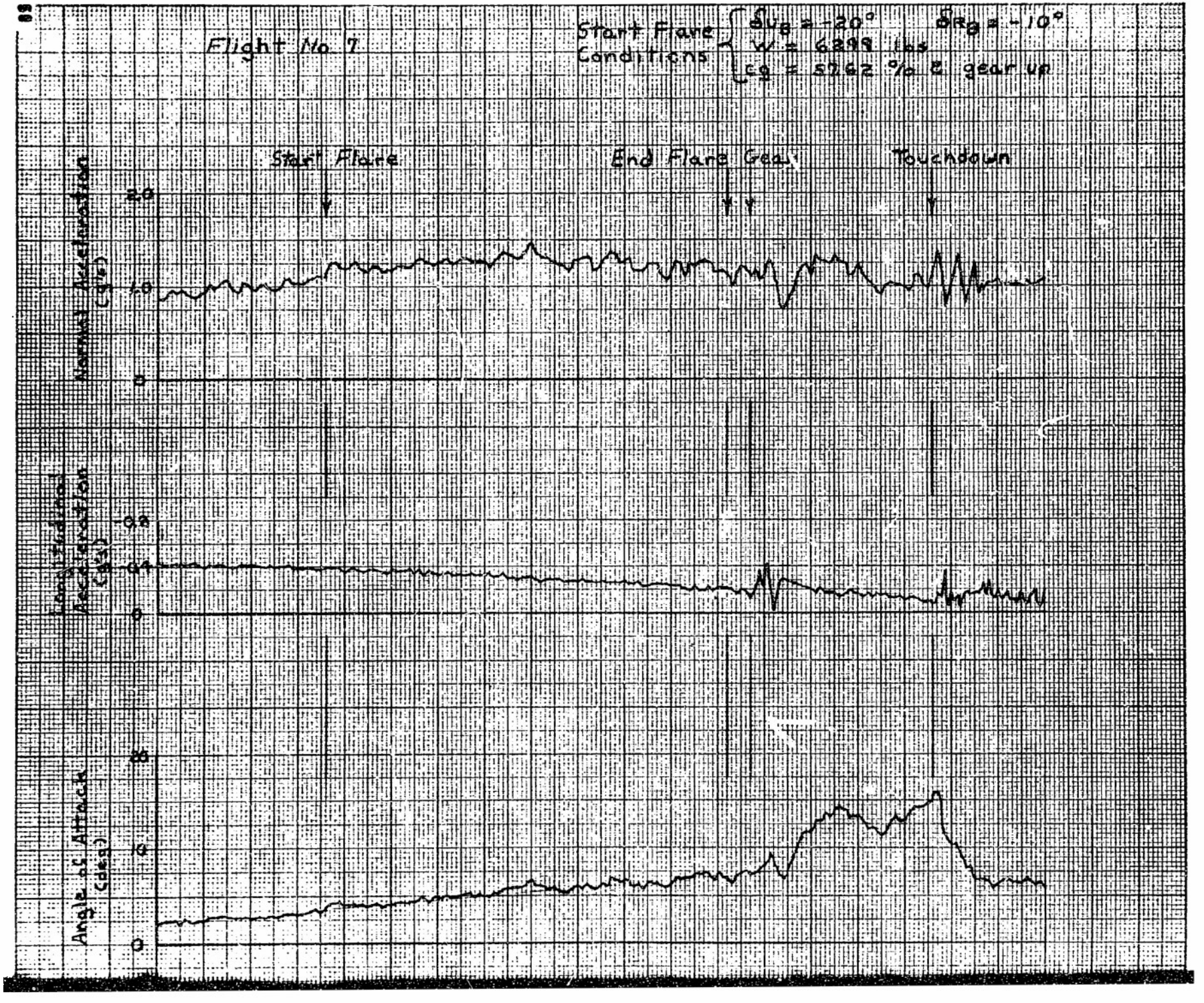
Flight No. 7
Start Flare Conditions
$\delta_{UB} = -20°$
$\delta_{RB} = -10°$
$W = 6299$ lbs
$c.g. = 52.62$ % $\bar{c}$ gear up
Start Flare
End Flare Gear
Touchdown
Normal Acceleration (g's)
2.0
1.0
0
Lateral Acceleration (g's)
-0.2
-0.4
0
Angle of Attack (deg.)
20
10
0

Figure 36. Flare and Landing Time History — Calibration Mode One

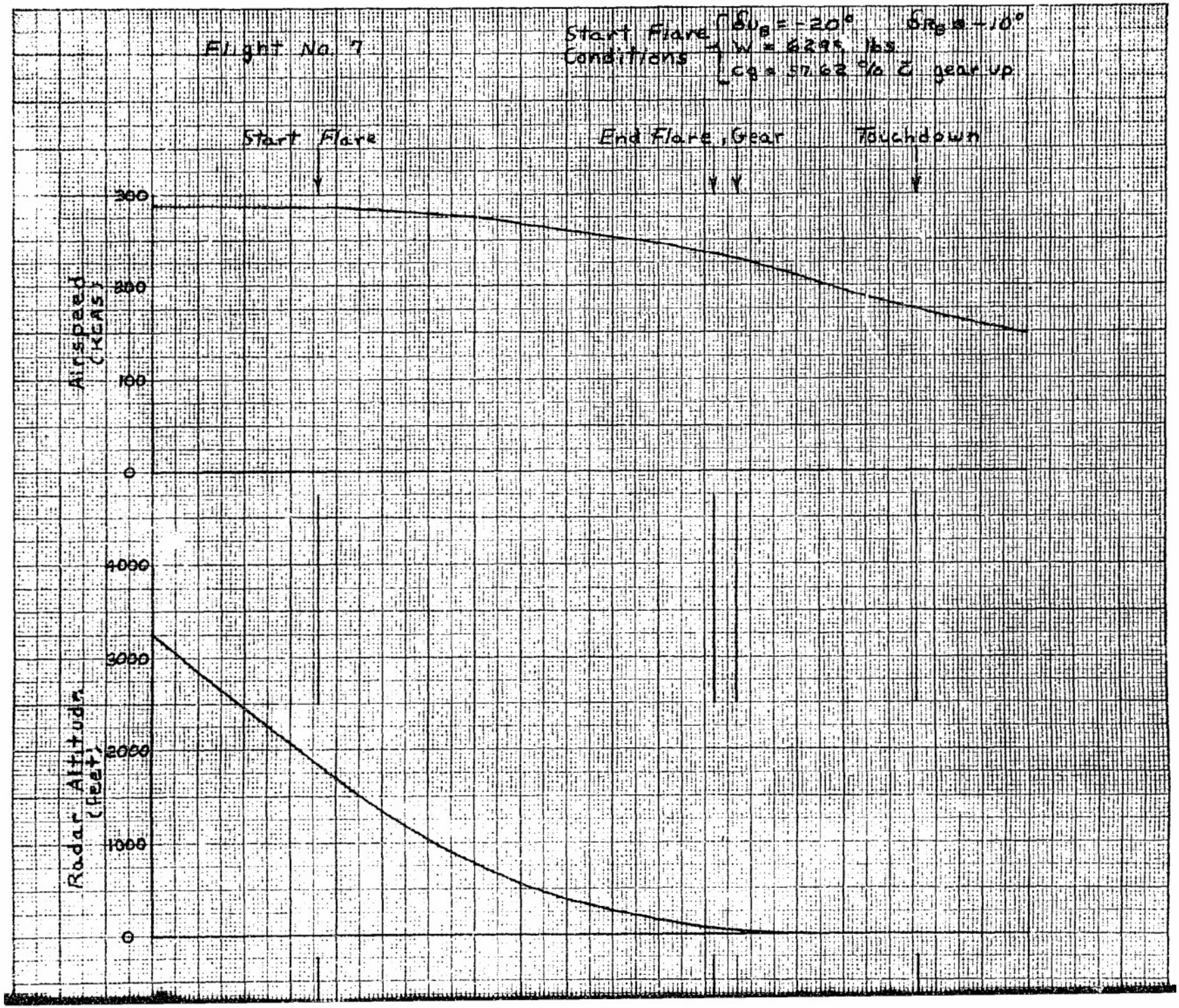
Flight No. 7
Start Flare Conditions
$\delta_{us} = -20°$
$\delta_{RS} = -10°$
W = 6295 lbs.
cg = 27.62 % $\bar{c}$ gear up
Start Flare
End Flare, Gear
Touchdown
Airspeed (KCAS)
300
200
100
0
Radar Altitude (feet)
4000
3000
2000
1000
0

Figure 3-6. Typical Landing Path Parameters Configuration Mode One

Flight No 8
Start Flare
Conditions
End Flare
Touchdown
Angle of Attack (deg)
Longitudinal Acceleration (g's)
Normal Acceleration (g's)

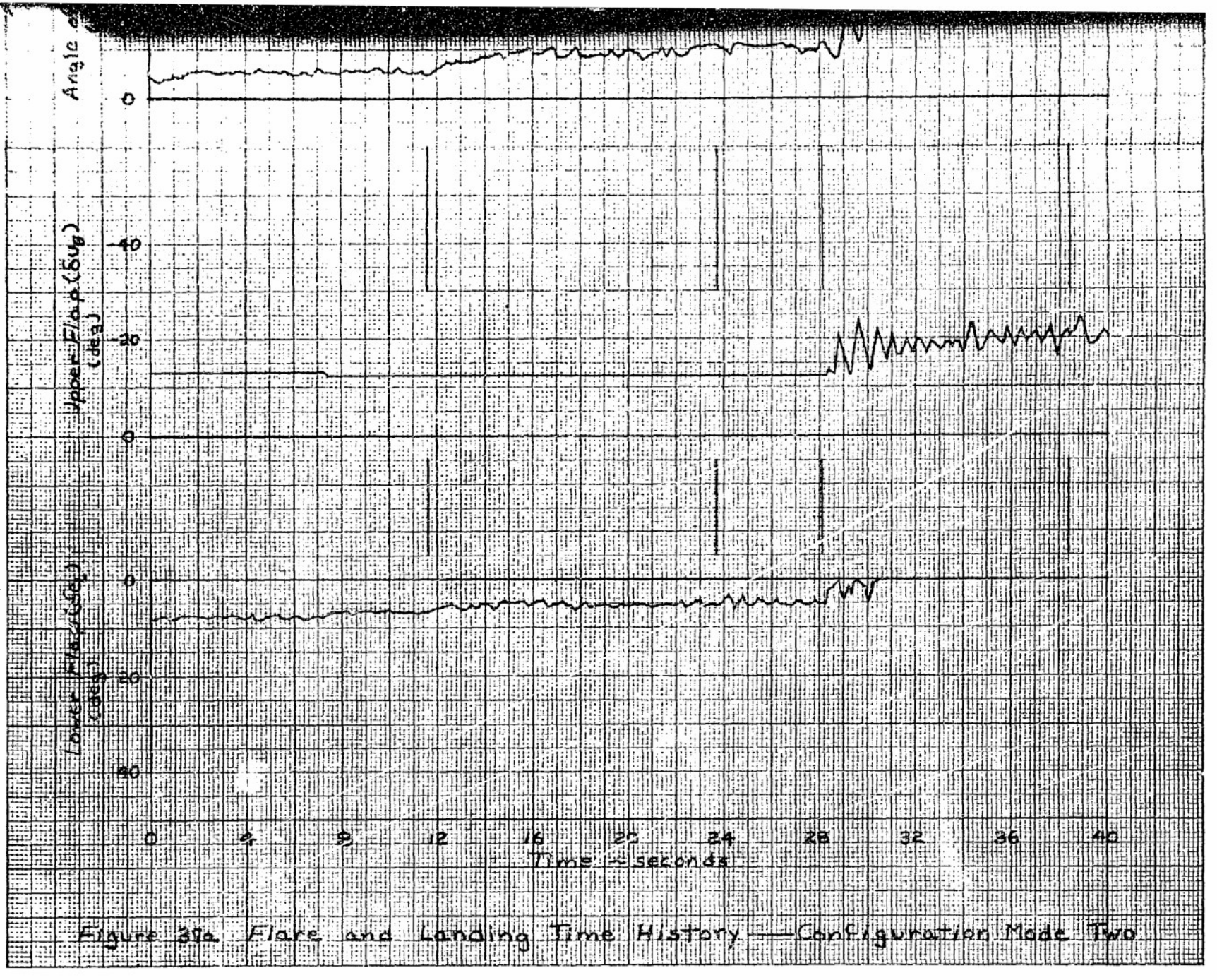

Figure 31a. Flare and Landing Time History — Configuration Mode Two

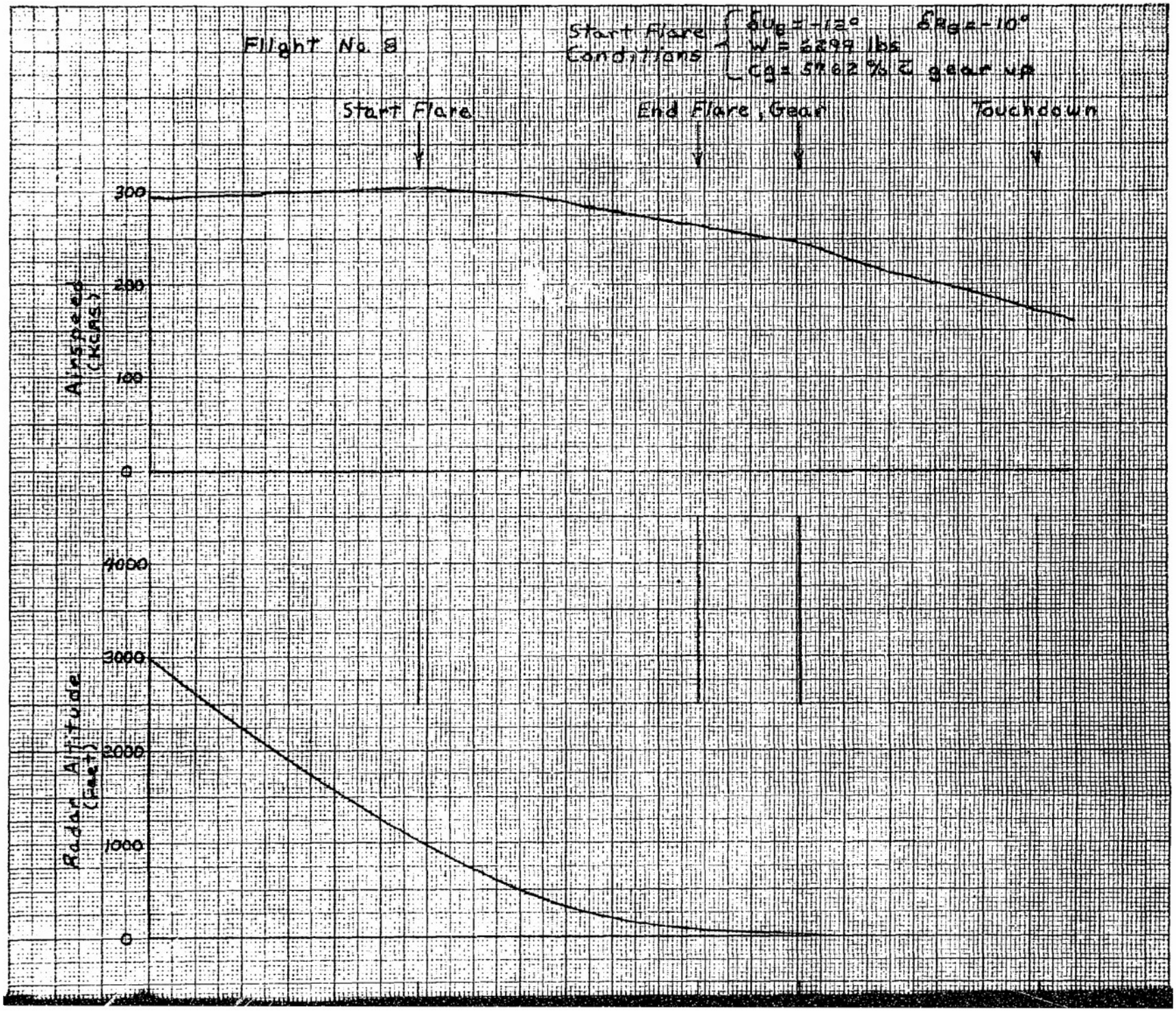
Flight No. 8
Start Flare Conditions
$\delta_{HS} = -12°$
$\delta_{Rud} = -10°$
W = 6299 lbs
cg = 57.62 % ℄ gear up
Start Flare
End Flare, Gear
Touchdown
Airspeed (Kcas)
300
200
100
0
Radar Altitude (Feet)
4000
3000
2000
1000
0

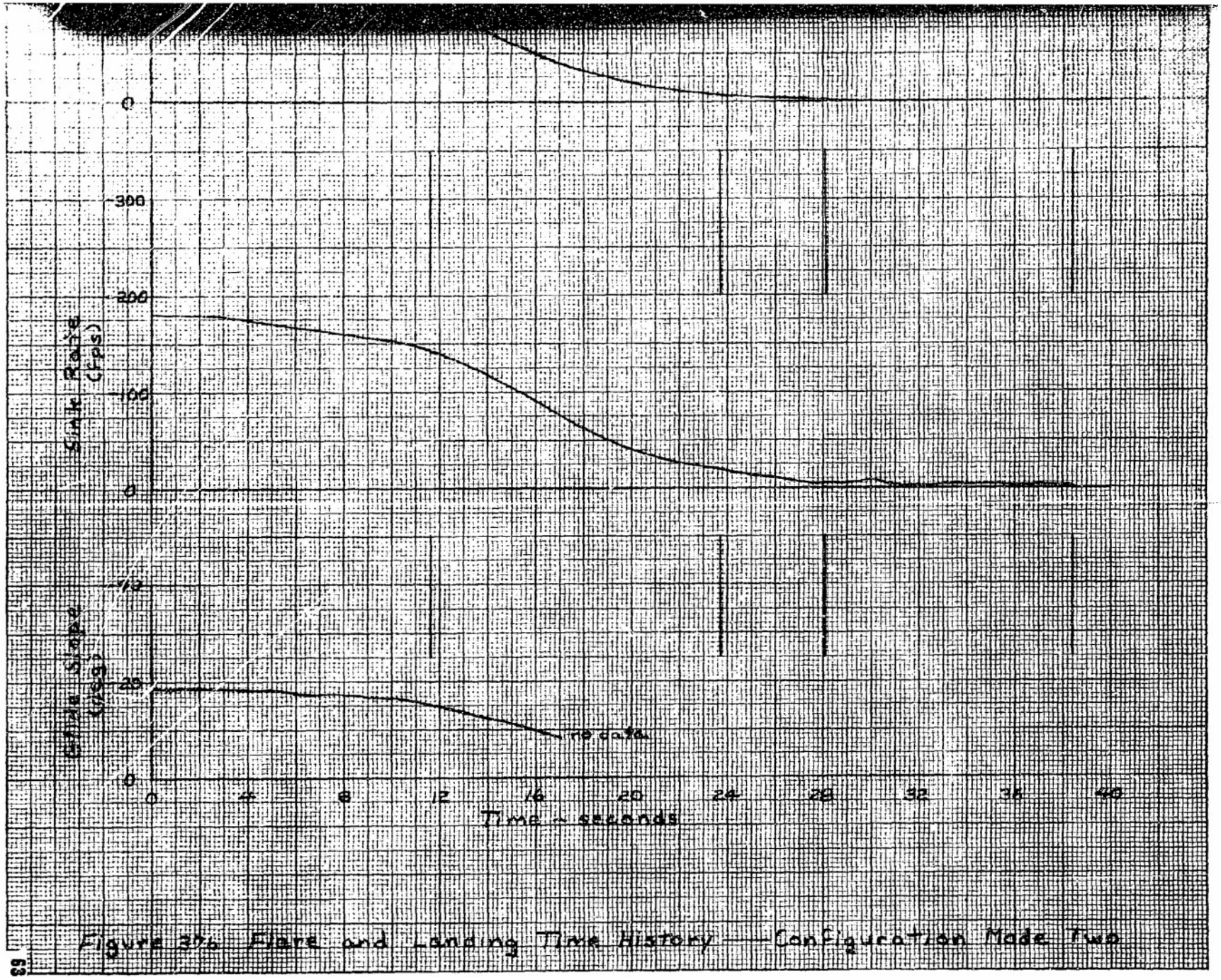

Figure 37b Flare and Landing Time History ——Configuration Mode Two

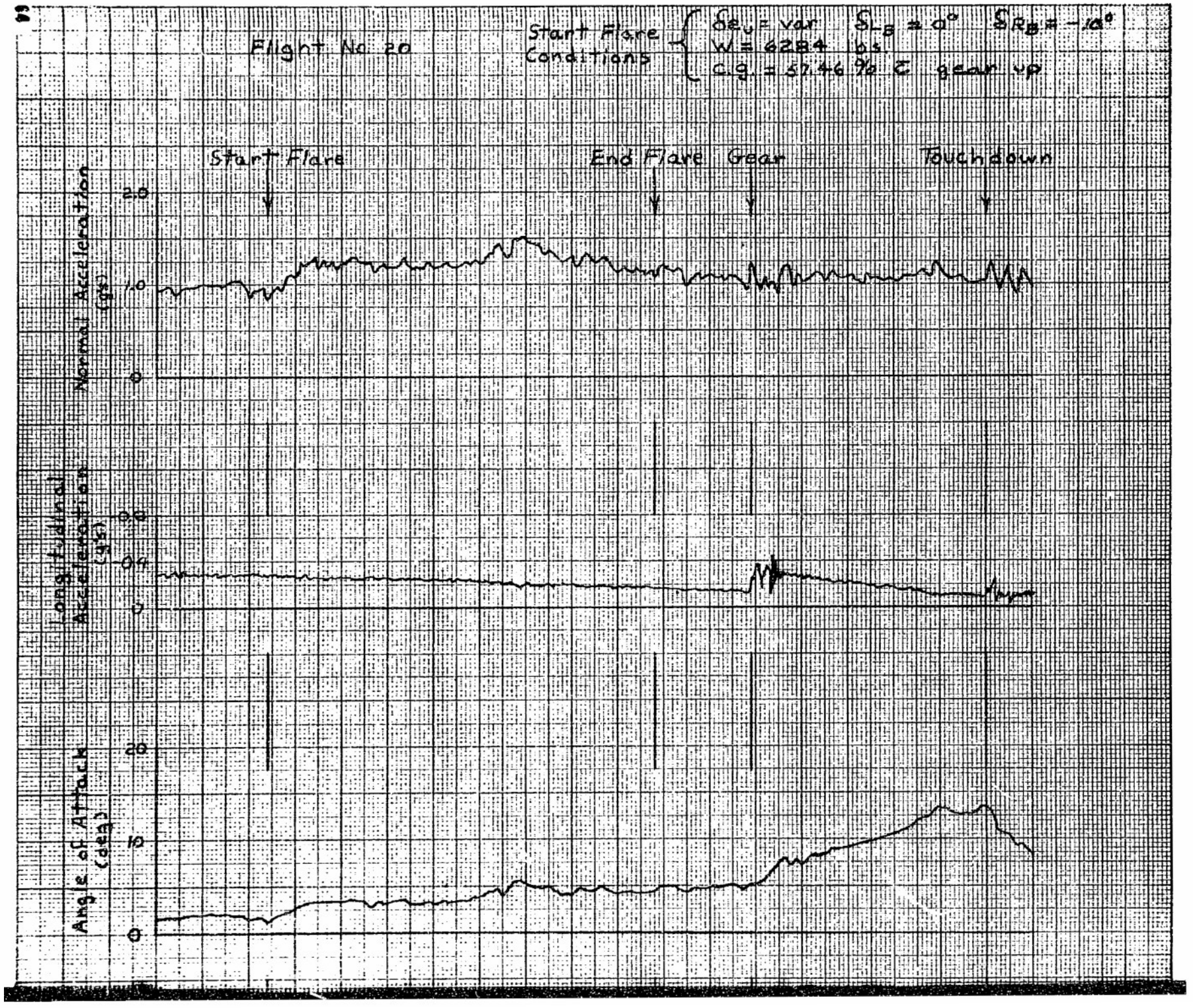
Flight No. 20
Start Flare Conditions
δe_u = var $\delta_{L_B} = 0°$ $\delta_{R_B} = -.4°$
W = 6284 lbs
C.g. = 57.46 % C gear up
Start Flare
End Flare
Gear
Touchdown
Normal Acceleration (gs)
2.0
1.0
0
Longitudinal Acceleration (gs)
-.2
-.4
0
Angle of Attack (deg)
20
10
0

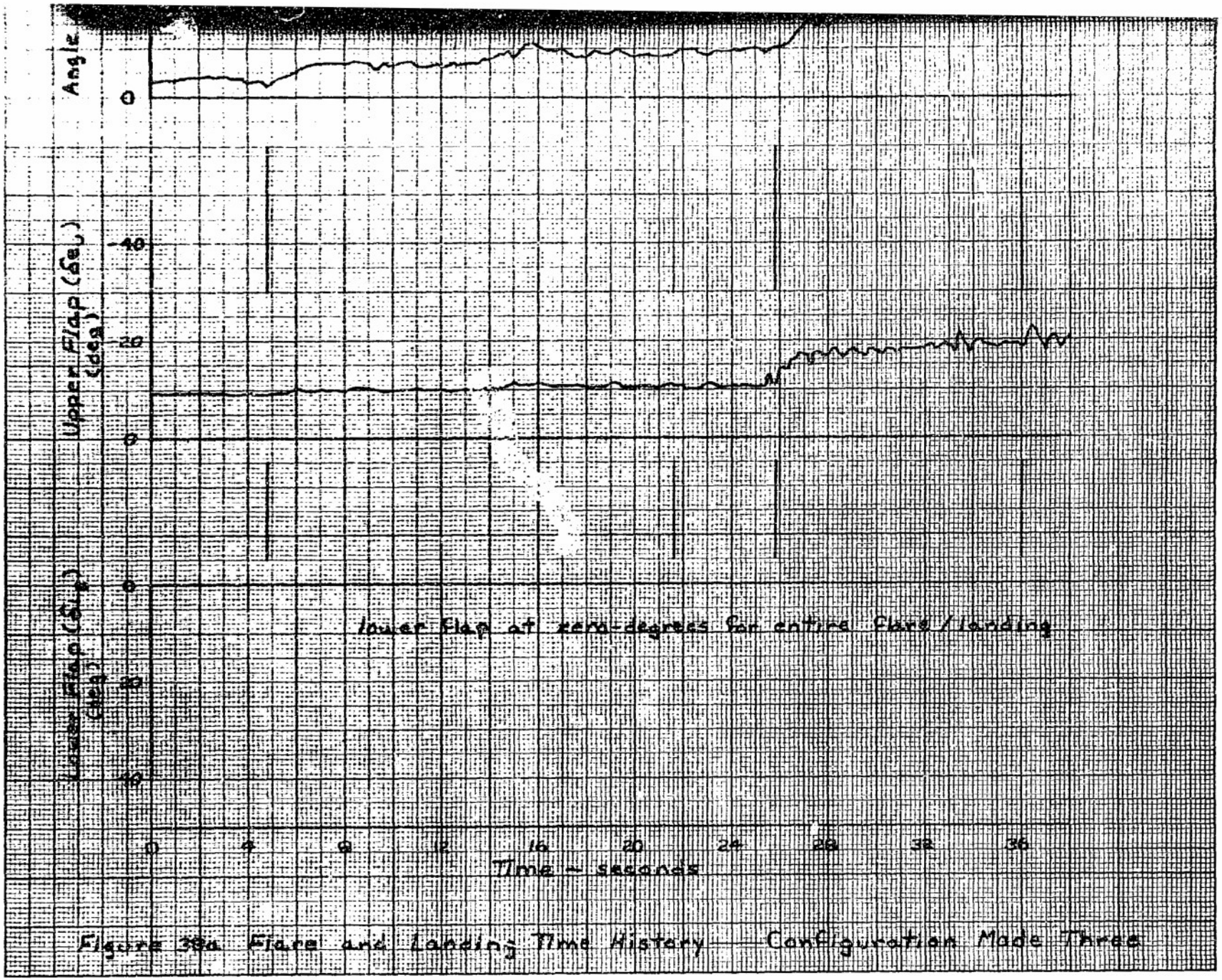

Figure 30a Flare and Landing Time History — Configuration Mode Three

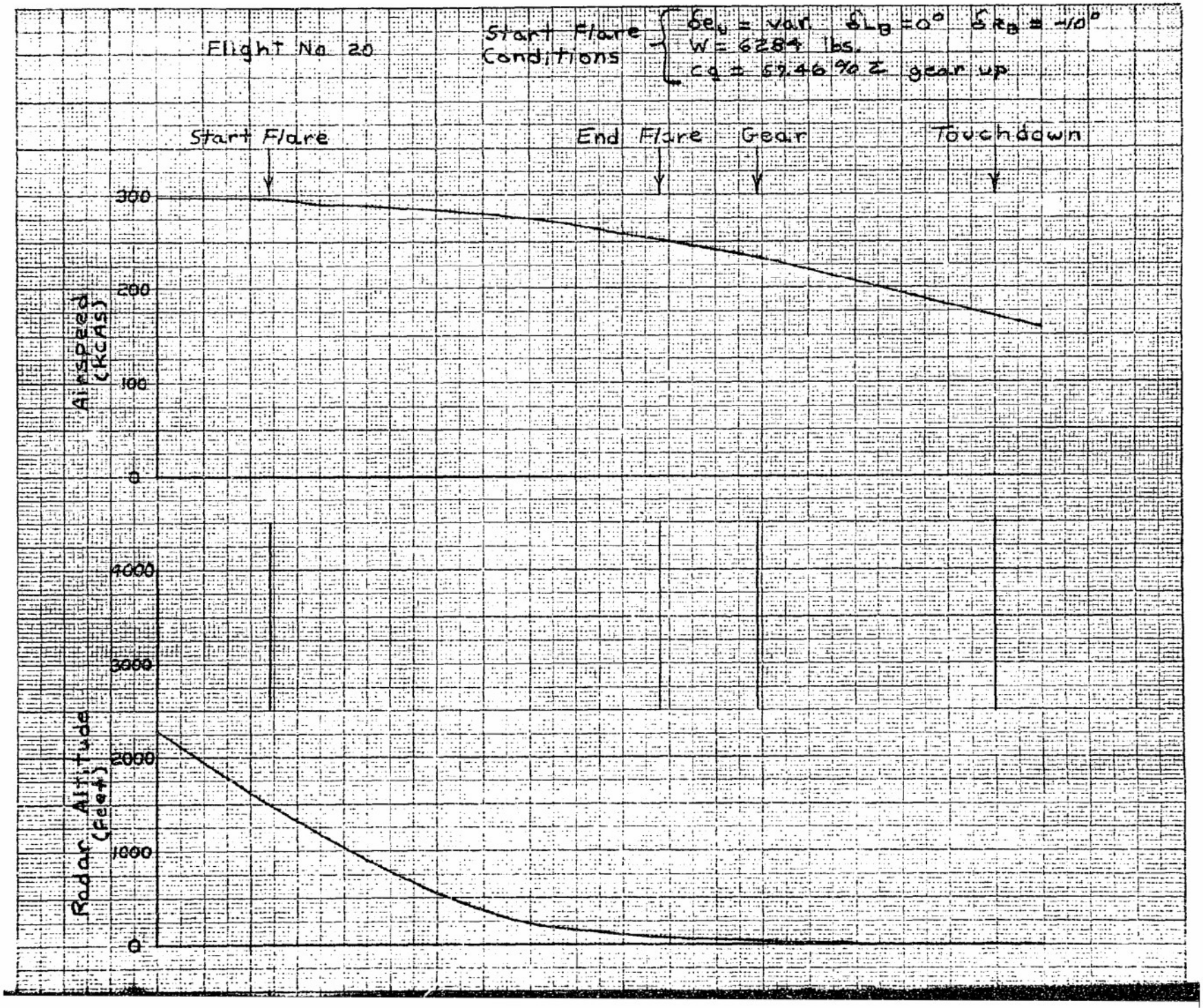
Flight No 20
Start Flare Conditions
δe_u = var $\delta L_B = 0°$ $\delta R_B = -10°$
W = 6284 lbs.
c_g = 59.46 % $\bar{c}$ gear up
Start Flare
End Flare
Gear
Touchdown
Airspeed (CKCAS)
300
200
100
0
Radar Altitude (Feet)
4000
3000
2000
1000
0

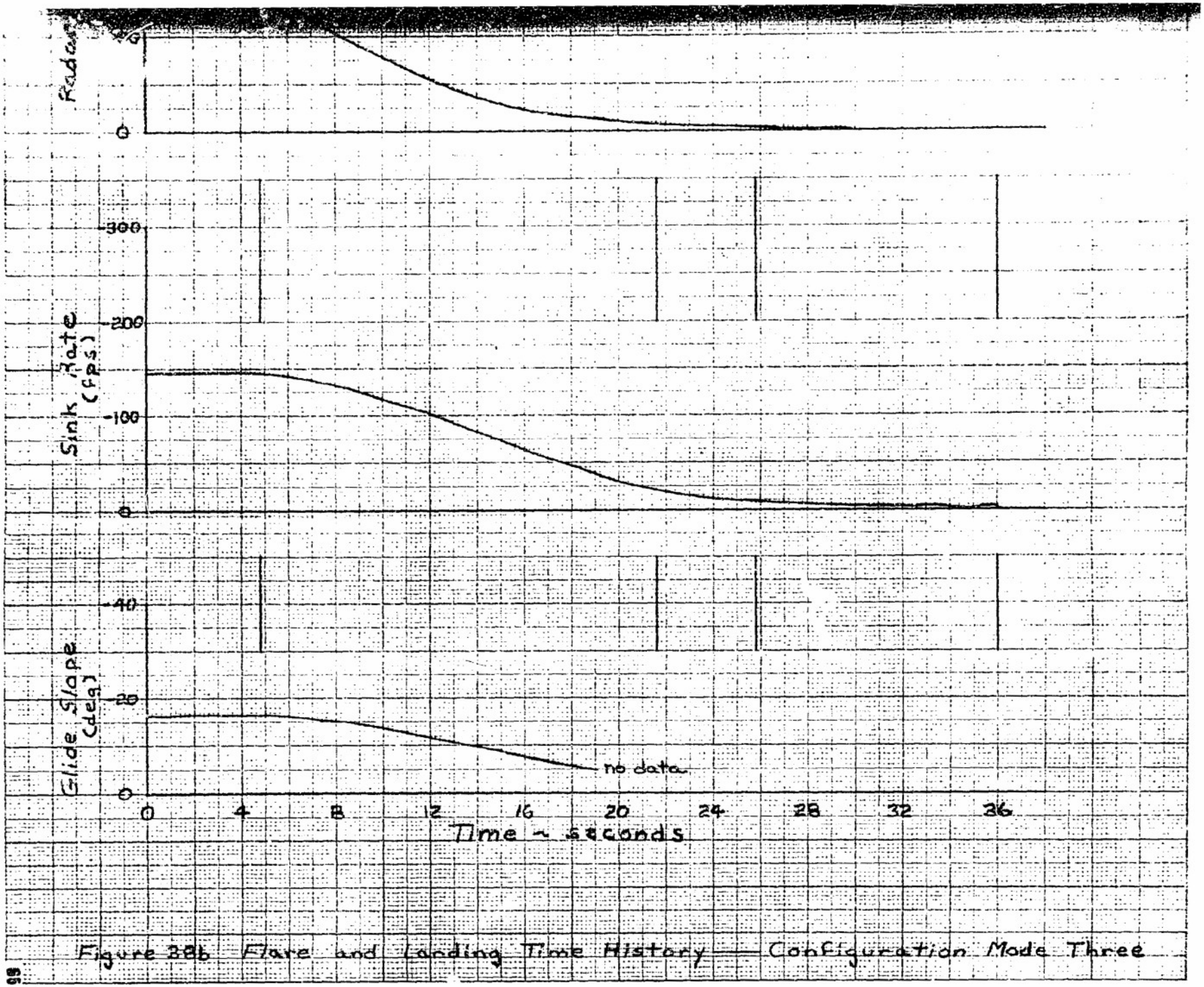

Figure 38b Flare and Landing Time History —— Configuration Mode Three

Landing Gear Characteristics

At or near flare completion (sink rate of 20 feet per second and an altitude of 40 to 130 feet AGL, table III), the landing gear was extended and the vehicle decelerated along a shallow glide path (less than 3 degrees) to the touchdown point.

The X-24A had a somewhat severe nosedown trim change associated with landing gear extension. A fast acting pneumatic landing gear extension system was used to deploy the gear. The average deployment time from pilot action until gear-down-and-locked was 1.2 seconds for the main gear and 1.5 seconds for the nose gear. The landing gear trim change was produced by both an aerodynamic effect which produced a nose-down moment and a forward shift in the center of gravity which also produced a nose-down moment. Reference 7 shows that this center of gravity shift with gear extension was about 2 inches (0.72 percent $\bar{c}$).

Longitudinal trim data for the three configuration modes during the approach, flare and landing are shown in figures 39 to 41. The lower flap increment (figure 39) required to compensate for the landing gear trim change was about 7 degrees or 2 inches of longitudinal stick. The upper flap increment (figure 41) required to compensate for the landing gear trim change was 5 degrees or 1.0 inch of longitudinal stick.

Figure 41 contains data from some tests on the X-24A in the full scale wind tunnel at NASA Ames Research Center. The incremental trim change due to the landing gear was accurately predicted by the full scale wind tunnel although the slopes were not. The X-24A fixed base simulator contained this trim change based on the full scale wind tunnel data and the gear up/down center of gravity measurements. However, an instantaneous trim change was used in the simulator, whereas flight experience indicated that there was a delayed trim change. Although the pilots were continually exposed to this trim change during their training, the first two pilots were caught by surprise on their first flights. A time delay was added to the simulator, and briefing of the third pilot by his predecessors prepared him for the delayed trim change. The pilots felt that even though they became accustomed to the gear trim change, and it was easily compensated for, it was still an undesirable feature especially in close proximity to the ground where the workload was high and other distractions could easily occur. However, there were occasions when the pilot extended the gear higher above the ground than usual and in these cases he knowingly used the nosedown trim change to converge with the ground.

In an effort to minimize the aerodynamic effect, a minor linkage modification was made to reposition the nose gear door in the extended position. It is seen in figure 40 that only a small change was realized, 1 or 2 degrees less flap required. This modification is discussed in appendix I.

The fixed upper flap settings and center of gravity location for the approach and landing on flights 1 through 7 were selected such that the lower flaps were used for pitch and roll control throughout the flight, thus avoiding the crossover region[4] (configuration mode 1, figure 39).

[4] Due to a certain amount of hysteresis in the control system linkage, there was a deadband of 2 degrees of control surface travel in conjunction with the crossover from the lower to the upper flaps (reference 8).

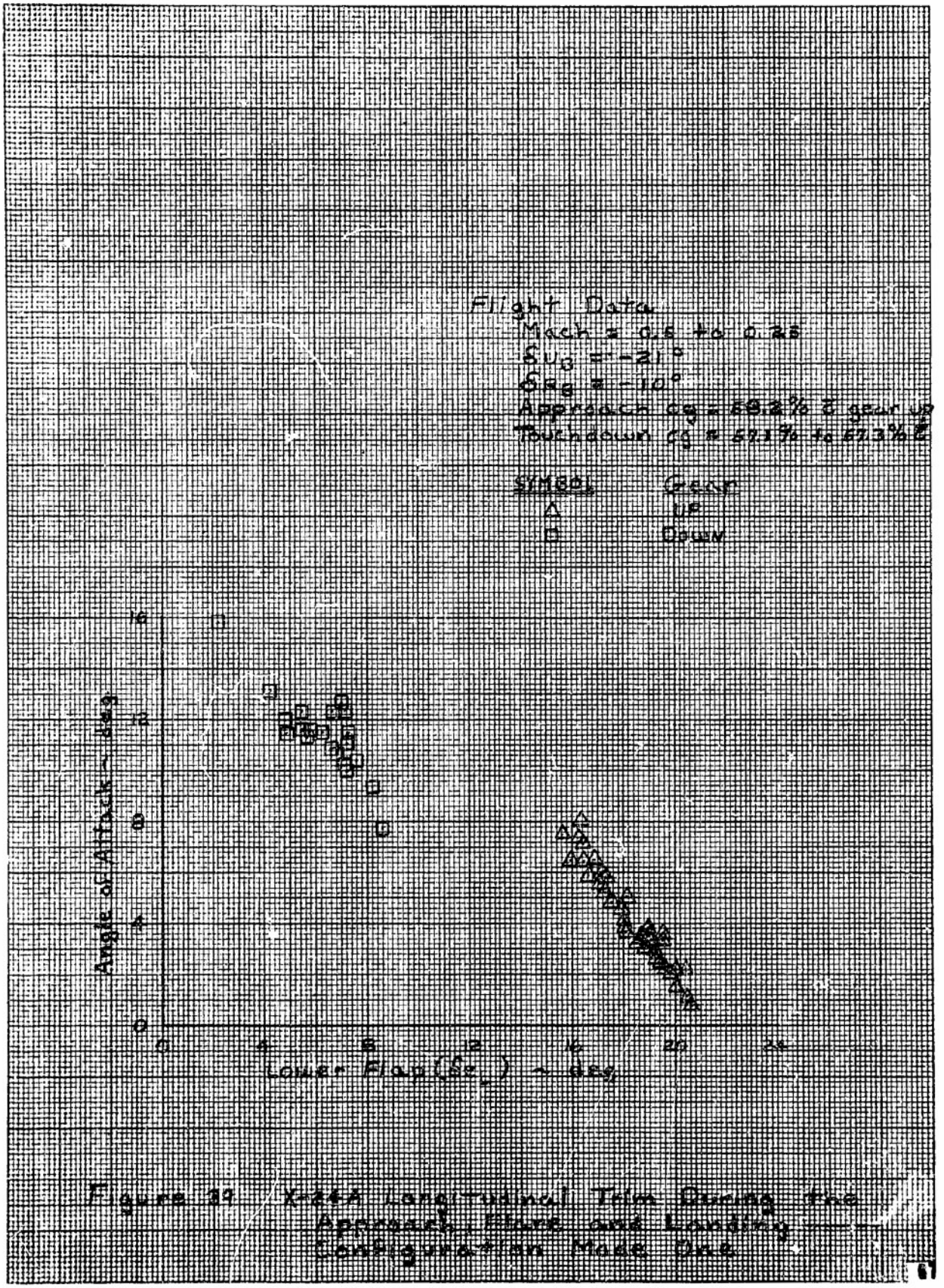

Figure 39 X-24A Longitudinal Trim During the Approach, Flare and Landing Configuration Made Once

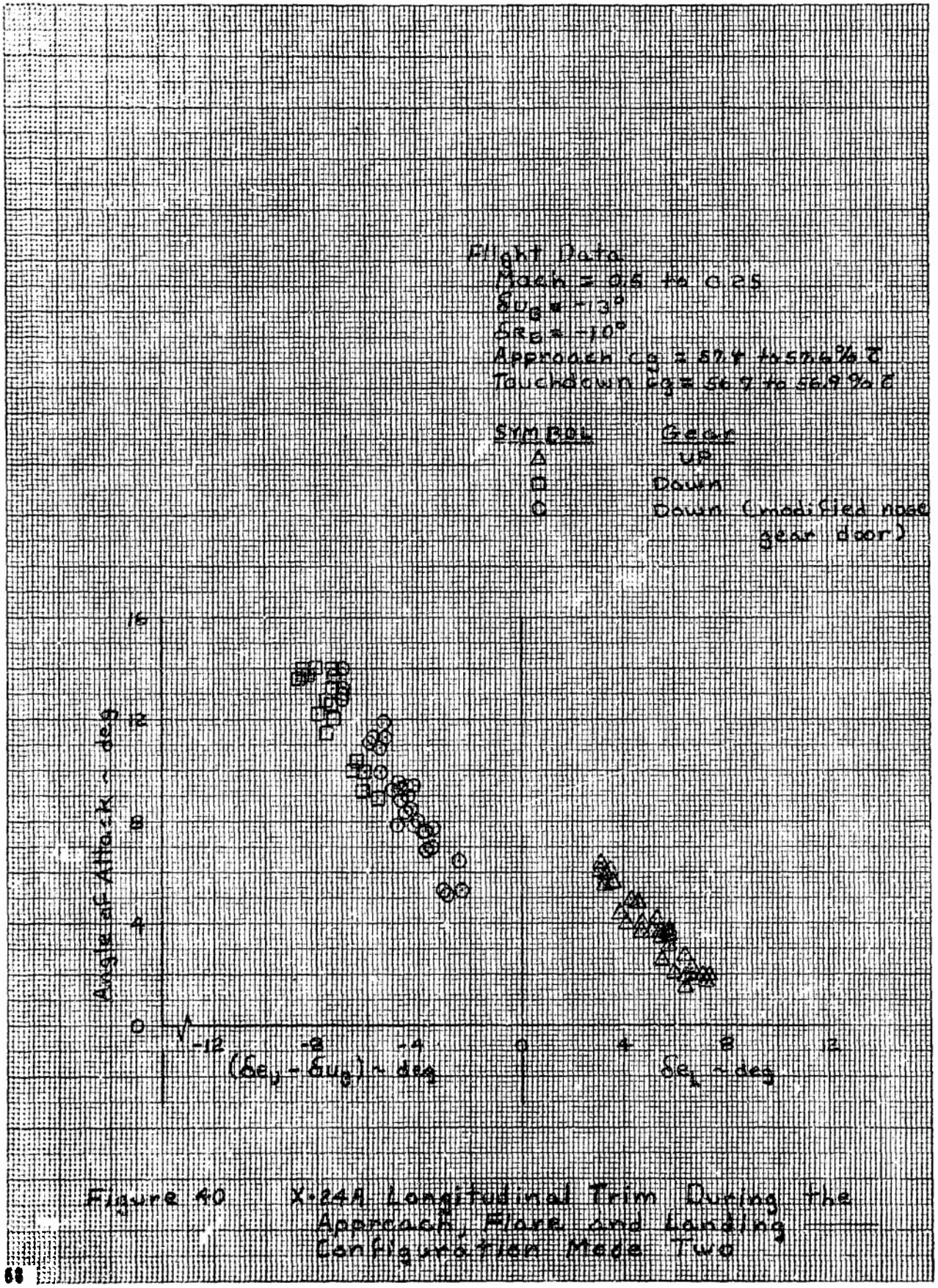

Figure 40 X-24A Longitudinal Trim During the Approach, Flare and Landing Configuration Mode Two

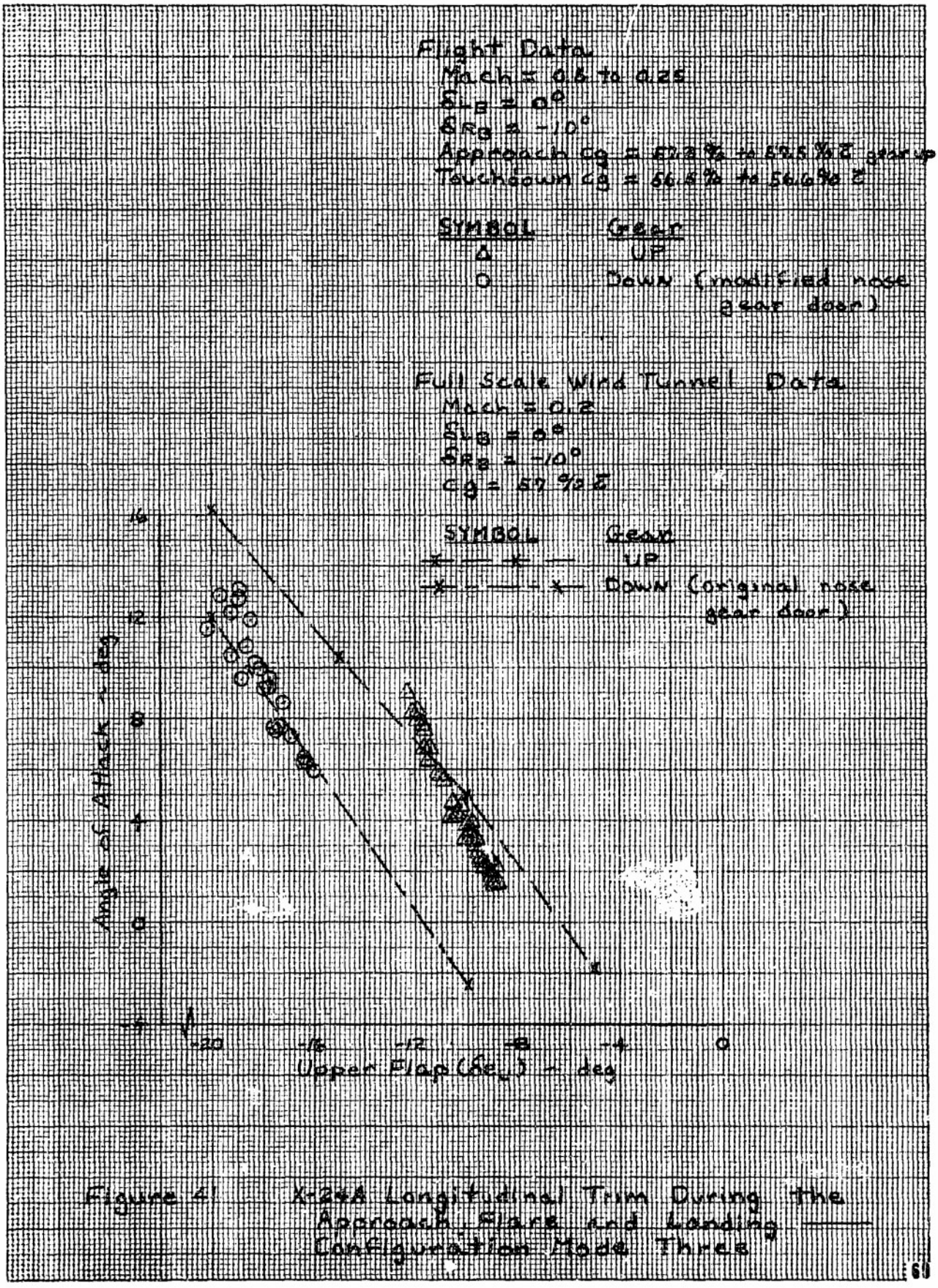

Figure 41 X-24A Longitudinal Trim During the Approach, Flare and Landing Configuration Mode Three

Test maneuvers were performed at altitude during these flights both in the crossover region and using only the upper flaps for control without adverse effects. Starting with flight 8 the upper flap setting (configuration mode 2, figure 40) was selected such that the landing gear trim change would result in a rapid crossover from the lower to the upper flaps, thus avoiding any extended time in the crossover region. The pilot was not aware of any obvious change in pitch sensitivity after gear extension for this mode, although the increased effectiveness of the upper flap is apparent in figure 40 by comparing the slopes (δe_L, δe_U vs α) before and after gear extension. The effect was probably masked by the rapid speed loss which occurred after gear extension. Note also that a comparison of the slopes before and after gear extension in figures 39 and 41 showed no trend in pitch sensitivity that could be attributed to the landing gear alone.

The gear-down data points shown in figures 39 through 41 encompassed the time span from gear extension to the instant of touchdown. A comparison of slopes of the gear-up/gear-down data showed no obvious trend in pitch sensitivity that could be attributed to ground effect. This is consistent with the limited wind tunnel results of reference 13 in which tests were accomplished with a landing gear and ground board. These wind tunnel tests could not be compared directly since the landing gear and gear doors were not the same as those on the vehicle.

The pilots were impressed with the good vehicle response close to the ground with the landing gear extended. They commented that it was easy to make small corrections in the vehicle attitude while decelerating to the touchdown point. The exceptions to this were the few landings when a strong ground crosswind existed (see the section titled Effect of Winds and Turbulence in the Approach Pattern and Flare).

Deceleration Phase

After the landing gear was extended the vehicle continued to decelerate to the touchdown point. An interesting phenomenon brought about by the gear trim change was the difference in deceleration before and after gear extension for configuration modes 1 and 3. The nose-up trim requirement at gear extension resulted in a reduction in trim drag and a reduction in lift-due-to-the-tail for mode 1 (lower flap closed, reduced base area). This, in combination with the angle-of-attack increase required at gear extension to compensate for the reduction in lift-due-to-the-tail resulted in the fact that the L/D (figure 42) and the deceleration did not change appreciably at gear employment in configuration mode 1. In configuration mode 3, the same trim requirement resulted in an increase in trim drag and a reduction in lift-due-to-the-tail (upper flap opened, increased base area). In this case, the L/D decreased with the result that a signficant increase in deceleration occurred at gear deployment for configuration mode 3. This trend is also apparent in the longitudinal accelerometer values before and after landing gear deployment (figures 36a and 38a) and the rate of change of airspeed (figures 36b and 38b and table VII).

The change in deceleration for configuration mode 2 (figure 37) was between those of modes 1 and 3, but closer to that of mode 3. The landing rockets, which were used during 3 of the 7 flights in configuration mode 1, decreased the deceleration by about 3 knots per second. There

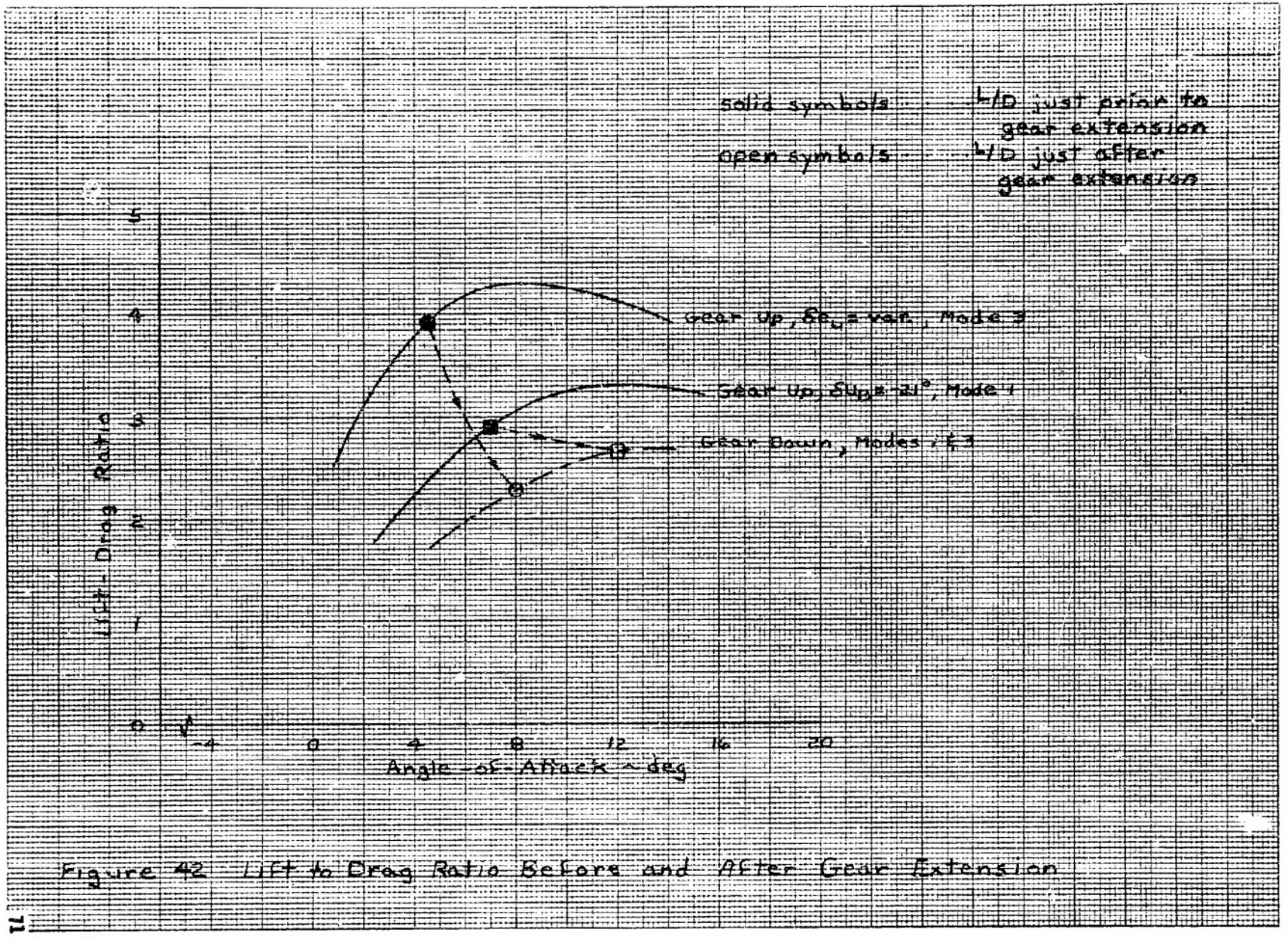

Figure 42 Lift to Drag Ratio Before and After Gear Extension

Table VII

SUMMARY OF THE DECELERATION
BEFORE AND AFTER GEAR EXTENSION

Configuration Mode	Landing Rockets Used	Deceleration Before Gear Extension (kt/sec)	Deceleration After Gear Extension (kt/sec)
1	Yes	3.7	5.0
1	No	6.7	7.4
2	No	4.0	7.7
3	No	3.9	7.0

were no pilot comments associated with this difference in deceleration between the different configurations. Apparently the pilot's attention was directed to altitude control and sink rate after gear deployment and he was not aware of, or concerned with, the difference in the rate of speed bleed-off.

Landing Rocket Usage

A description of the landing rocket system is given in appendix I. This system was available for use at the pilot's discretion to decrease the rate of sink and extend the glide by producing an increase in the effective L/D. The burn time available varied from 27 seconds for glide flights to approximately 10 seconds following powered flights using the XLR-11 rocket engine.

The first pilot to fly the X-24A used the landing rockets during the first three flights. He elected not to maintain the desired high energy approach airspeed (300 KIAS) due to handling qualities problems. He therefore used an approach airspeed of 260 to 280 KIAS while relying on the landing rockets for additional energy during the flare and landing. After accomplishing several modifications to the control system, and as the pilot became more familiar with the vehicle response in light turbulence, landings were performed without the use of the landing rockets. Also, as the flights progressed and airspeed calibration data were obtained, it became evident that the X-24A had a larger positive position error than expected (11 knots at an airspeed of 300 KIAS and a Mach number of 0.5, reference 4).

Table VIII compares average values of various flare parameters with and without use of the landing rockets in configuration mode 1. The average time that the glide was extended by using the landing rockets was five seconds and would have been greater if the average touchdown airspeeds with and without the use of the landing rockets had been the same.

Table VIII

SUMMARY OF LANDIN· ROCKET EFFECTS ON THE FLARE AND LANDING CHARACTERISTICS
(average values)*

Landing Rockets Used	Time Start Flare to Touchdown (sec)	Time Gear to Touchdown (sec)	Time Start Flare to Rockets "On" (sec)	Rocket Burntime Used (sec)	Airspeed at Start Flare (KCAS)	Altitude at Start Flare (ft AGL)	Airspeed Lost During Flare (KCAS)	Airspeed at Landing Gear Extension (KCAS)	Airspeed at Touchdown (KCAS)	Angle of Attack at Touchdown (deg)
Yes	29.0	8.8	2.8 to 8.6	24.6	280	1,840	46.1	230	184	14.0
No	24.0	6.8	----------	----	282	1,820	54.6	224	175	14.8

*Values in the first row were averaged over three flights. Values in the second row were averaged over four flights.

Landing Accuracy and Rollout Distance

Each pilot specified his intended touchdown point prior to most flights. This point was usually one and a quarter statute miles beyond the preflare aim point. Figure 43 shows the frequency distribution of the longitudinal distance from the intended touchdown point for 19 X-24A landings. This figure shows that 32 percent of these landings were made within 250 feet of the intended touchdown point and that all landings were within 2,000 feet. Although this is a small sample of landings, these results are similar to the X-15 findings of reference 14 which covered 94 landings, in which 20 percent were within 250 feet and 84 percent were within 2,000 feet of the intended touchdown point. Reference 15 contains the touchdown accuracy data for the other two lifting body vehicles.

The data in figure 43 must be qualified by the fact that the pilots were not always allowed to devote their entire attention to the landing from low key to touchdown as would be necessary to make an accurate touchdown. As a result seven flights (asterisked values in figure 44) were excluded from the statistics. For flights 7, 8, 19, and 20, a new approach configuration was being evaluated. For flights 17 and 18, the pilot flew the landing pattern at a specified airspeed of 270 KIAS. On flight 10 (the first powered flight) the pilot realized he was high in energy, but expressed concern that if he used extensive speed brakes he might lose the chase aircraft; therefore, he decided to forego the accuracy landing. The pilots found that an effective speed brake was an absolute necessity to consistently make accurate landings.

Pilot A stated that his tenth flight in the X-24A (flight 12) was the first flight in which he was able to devote his entire attention to the approach and landing with the results that his touchdown occurred 197 feet short of the intended touchdown point. Likewise for pilot B, his eighth flight in the X-24A (flight 21) was the first one in which he really concentrated on achieving a touchdown point (although there was no touchdown marker), and for that flight, the touchdown occurred 385 feet beyond the intended point. It should also be pointed out that the last eight flights of the X-24A program were flown to a new runway without a marker at the intended touchdown point.

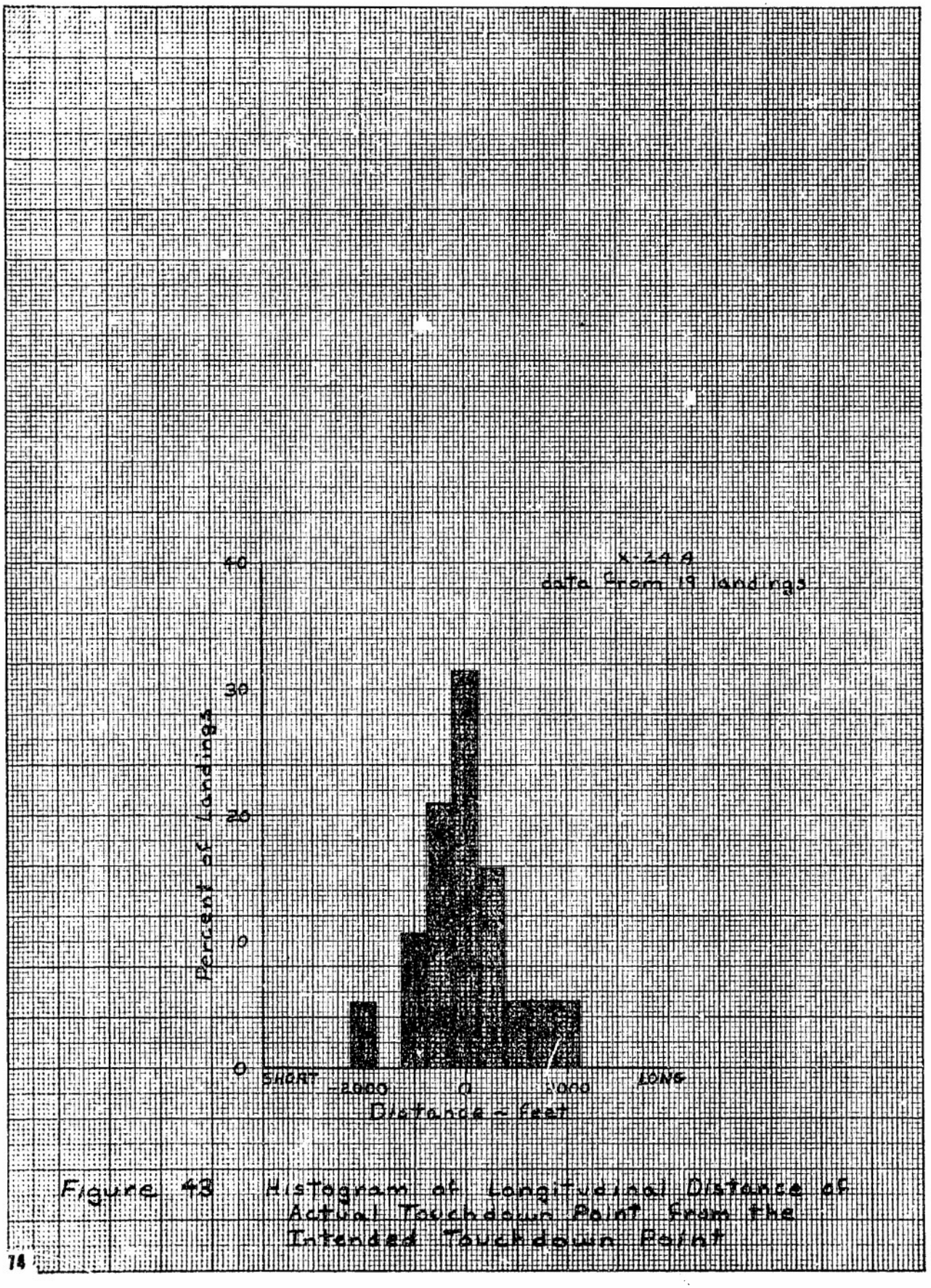

Figure 48 Histogram of Longitudinal Distance of Actual Touchdown Point from the Intended Touchdown Point

Figure 44 Summary of the Landing Accuracy for Each X-24A Flight

Figure 45 is a plot of landing rollout distance as a function of touchdown airspeed and braking. The braking technique varied from moderate to no braking with or without speed brakes. All braking began at approximately the same airspeed, 100 to 120 KIAS, and was defined in terms of toe pressure. Light braking meant light toe pressure on the brakes with periods of no braking, whereas moderate braking consisted of moderate toe pressure on the brakes. Figure 45 shows an increased rollout distance with increased touchdown airspeed, as expected.

The task after touchdown was primarily to maintain a desired ground track (straight down the runway). The stopping distance and/or braking effectiveness were of academic interest only.

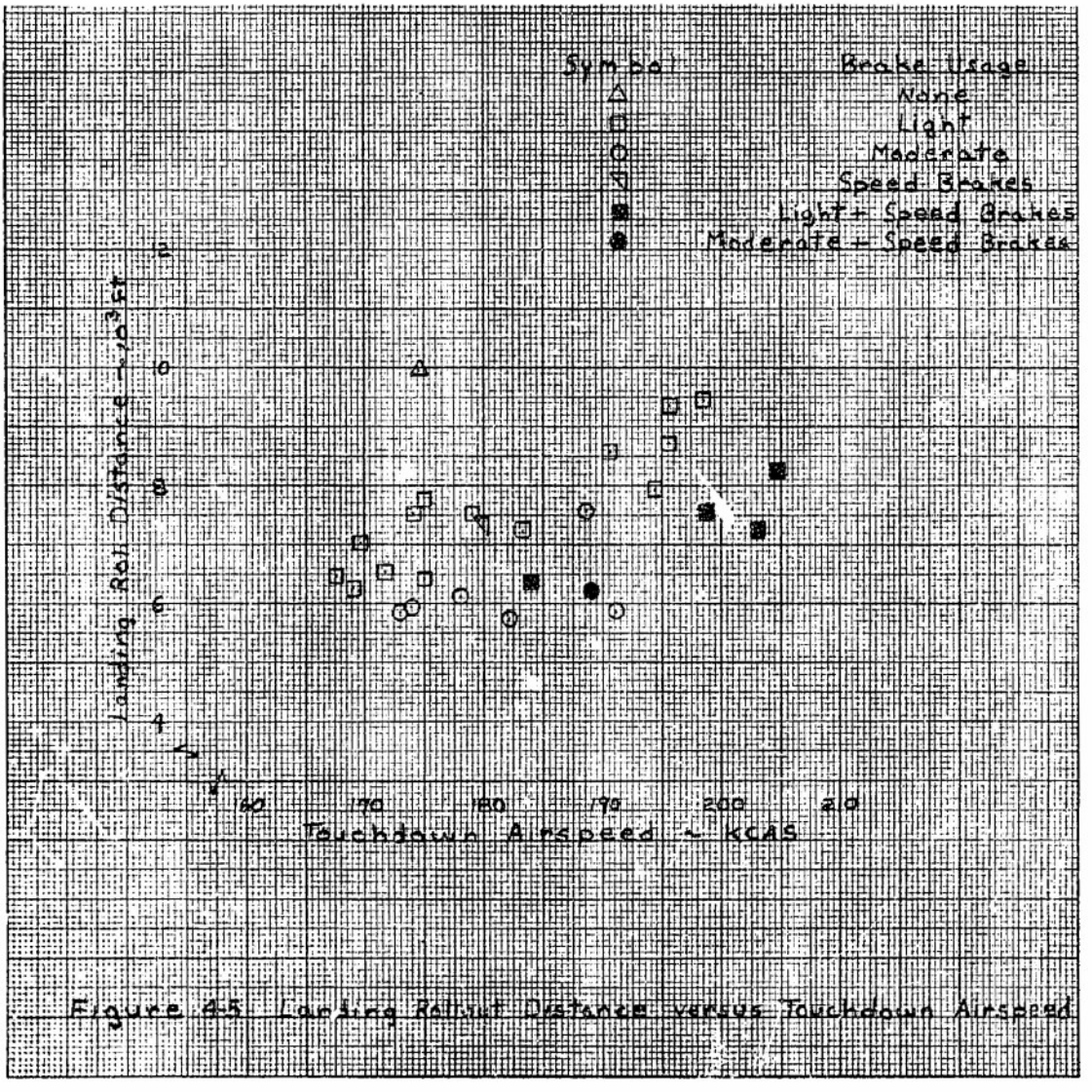

Figure 45 Landing Rollout Distance versus Touchdown Airspeed

Planform Loading Effects in the Approach, Flare, and Landing

The range of wing loadings experienced during the X-24A approach and landings was very limited (38.0 to 43.4 pounds per square foot). The heaviest weight during the approach/ landing occurred on flight 15 (there were no pilot comments relating to the heavy weight condition). In analyzing the actual data it was difficult to differentiate between planform loading effects, wind effects or off-nominal patterns because the pilot compensates for each in the same manner using airspeed, speed brakes, and bank angle.

Effects of Wind and Turbulence in the Approach Pattern and Flare

The low key point that the ground controller was guiding the pilot toward was not adjusted for winds. However, there was adequate excess energy in the standard approach pattern to allow the pilot to visually compensate for winds using airspeed, bank angle, and/or speed brakes.

Winds aloft were determined from early morning weather balloon data. These data were made available to the pilot prior to cockpit entry and were updated just before launch if later balloon data were available. Also, on the morning of each X-24A flight the pilot, flying in the in-flight performance simulator (F-104), had an opportunity to practice the X-24A approach and thus experience the effects of wind to be expected during the actual X-24A flight. Based on this information, the pilot could adjust the pattern inside or outside of the non-wind-corrected low key point before reaching the low key altitude. Crosswinds on final approach and landing were compensated by a combination of crab and bank angle.

The effect of wind and the compensation technique used during X-24A approaches were similar to those experienced on standard fighter aircraft with the exception of the turbulence and surface winds. The response of the X-24A to atmospheric turbulence was somewhat different than that of most winged vehicles because of its unusually large dihedral effect. Although all three axes were disturbed by the turbulence, the pilot was more aware of the lateral response of the vehicle than either the pitch or yaw. These unexpected lateral upsets were somewhat disconcerting to the first pilot on his first few flights, especially during the final approach at high airspeed and below 10,000 feet. Once the pilot was able to associate these motions with atmospheric turbulence rather than with a degradation in lateral stability, he was able to ride through turbulence on subsequent flights without apprehension.

Even through the flare, no difficulty was experienced in compensating for the winds right up through gear extension and touchdown within the specified wind limits (see the Ground Handling and Surface Winds section). The exceptions to this were the few flights in which the surface crosswind was near the limit value, and gusts and turbulence were heavier than usual; the pilot experienced several disconcerting lateral upsets between landing gear extension and touchdown.

Ground Handling and Surface Winds

The initial X-24A configuration incorporated nosewheel steering for ground handling. A series of taxi tests was conducted to evaluate

ground handling characteristics with and without nosewheel steering engaged. Vehicle response with nosewheel steering engaged was too sensitive. The use of differential braking for directional control was concluded to be adequate for landings on a dry lakebed; consequently, the nosewheel steering was deleted prior to the first flight of the vehicle.

The primary task after touchdown was to maintain a desired ground track (straight down the landing runway). For the landings in which no surface crosswind existed, the desired ground track was maintained through the use of differential braking and rudder/aileron deflection. The deceleration technique during rollout varied from moderate to no braking, and on six occasions by opening the upper flaps to full deflection for maximum aerodynamic braking after touchdown. Pilot comments on ground handling under conditions of little or no crosswind indicated no significant vehicle deficiencies and satisfactory results of both brakes and deflected control surfaces in maintaining the desired ground track.

The surface wind limit used during the X-24A program was an arbitrary limit based on experience with earlier lifting body programs. This limit for flights 2 through 6 and 22 was a maximum surface wind of 10 knots or a crosswind component of 5 knots. For the balance of the X-24A flights, this limit was a maximum surface wind of 15 knots or a crosswind component of 10 knots.

The surface wind direction and velocity as listed in table III were obtained from a combination of instruments all located a mile or more from the touchdown point. In some cases, the wind reading was not taken until some time after touchdown. In any case the best available data were used for the wind values in table III.

Two landings (flights 19 and 24) were accomplished with crosswind components at or near the maximum allowable. The pilots rated the vehicle ground handling characteristics as poor on these landings. The vehicle was blown downwind and on flight 24 despite moderate-to-heavy differential braking applied concurrently with maximum control surface deflection, the vehicle came to a stop approximately 2,500 feet laterally displaced from the touchdown point. The wind direction for this landing (figure 46) produced a surface headwind component. As the vehicle was blown downwind, the crosswind component tended to increase until the wind was almost perpendicular to the ground track. The pilot did not have adequate control or inherent vehicle ground stability to prevent this heading divergence.

On flight 19 using the same control techniques, the lateral displacement was 300 feet. The wind direction for this landing (figure 46) was such that there was a surface tailwind component. In this case, as the vehicle was blown downwind, the crosswind component decreased until the wind was almost all tailwind. As the vehicle slowed, the pilot was able to gain control and turn to the runway heading once again.

In addition to the poor handling characteristics, the riding qualities during ground rollout in a crosswind were unpleasant. The vehicle turned away from the wind and the downwind landing gear strut was compressed. On flight 19 this compression (the difference between windward and downwind strut positions) amounted to about 1.5 inches, and on flight 24 it was 2.2 inches.

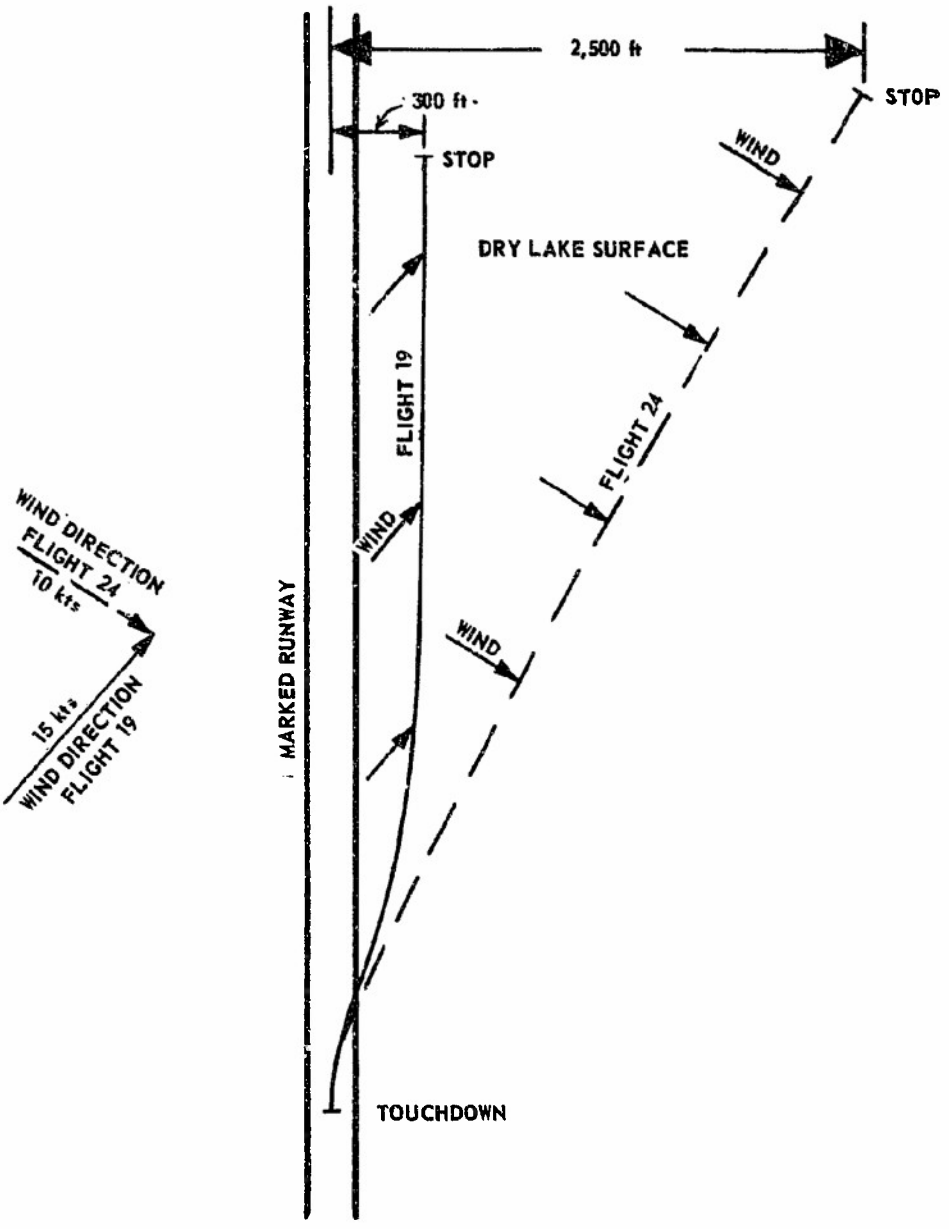

Figure 46 Ground Rollout Track of High Crosswind Landings

Due to vehicle geometry (narrow wheel base and high center of gravity above the ground, figure 47) the strut compression was experienced by the pilot as an uncomfortable "heeled over" attitude downwind. In attempting to maintain ground track against the crosswind, the downwind strut compression was even greater, aggravating the poor riding qualities. This "heeled over" attitude was experienced on all of the lifting body vehicles and the pilots felt that if they had tried to steer into the wind the vehicle might have overturned. The use of braking on the windward wheel was not satisfactory because that wheel was lightly loaded and because of the potential tire blowout problem. The pilots were reluctant to use the brakes until the vehicle had decelerated to below 120 knots.

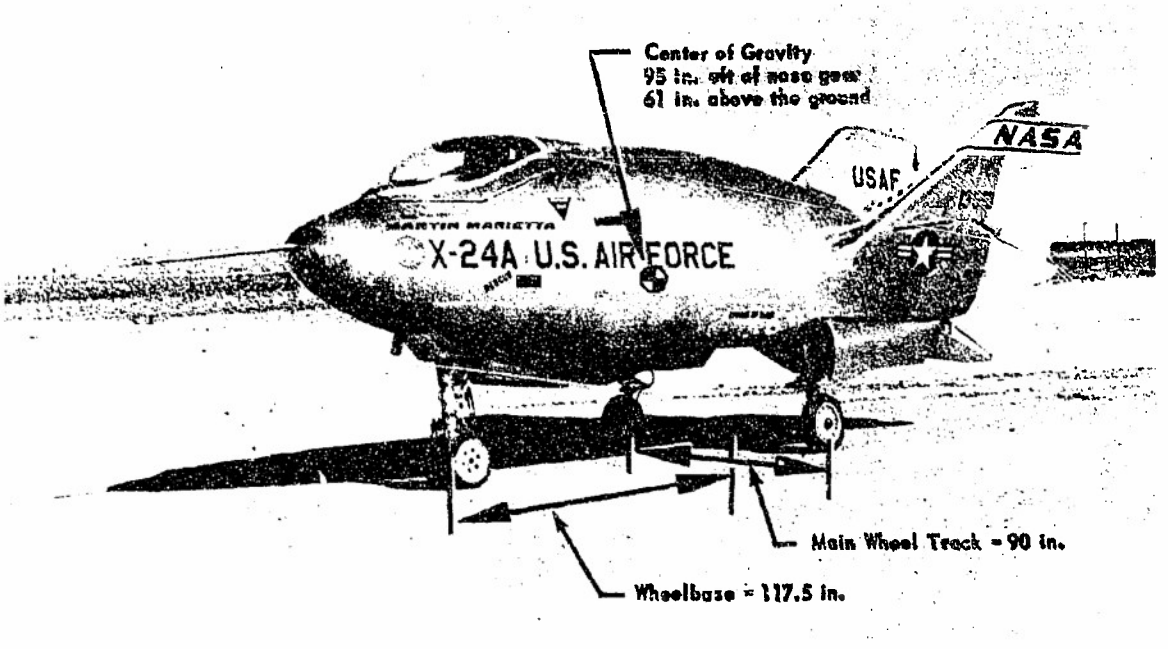

Figure 47 X-24A Landing Gear Configuration

Visibility During the Approach, Flare, and Landing

The canopy on the X-24A was an acrylic resin bubble canopy (figure 48) very similar to the canopies on many fighter aircraft. However, the X-24A canopy/cockpit was quite wide, which limited the over-the-side visibility somewhat.

The pilots felt that the X-24A had superior visibility compared to the other two lifting body vehicles (M2-F2 and HL-10) and compared it favorably with the visibility from an F-104. The forward visibility and depth perception in the X-24A were outstanding, and the pilots never lost sight of the runway even when landing at the slower speeds. A pressure suit degraded the visibility slightly primarily because it restricted the pilot's head movements.

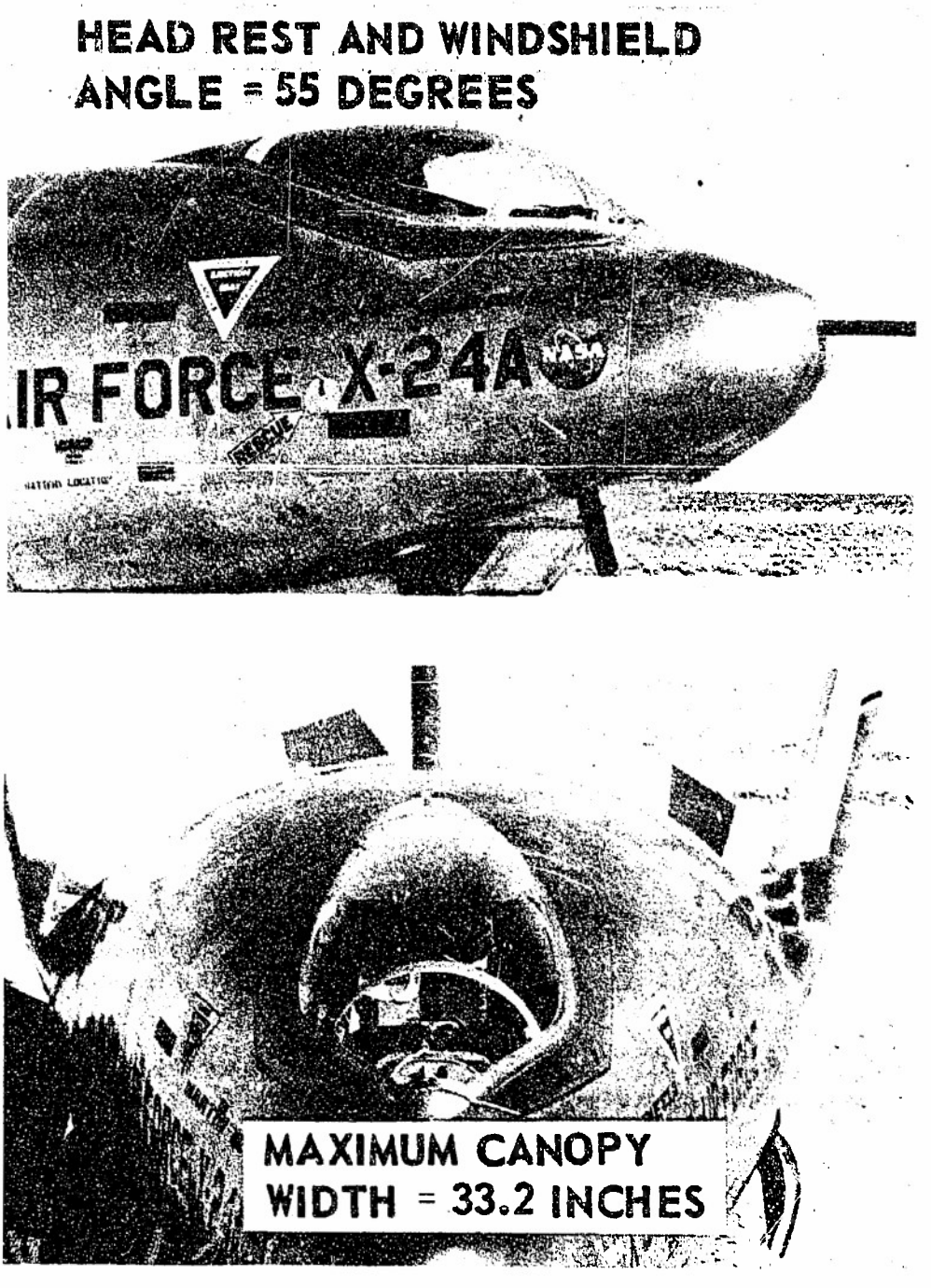

Figure 48 Canopy of the X-24A

CONCLUSIONS

Three pilots, after a suitable period of training, flew the X-24A lifting body vehicle and found that the unpowered visual approach and landing task was relatively easy after extensive F-104 low/medium L/D practice. There were several factors found important when performing an unpowered low/medium L/D approach and landing.

An effective method of energy management was necessary to perform accurate landings. The use of the flap bias feature as a speed brake proved to be quite effective and valuable during the approach and landing phases. The landing accuracy during the X-24A program was similar to that observed on other lifting body vehicles.

The external visibility, and consequently the canopy configuration, were important in the performance of low/medium L/D landings. The X-24A visibility was better than that of either of the two previous lifting bodies. The depth perception during the flare and landing was excellent, and the pilot never lost sight of the runway.

Good handling qualities were very important. Following control system developments early in the test program the handling qualities of the X-24A in the approach and landing configuration were excellent. However, lateral upsets due to turbulence were disconcerting to the pilot, particularly in close proximity to the ground.

Any large trim changes during approach and landing increased pilot workload. The trim change associated with biasing the flaps for speed brakes was minor and easily controlled in the X-24A. The landing gear trim change was large and somewhat objectionable to the pilots although it was easily compensated for.

As with past lifting body programs, the use of an inflight landing simulator was very valuable. Without this the pilot experience level would probably have been significantly lower and possibly inadequate.

An effective method of steering on the ground was necessary to stay within the limits of the marked lakebed runway. Without a crosswind, the X-24A had good ground handling and the desired ground track could be maintained through the use of differential braking and rudder/aileron deflections. With a crosswind these methods were not adequate to maintain the desired ground track.

The total time from flare initiation to touchdown was important in accomplishing the piloting tasks associated with the flare and landing. The pilots, combining their experience in the X-24A and other low to medium L/D lifting body vehicles, suggest that 20 to 30 seconds is adequate to arrest the sink rate, extend the landing gear and adjust the sink rate to an acceptable touchdown value. The X-24A flare data fell within this time band. The energy at flare initiation was very important in order to give the pilots this necessary time interval.

APPENDIX I
SUBSYSTEMS DESCRIPTION

LANDING GEAR SYSTEM

The landing gear was a conventional tricycle arrangement with cantilevered air-oil shock struts. The nose gear was similar to the nose gear used on the North American T-39. The vehicle originally had nosewheel steering, but it was removed before the first flight as the result of the taxi tests which indicated that the steering was too sensitive. The nosewheels were free-swivelling through a $\pm$35 degrees steering angle. Cams in the nosewheel strut provided centering of the wheels when the strut was fully extended. Shimmy was prevented by means of two co-rotating wheels. The nose gear was operated by a pneumatic actuator with an integral lock in the extended position, functioning both as an actuator and a drag brace.

Each main gear had a single wheel and was similar to the main gear on the T-38 and the F-5A. The X-24A main gear had a folding drag brace with a pneumatic actuator connected at the folding joint of the drag brace. The actuator had an internal lock to hold the drag brace in the extended position.

Both the nose and main gear retracted aft with the strut in the fully extended position. The nose gear strut contained a floating piston to separate the oil and the air in the strut. To ensure reliable gear extension, a direct mechanical link was provided from the pilot's gear handle to the gear actuation valve. Gas flow for gear extension was supplied simultaneously from the emergency helium supply tank and from the landing gear helium supply bottle. The main and nose gear were automatically locked in the extended position by positive mechanical locks. During flight the gear could only be extended; there was no capability for inflight retraction. There were no cockpit indicators to tell if the gear was down and locked; however, the chase aircraft pilot verified that the gear was down.

During the full scale wind tunnel tests at Ames Research Center, some gear extension tests were run with a dynamic pressure of 108 pounds per square foot. These tests indicated that the average time from when the gear handle was pulled until the gear was down and locked was:

left main gear - 1.17 seconds
right main gear - 1.13 seconds
nose gear - 1.48 seconds

The full scale wind tunnel tests indicated that 75 percent of the gear-down aerodynamic pitch trim change was due to the nose gear system alone and 30 percent of this was due to the nose gear forward flap assembly (figure 1). The original assembly was mounted so that the angle relative to the vehicle horizontal reference line (waterline) was 90 degrees in the gear-down position (figure 1); however, prior to flight 9 a modification was completed in which this angle was reduced to 45 degrees (figures 2 and 3). The planform area of this assembly was 1.75 square feet.

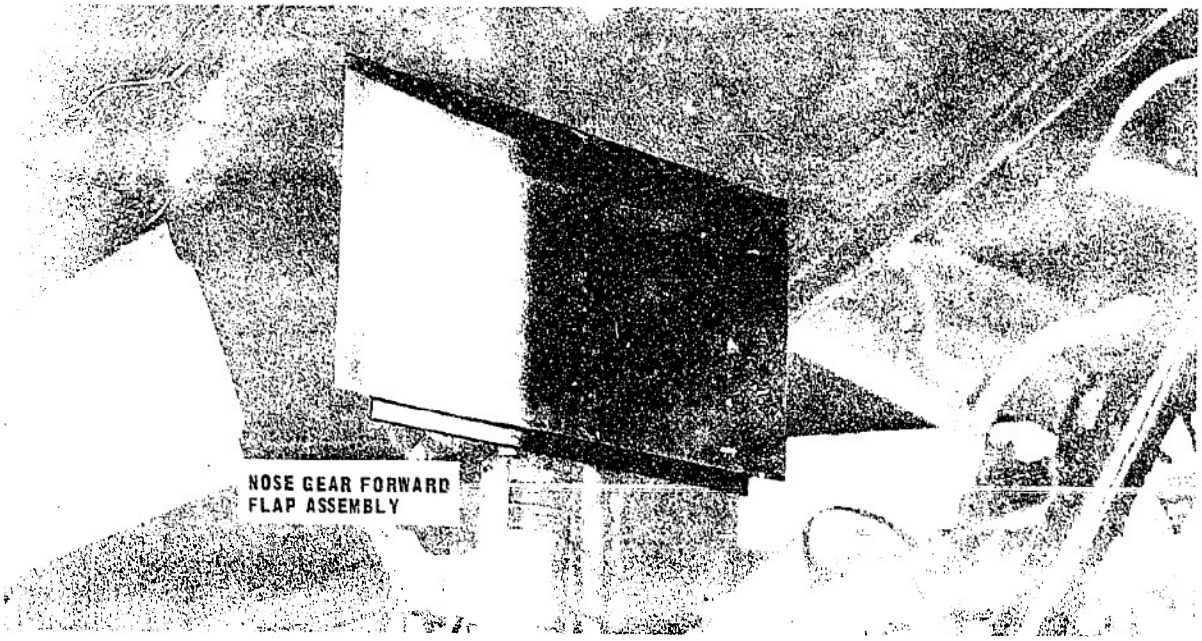

Figure 1 Old Nose Gear Door

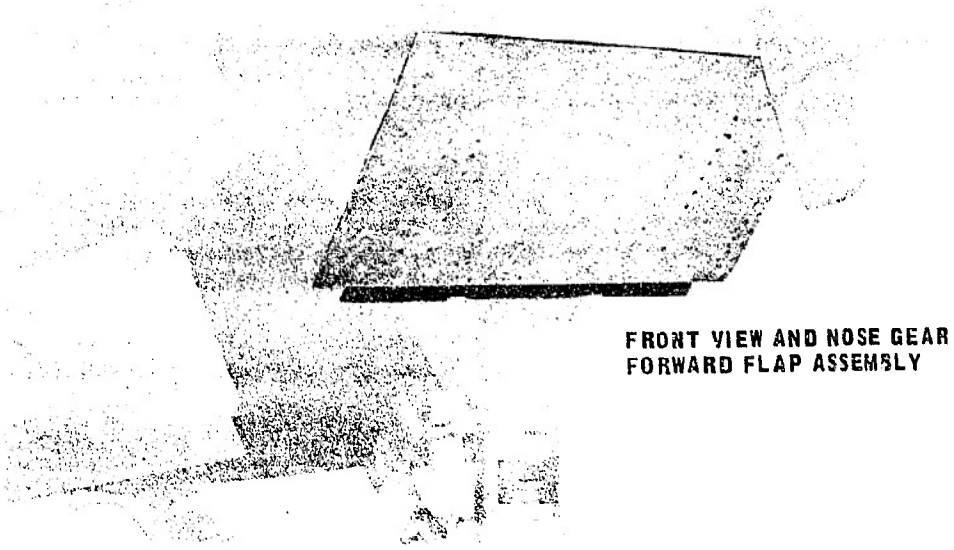

Figure 2 New Nose Gear Door

Figure 3 New Nose Gear Door

LANDING ROCKET SYSTEM

This system was used by the pilot if required to stretch the glide or reduce the rate of descent by an increase in the effective L/D. This system consisted of two variable thrust Bell monopropellant rocket motors. They were rated at 500 pounds thrust each and used hydrogen peroxide as a propellant. These motors were originally developed for the Lunar Landing Research Vehicle.

Since the hydrogen peroxide was also used to run the gas turbine for the turbopumps in the primary propulsion system, the burn time of the landing rockets was a function of the burn time of the main engine. The maximum landing rocket burn time was 27 seconds as confirmed by flight test data. The burn time available after a complete burn of the main rocket was approximately 10 seconds.

RADAR ALTIMETER

The radar altimeter was a Honeywell YG9000D1 electronic altimeter set which operated on the Doppler shift principle. The unit contained outputs for altitude rate ($\pm$300 and $\pm$60 feet per second) in addition to two altitude ranges (0 to 1,000 feet and 0 to 5,000 feet). The manufacturer's stated altitude accuracy was $\pm$5 feet plus 3 percent of actual altitude. The altitude accuracy was checked against a ground-based beacon tracking radar and was found to be within the manufacturer's specifications.

No accuracy was given for the altitude rate data; however, a comparison between ground-based radar and the Honeywell unit revealed that the radar altimeter had good accuracy at altitude. No comparison could be made near runway level because of ground reflection problems with ground-based radar. The unit read zero on the ground unless there happened to be a zero shift in telemetry data. The accuracy was a function of the type of terrain over which the vehicle flew. The data over the hard, flat lakebed runway looked good. The ±60 foot per second output was not available until flight 15.

A problem with this particular unit was reliability. The unit had a 2.5 second per cycle search mode and should have acquired a trackable signal within one cycle. However, this unit often took several cycles to acquire a signal. This appeared to be a malfunction in this particular unit and should not have affected its accuracy. The output was not presented to the pilot and was used only for data purposes.

DATA ACQUISITION SYSTEM

Table I presents a summary of the parameters used in this study including their range, sampling rate, and estimated accuracy. The accuracy values given in table I included the processing, sensor, onboard pulse code modulation (PCM), power supply and the calibration accuracies.

A standard NASA noseboom was used to measure the total and static pressure and the angle of attack. The bank angle and pitch angle were obtained from attitude gyros. The flap, rudder, stick, and landing gear strut positions came from several control position transducers. The normal and longitudinal accelerations were measured by sensitive accelerometers mounted close to the vehicle's center of gravity. The landing rocket chamber pressure was measured by a pressure transducer. All of the data were telemetered to the ground station through a PCM data acquisition system. The raw data were recorded on a magnetic tape at their respective sampling rates of 200 or 50 samples per seconds (SPS). Calibrations and corrections were applied to the raw data and the results were listed in engineering units at 10 SPS.

A surveyor's wheel was used to measure the longitudinal distance from the intended to the actual touchdown point and the rollout distance.

Ground-based beacon tracking radars were used for space positioning data. A MPS-19 long-range radar was used to provide real time space position data in the control room which were used among other things to guide the pilot to the low key point. Data from an FPS-16 long-range radar were recorded on magnetic tape for later examination and were used for the plots of altitude, ground track, and glideslope in this report.

Table I

PARAMETERS USED DURING THE POSTFLIGHT ANALYSIS
OF THE X-24A APPROACH AND LANDING

Parameter	Range	Sampling Rate (SPS)	Accuracy (RMS pct)
Angle of attack	-13 to 20 deg	200	1.28
Airspeed pressure sensor (fine scale)	72 psf/turn, (10 turns)	50	1.62
Altitude pressure sensor (fine scale)	210 psf/turn, (10 turns)	50	1.62
Radar altitude	0 to 5,000 ft 0 to 1,000 ft	200 50	±5 ft +3%
Radar altitude rate	±60 ft/sec	50	none given
Bank angle	±90 deg	50	1.17
Pitch angle	±90 deg	50	1.17
Upper flap	4 to 57 deg	200	1.08
Lower flap	0 to 42 deg	200	1.08
Rudder bias	±10 deg	200	1.08
Normal acceleration	-1 to 3 g's	200	0.38
Longitudinal acceleration	±0.5 g's	200	0.41
Gear strut position	1 to 12 in.	50	1.07
Longitudinal stick position	-4.75 to 6.75 in.	50	1.07
Lateral stick position	±6.25 in.	50	1.07
Landing rocket chamber pressure	0 to 500 psi	200	1.62

APPENDIX II
DATA REDUCTION EQUATIONS

FLIGHT DATA EQUATIONS

The final approach L/D and flightpath angle (γ) were calculated using equations derived in reference 16.

$$L/D = \frac{n_{z_b} \cos \alpha + n_{x_b} \sin \alpha}{n_{z_b} \sin \alpha - n_{x_b} \cos \alpha} \tag{1}$$

$$C_L \, S/W = \frac{295 \, n_{z_s}}{V_e^{\,2}} \tag{2}$$

where V_e is in knots

$$n_{z_s} = n_{z_b} \cos \alpha + n_{z_b} \sin \alpha$$

$$\cot \gamma = A_f \, L/D \tag{3}$$

Almost all of the parameters for these equations came from the X-24A data system as outlined in appendix I. The weight (W) came from reference 7 and the acceleration factor (A_f) was from reference 17.

THEORETICAL EQUATIONS - TURN PERFORMANCE

To more easily compare the flight values of turn rates which were a function of altitude, airspeed, L/D, and bank angle, a theoretical equation was calculated for use in appendix III. This equation came from reference 16. It was derived by summing the forces along all three axes of a vehicle in banked descending flight and using the glide flight energy dissipation equation where the rate of change of total energy was equal to the drag times the airspeed. The final equation was

$$\text{Turn rate (heading change per altitude)} = \frac{\sqrt{1 - \zeta^2}}{R \, \zeta} \tag{4}$$

where

$$R = \text{turn radius} = - \frac{V_t^{\,2}}{g \, (A_f) \, (L/D) \sin \phi \, \zeta}$$

and

$$\zeta = \frac{L/D \cos \phi}{2} - \sqrt{\left(\frac{L/D \cos \phi}{2}\right)^2 + \frac{1}{A_f}}$$

It was important to realize that the L/D in turning flight was not the same as the L/D used in level flight. The L/D for turning flight was obtained from a C_L based on the following lift force which was found by summing the forces along the vertical axis and assuming that the vertical acceleration was zero.

$$L = \frac{W}{\cos \phi \cos \gamma + \frac{\sin \gamma}{(L/D)}} \qquad (5)$$

The flightpath angle (γ) came from equation (3) modified for turning flight.

$$\cot \gamma = A_f \, L/D \cos \phi \qquad (6)$$

It was apparent that the lift force was dependent upon L/D which in turn was a function of C_L. To determine the lift and, consequently the lift coefficient, required an iterative process. An L/D was assumed and used to determine γ from equation (6). With γ and L/D, the lift force was computed from equation (5). With C_L, a new L/D was obtained from the vehicle's L/D versus C_L curve. The next computation of lift and C_L was carried out. With any reasonable selection of the initial value of L/D only one iteration would have been required.

APPENDIX III
ENERGY MANAGEMENT DURING THE APPROACH

There were three methods available to the pilots for energy management during the approach:

1. Airspeed modulation
2. Bank angle modulation
3. Flap bias as a speed brake

All of the approaches were made on the high-speed "front side" of the L/D curve. It was instinctive for the pilot to fly on the front side of the L/D curve, because when he pushed over, the airspeed increased, the L/D decreased, the flightpath angle became steeper, and the range decreased. If he pulled up, the airspeed decreased, the L/D increased, the flightpath angle became shallower, and the range increased. However, if the pilot were to fly on the low-speed "back side" of the L/D curve, any energy management would have been contrary to pilot instinct because (unlike the front side) an increase in airspeed would have increased the L/D and thus, the range.

The variation in L/D and flightpath angle due to airspeed is summarized in figure 1 which was based on flight data reduced to flightpath angle by means of equation (3) in appendix II. The interesting characteristic of these curves was that as the L/D versus C_L slope decreased (refer to figure 10 of the body of this report), a small change in lift-drag ratio ($\Delta L/D$) produced a larger change in flightpath angle ($\Delta\gamma$). For example, a $\Delta L/D$ of -0.5 represented a $\Delta\gamma$ of -3.3 degrees for configuration mode 1 and the same $\Delta L/D$ represented a $\Delta\gamma$ of only -1.5 degrees for configuration mode 3. This factor was of no major consequence to the X-24A, and the pilots did not comment on it.

By increasing or decreasing the bank angle, the turn rate will increase or decrease, and the turn radius will consequently decrease or increase. The turn rate at an altitude of 15,000 feet is shown in table II in the main body of this report. This data came from ground-based radar tracking. By examining this data it was not readily apparent that any correlation existed between turn rate, bank angle and L/D. In an effort to show this correlation, the turn rate was calculated based on theoretical equations as presented in appendix II. These equations used L/D data based on flight data. Figures 2 and 3 show the theoretical turn rate as well as the actual values for configuration modes 1 and 2.

On the X-24A there were no speed brakes per se; however, by biasing the upper and lower flaps a very effective speed brake was realized. Speed brake (δSB) was expressed in terms of the upper flap bias position (δU_B). The zero speed brake position was considered to be the point at which δU_B = -13 degrees. Note that the lower flap position was dictated by the trim requirements for a particular angle of attack; therefore, drag effects must also be compared at the same angle of attack.

The rudder bias position, which was a function of upper flap bias position, figure 4, also contributed to the speed brake effectiveness. Figure 5 shows the drag increment due to speed brakes. Figure 6 shows the flightpath angle and range loss as a function of speed brake position. These figures concurred with the pilot comments that the use of the flap bias feature as a speed brake was very effective. The trim change associated with the use of speed brakes was easily compensated for by the pilots (figure 7).

As a result of the unknowns involved when flying at several upper flap positions, it was decided that no speed brakes would be used during the first several X-24A flights. Starting with configuration mode 2, the speed brakes were used. No speed brakes were available when flying with the upper flaps (configuration mode 3) because any attempt to bias the upper flaps would result in a crossover to the lower flaps for control; this would result in loss of the flight objective to use the upper flaps for control.

Altitude = 13,000 Ft msl
W = 6360 lbs
cg = 62 % MAC

Configuration Mode	$V_{C_{max}}$	V_C @ L/D_{max}
1	300 kts	164 kts
2	300	186
3	300	200

The nominal airspeed for each configuration was 250 kts

$\Delta L/D = L/D - L/D_{@\ V_C = 250\ kts}$

$\Delta \gamma = \gamma - \gamma_{@\ V_C = 250\ kts}$

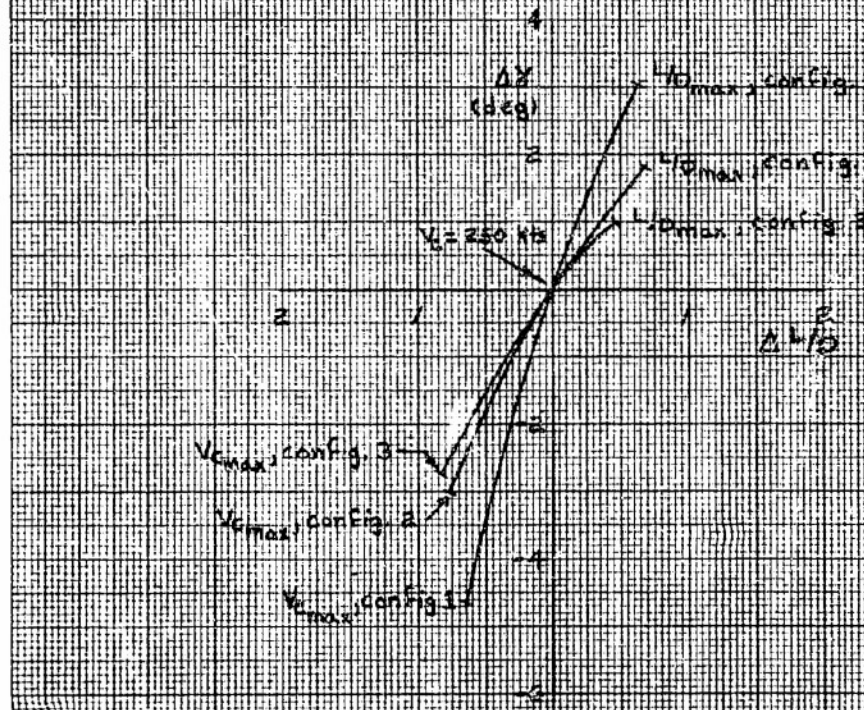

Figure 1 Airspeed as an Energy Management Device

Theoretical Data H = 15,000 ft

SYM	δ_{L_B}	δ_{R_B}	W	CG
———	-21°	-10°	6360 lb	58.9%c

Flight Data H = 15,000 ft

SYM	ϕ (deg)	δ_{L_B} (deg)	δ_{R_B} (deg)	W (lbs)	CG (%c)
△	50	-21.0	-10.0	6362	58.8
○	43	-20.9	-9.5	6353	58.8
◇	42	-20.6	-9.8	6353	58.7
▽	40	-20.0	-7.9	6394	57.0
□	37	-20.4	-9.8	6435	58.5

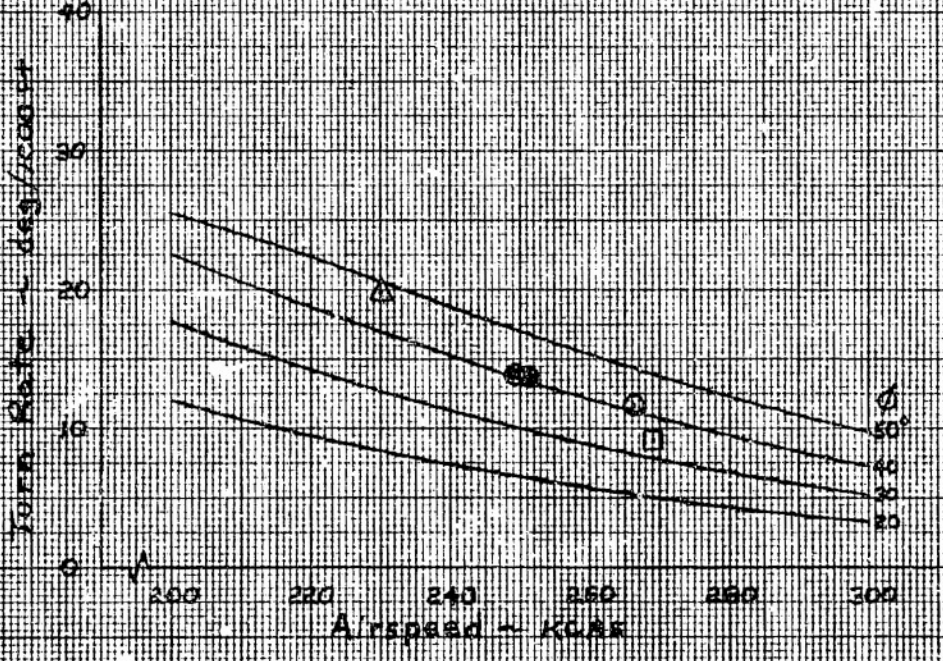

Figure 2 Turn Rate — Configuration Mode One

Theoretical Data H = 15,000 Ft

SYM	δu_B	δa_B	W	CG
	-13°	-10°	6360 lb	57.7%

Flight Data H = 15,000 Ft

SYM	ϕ (deg)	δu_B (deg)	δR_B (deg)	W (lbs)	CG (%c)
○	43	-11.8	-9.8	6249	57.6
◇	34	-13.2	-9.1	6690	56.2
□	30	-13.5	-9.2	6666	56.4
■	28	-12.2	-9.8	6596	56.7
⊡	30	-12.3	-10.0	6417	56.7
◧	31	-13.3	-9.6	6324	57.3
△	24	-12.7	-9.8	6393	56.7
▲	23	-13.7	-10.0	7024	56.1
▽	20	-13.2	-9.4	6336	57.7

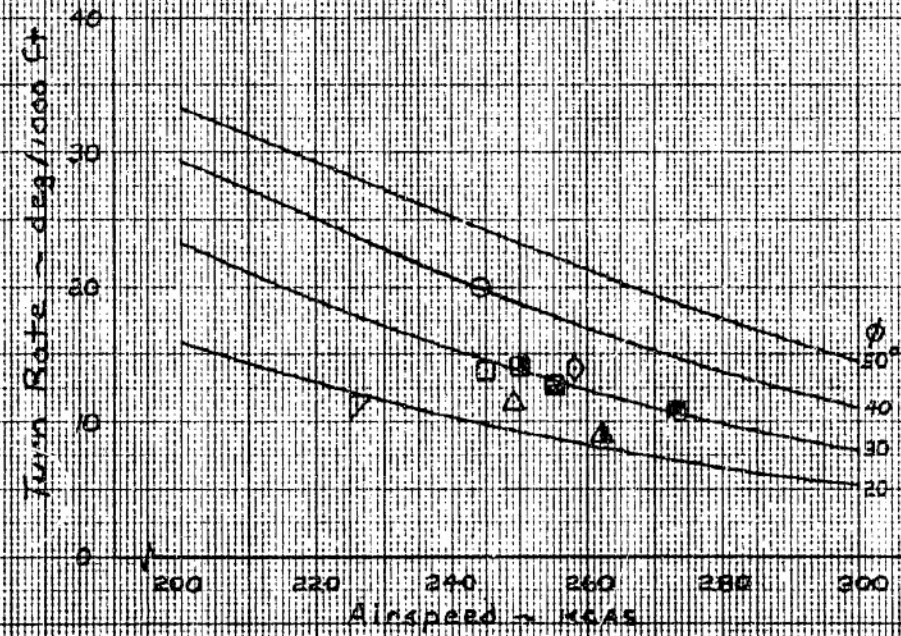

Figure 3 Turn Rate ——Configuration Mode Two

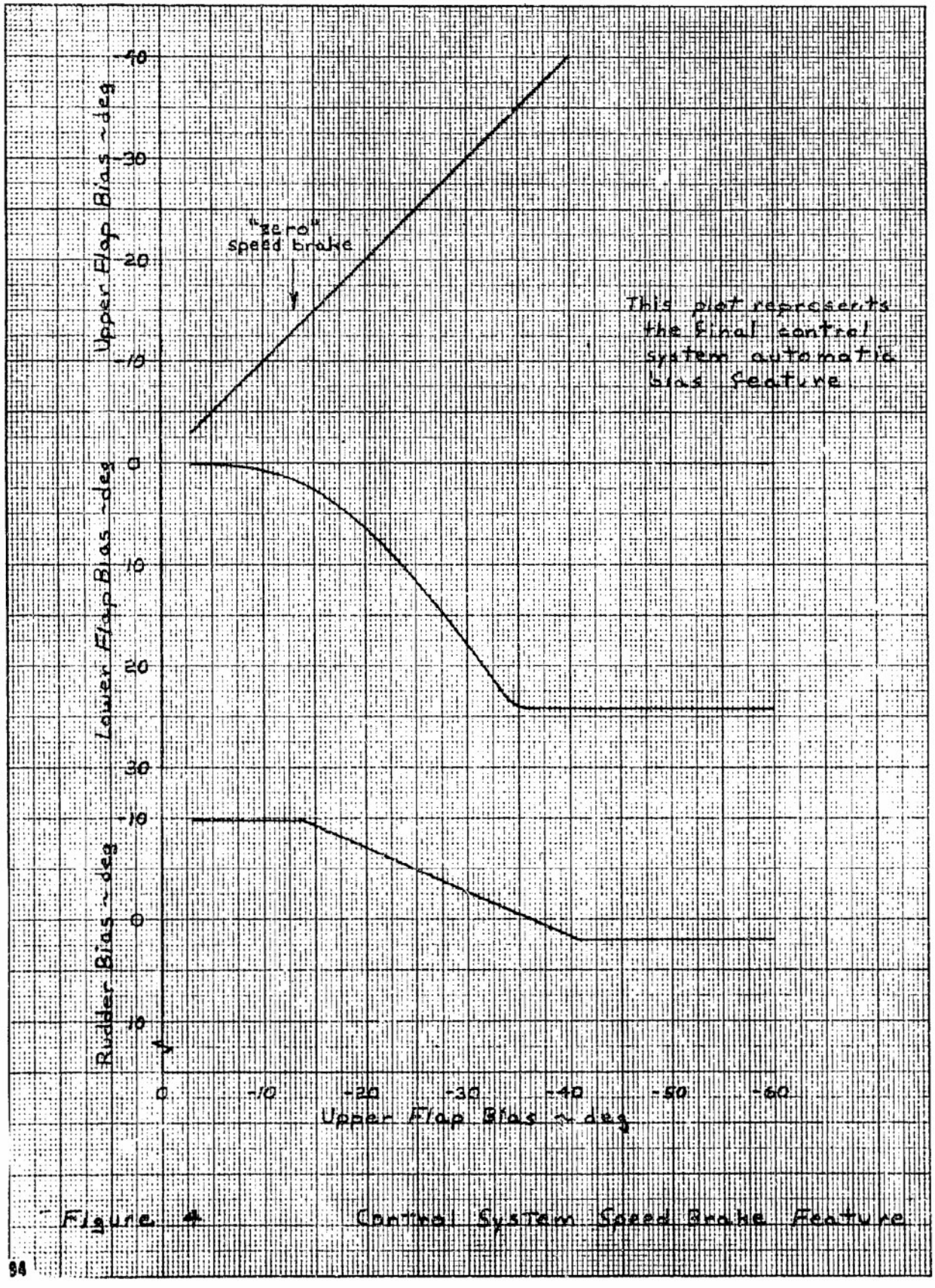

Figure 4. Control System Speed Brake Feature

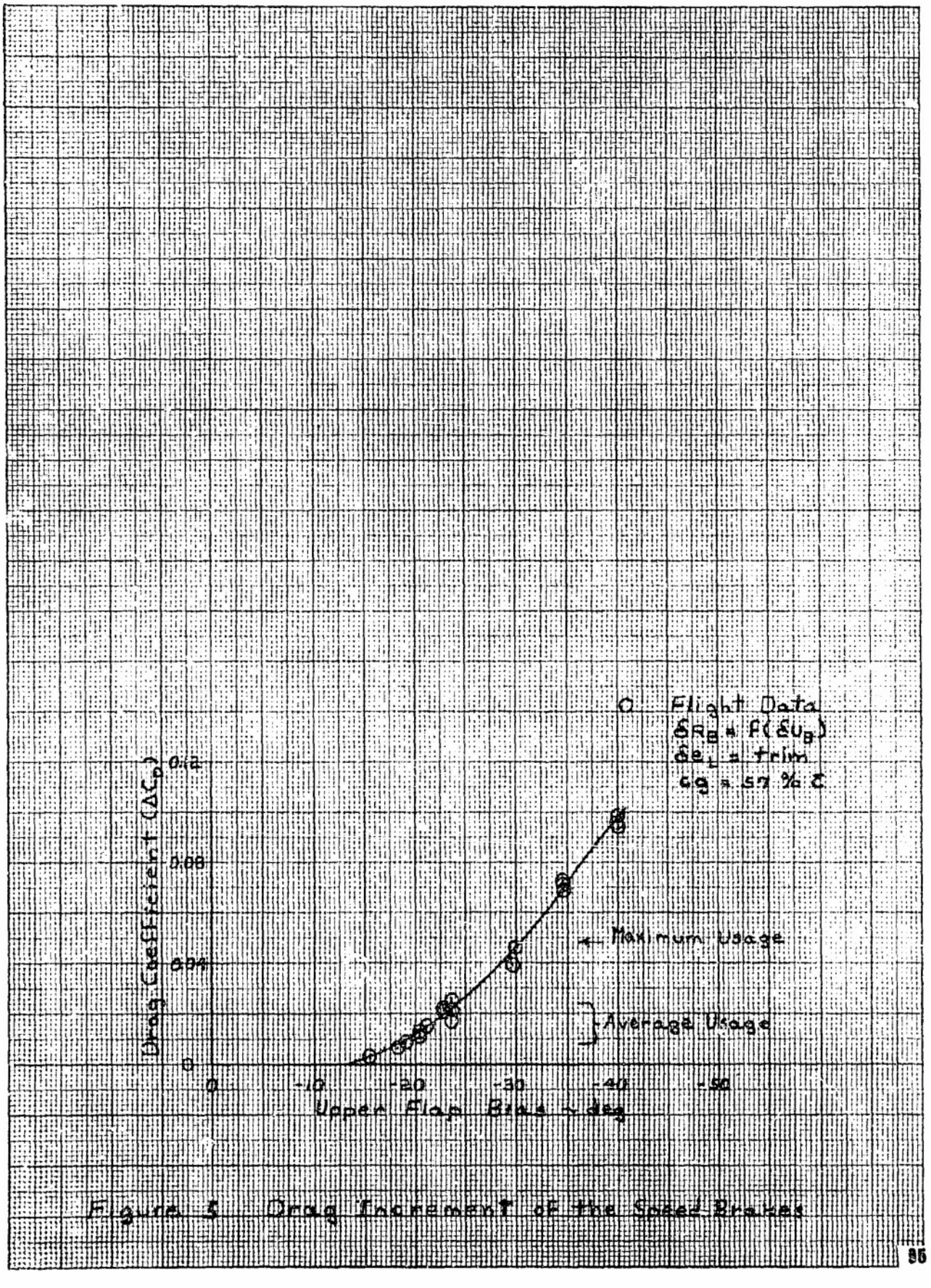

Figure 5 Drag Increment of the Speed Brakes

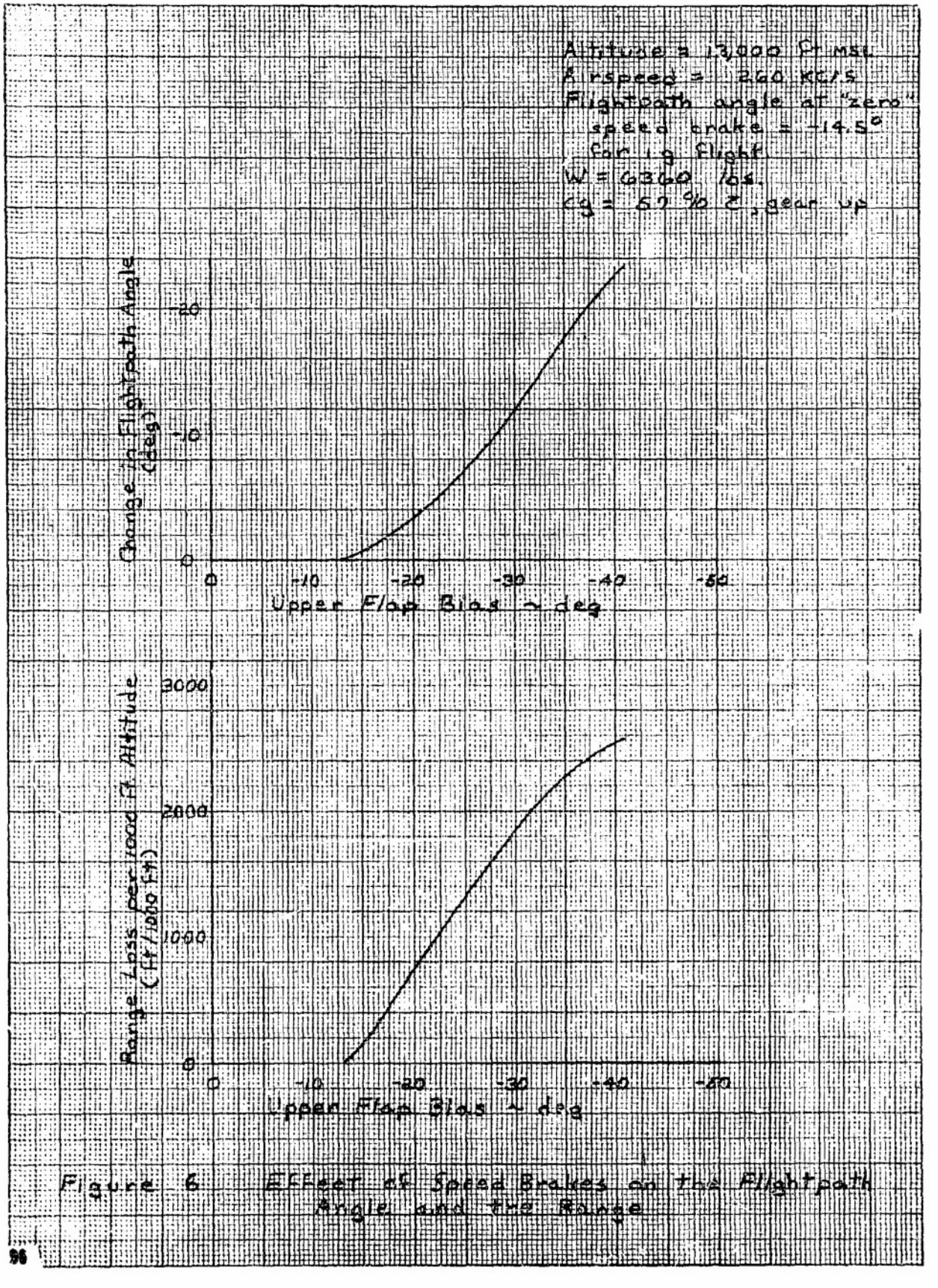

Figure 6 Effect of Speed Brakes on the Flightpath Angle and the Range

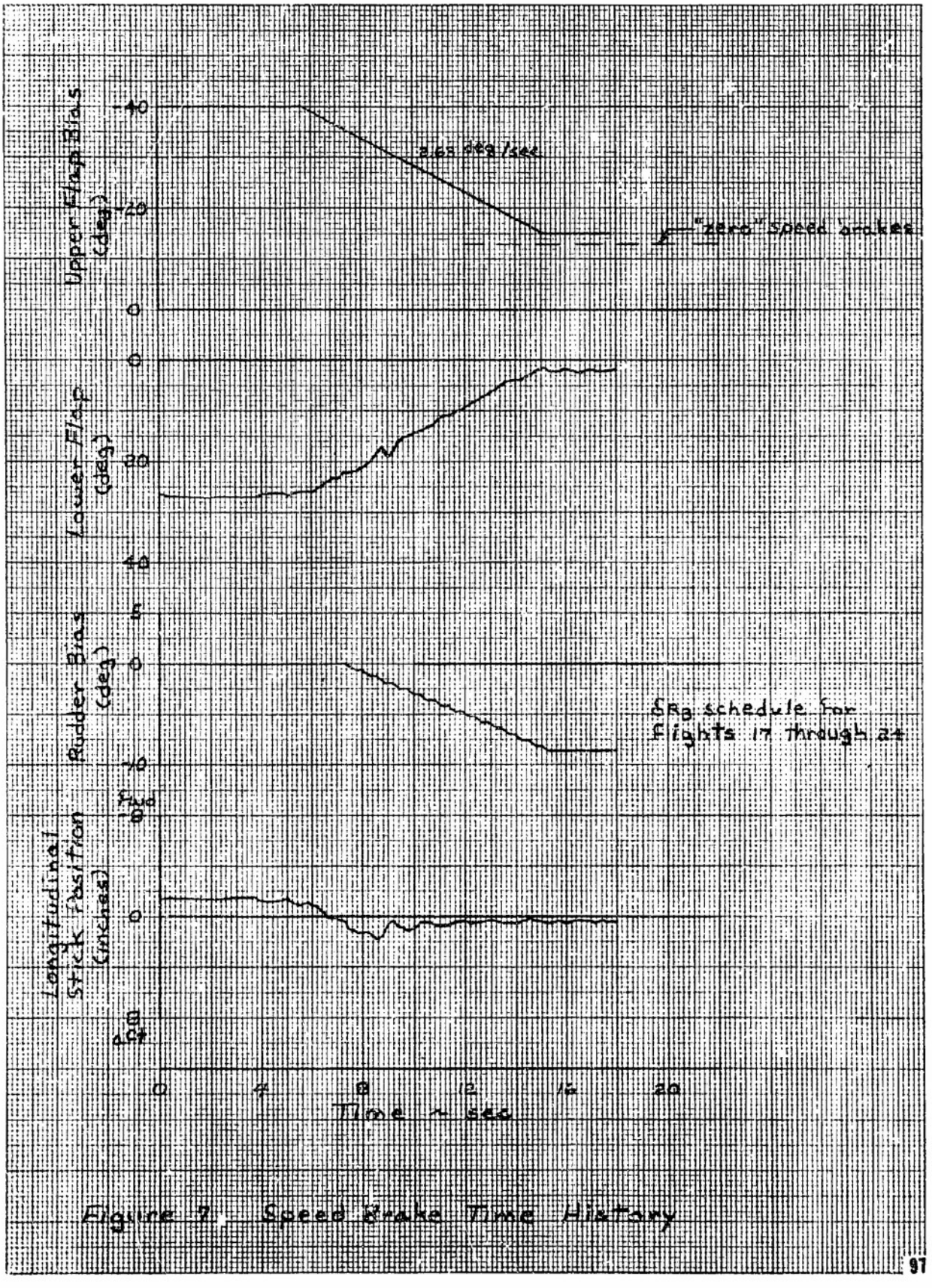

Figure 7. Speed Brake Time History

Figure 7 Speed Brake Time History (concluded)

APPENDIX IV
F-104A LOW L/D DATA

Early in the X-15 program a brief flight test program was initiated to evaluate the capability of the F-104A to simulate low/medium L/D landing patterns. Flight test information was obtained at idle power with various combinations of speed brake, landing gear and flap. Several configurations were flown using power settings above idle.

The effective lift-to-drag ratio[5] was obtained by establishing the airplane in a constant-indicated-airspeed descent in the desired configuration. The descent from 17,000 to 13,000 feet indicated altitude was manually timed and the resulting rate of descent was corrected for the change in true airspeed by the equation

$$\text{corrected rate of descent, } R/D_c = R/D \left(1 + \frac{V_{t_{avg}}}{g} \frac{\Delta V_t}{\Delta h}\right)$$

where $\Delta h = 4{,}000$ ft

and $\Delta V_t = V_{t_{17,000}} - V_{t_{13,000}}$

The true airspeed was calculated from the airspeed, altitude, and atmospheric temperature.

The effective lift-to-drag ratio was determined as follows:

$$L/D_{eff} = \cot \gamma_c$$

where γ_c was the corrected flightpath angle,

$$\sin \gamma_c = \frac{R/D_c}{V_{t_{avg}}}$$

The fuel remaining was recorded during each run for weight determination. The lift coefficient was calculated from

$$C_L = \frac{\cos \gamma_c}{q} \frac{W}{S}$$

where the dynamic pressure (q) was calculated from

$$q = 1/2 \, \rho_{SL} \, V_e^2$$

and S = 196 square feet and the empty weight = 13,850 pounds.

---

[5] The effective lift-to-drag ratio included the effect of engine thrust, $L/D_{eff} = \frac{L}{D-T}$

Figure 1 presents a summary of the L/D_{eff} data obtained for the F-104A.

In addition to the F-104A, the F-104B, C, and D models were available for use as inflight performance simulators and chase aircraft. There were no appreciable differences between these models that would affect the basic unpowered L/D other than the idle thrust engine differences.

The T-38 aircraft had high drag characteristics which made it suitable for use as a chase airplane, but not as an inflight performance simulator. During the flare, the T-38 had too great an L/D to accurately simulate that portion of the flight.

The F-5D aircraft was used both as an inflight performance simulator and a chase airplane, but there was only one available and it was phased out early in the X-24A program.

Note: 1. L/D values obtained during constant IAS descents and corrected for changing true speed
2. All points are at idle power unless noted otherwise.

SYMBOL	CONFIGURATION	SYMBOL	CONFIGURATION
■ PWR	Land Flap, Speed Brakes, Gear & Power	□	T/O Flap
⊠	T/O Flap, Speed Brakes & 80% RPM	●	Land Flap & Gear
⊗	T/O Flap & Speed Brakes	⊙	Speed Brakes
◑	T/O Flap, Speed Brakes & Gear		
+	Simulated Flame-Out		
◨	T/O Flap, Speed Brakes, Gear & 80% RPM		

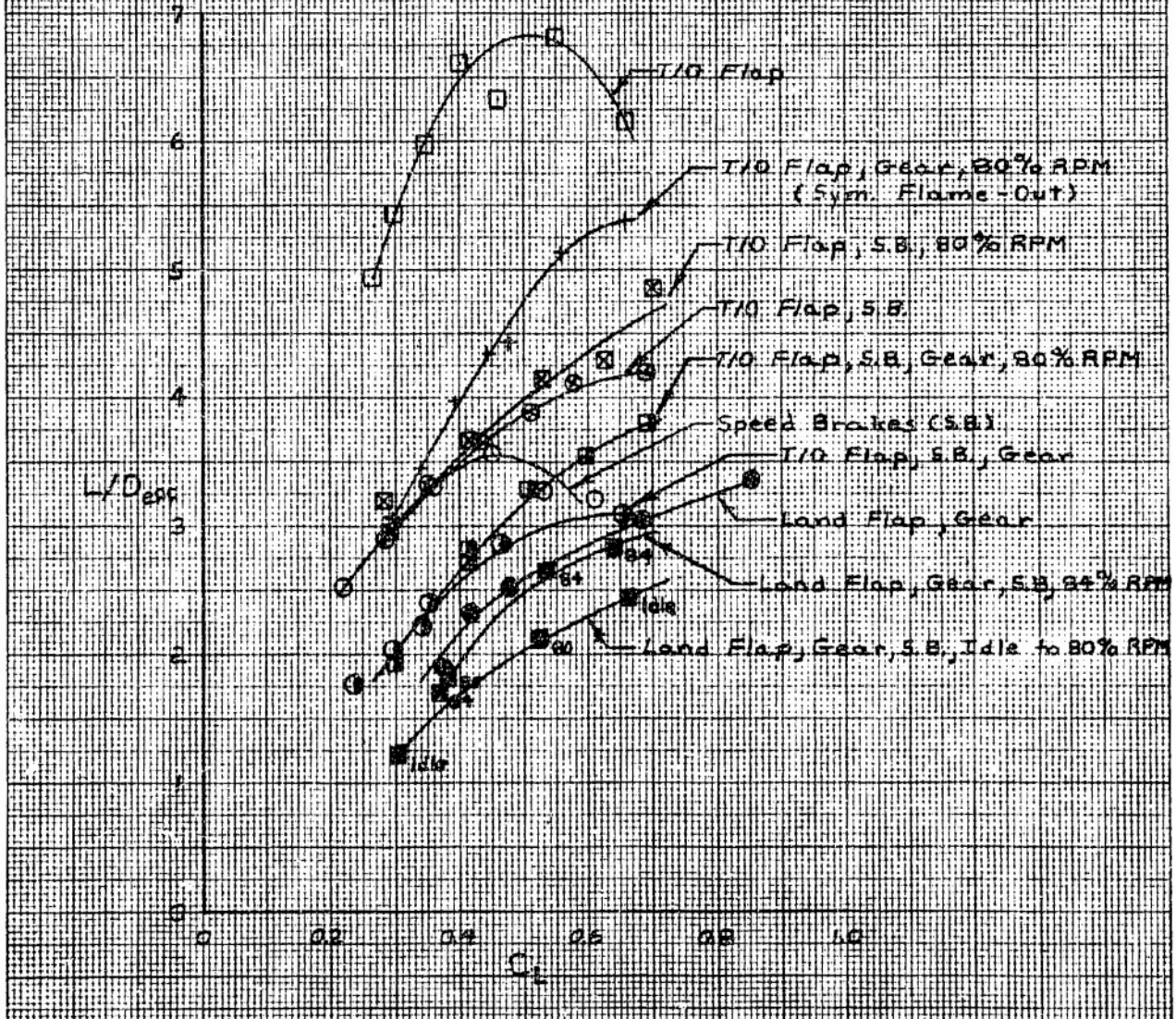

Figure 1 Lift-Drag Ratios of the F-101A

APPENDIX V
SIMULATION TEST RESULTS

FLIGHT SIMULATED LANDING PATTERNS

The value of inflight performance simulation of the unpowered landing patterns of low to medium L/D research vehicles was established prior to the first X-15 flight. This philosophy has continued throughout the lifting body program. Before the first X-24A flight, extensive inflight simulation of the predicted X-24A landing pattern was performed using an F-104. The F-104 configuration which best matched the L/D values of the X-24A during approach and landing was takeoff flaps, speed brakes and landing gear extended. Thrust modulation was used to vary the effective L/D and to adjust for the reduction in wing loading as fuel was burned (figure 1).

Baseline data for several F-104 configurations are included in appendix IV. Figure 2 is a comparison between an X-24A pattern and several F-104 simulations of that pattern.

Each pilot made 50 to 60 low L/D landings in the F-104 during the two-week period prior to each X-24A flight including at least five landings the morning of the actual X-24A flight. This allowed him to practice normal and alternate approaches to the primary and alternate runways. The use of such inflight performance simulation practice permitted a high level of pilot proficiency to be maintained even though actual lifting body flights were short and relatively infrequent. It also allowed efficient utilization of the available data gathering time on any one X-24A flight since the pilot was not overly preoccupied with the landing task.

FIXED BASE SIMULATION OF THE FLARE AND DECELERATION

Since before the first X-24A flight there has existed a six-degree-of-freedom, fixed base, hybrid simulator at AFFTC. Prior to the first flight and throughout the flight test program, the pilots used this simulator to predict (among other things) the X-24A flare characteristics, primarily the flare initiation altitude. With this information on hand, they used the inflight performance simulator (F-104 in high drag configuration) to simulate the complete X-24A landing pattern, including the flare.

After determining the flare techniques being used by the pilots, a simulator study was made using these flare techniques to observe how well the fixed base simulator matched the actual X-24A flare characteristics. Configuration modes 1 and 2 were used for this study. The flare technique used with configuration mode 1 was a constant 1.3 g rotation to a sink rate of 20 feet per second (see the section title Flare Technique). For configuration mode 2, the flare technique was to pull to an initial normal acceleration of 1.5 g's and then hold the angle of attack constant until reaching a sink rate of 20 feet per second. The gear extension and touchdown airspeeds used in the simulator study are in table I. The simulator flares with configuration mode 1 were done with and without the use of landing rockets.

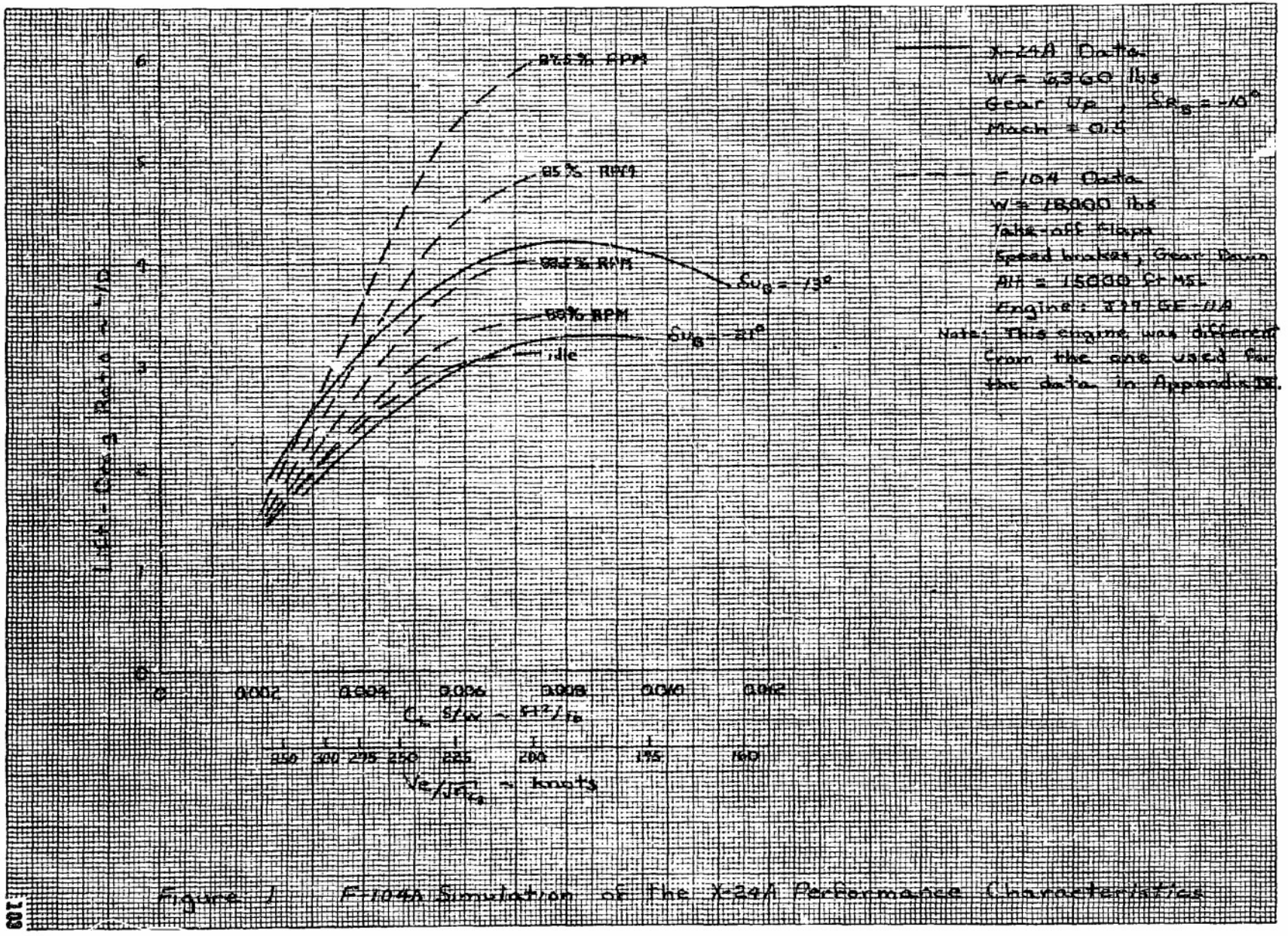

Figure 1 F-104B Simulation of the X-24A Performance Characteristics

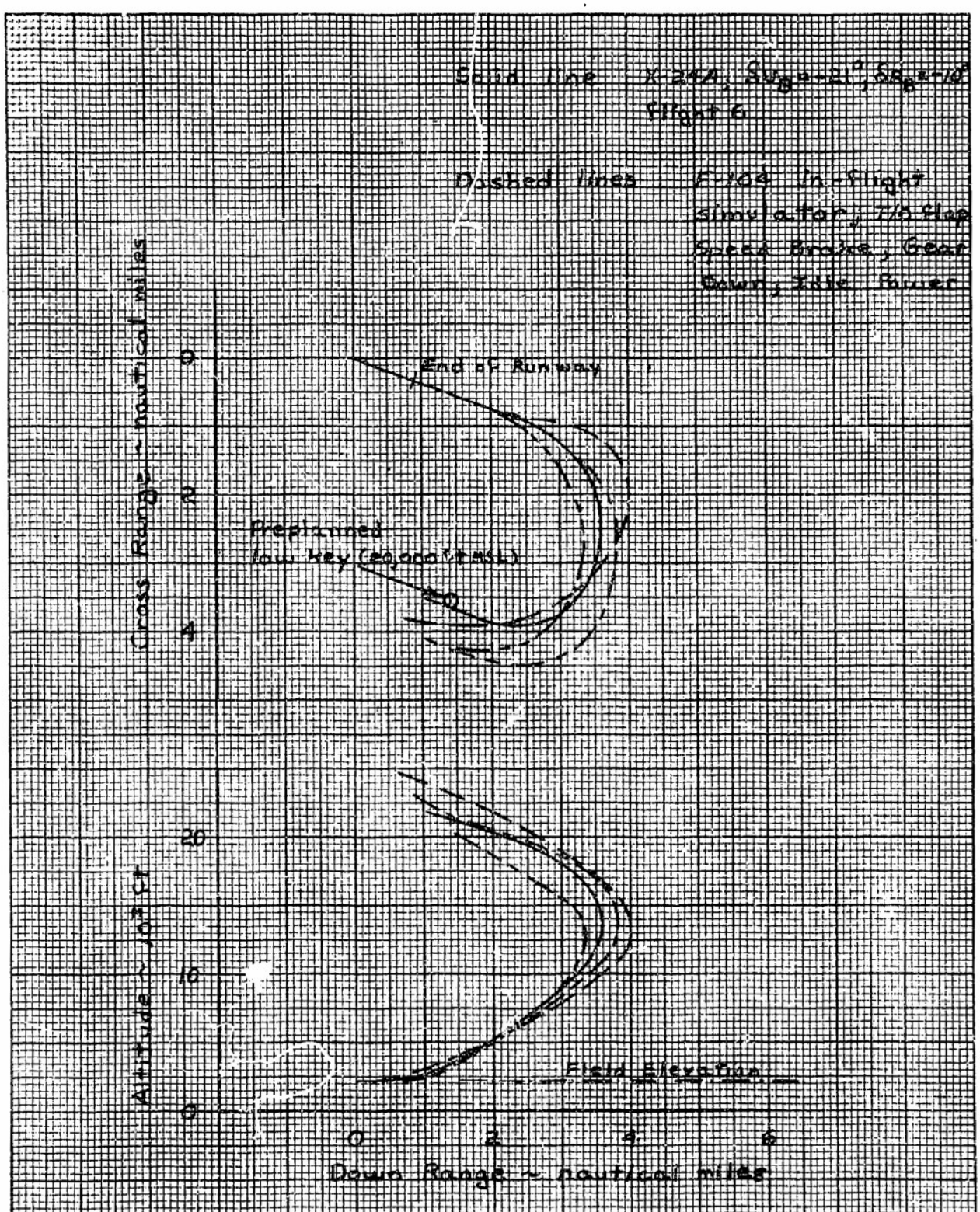

Figure 3 Comparison of an X-24A Landing Pattern With Patterns Simulated Using an F-104

Table I

AIRSPEEDS USED DURING THE FIXED-BASE SIMULATION
OF THE X-24A FLARE CHARACTERISTICS

Configuration Mode	Flare Initiation Airspeed (KCAS)	Rockets "ON" Airspeed (KCAS)	Gear Extension Airspeed (KCAS)	Touchdown Airspeed (KCAS)
	270	none used	230	170
	270	269	228	170
1	280	none used	229	175
	280	278	228	175
	290	none used	229	180
	290	281	230	180
2	280	none used	240	175
	290	none used	250	180
	300	none used	258	190
	310	none used	260	195

REFERENCES

1. Flight Planning and Conduct of the X-24A Lifting Body Flight Test Program, FTC-TD-71-10, Air Force Flight Test Center, Edwards AFB, California, to be published.

2. X-24A Lifting Body Systems Operation and Performance, FTC-TD-71-13, Air Force Flight Test Center, Edwards AFB, California, to be published.

3. Flight Measured X-24A Lifting Body Control Surface Hinge Moments and Correlation with Wind Tunnel Results, NASA TN , to be published.

4. Ash, Larry G., Captain USAF, Flight Test and Wind Tunnel Performance Characteristics of the X-24A Lifting Body, FTC-TD-71-8, Air Force Flight Test Center, Edwards AFB, California, June 1972.

5. Handling Qualities of the X-24A Lifting Body, FTC-TD-71-11, Air Force Flight Test Center, Edwards AFB, California, to be published.

6. Kirsten, Paul W., Wind Tunnel and Flight Test Stability and Control Derivatives for the X-24A Lifting Body, FTC-TD-71-7, Air Force Flight Test Center, Edwards AFB, California, April 1972.

7. Retelle, John P., Jr., Captain USAF, Measured Weight, Balance, and Moments of Inertia of the X-24A Lifting Body, FTC-TD-71-6, Air Force Flight Test Center, Edwards AFB, California, November 1971.

8. Measured Characteristics of the X-24A Lifting Body Flight Control System, FTC-TD-71-12, Air Force Flight Test Center, Edwards AFB, California, to be published.

9. Matranga, Gene J., and Armstrong, Neil A., Approach and Landing Investigation at Lift-Drag Ratios of 2 to 4 Utilizing a Straight-Wing Fighter Airplane, NASA TM X-31, August 1959.

10. DiFranco, Dante A., and Mitchell, John F., Preliminary Handling Qualities Requirements for Lifting Re-Entry Vehicles During Terminal Flight, AFFDL-TR-71-64, Air Force Flight Dynamics Laboratory, Wright-Patterson AFB, Ohio, August 1971.

11. Pyle, Jon S., and Swanson, Robert H., Lift and Drag Characteristics of the M2-F2 Lifting Body During Subsonic Gliding Flight, NASA TM-X-1431, August 1967.

12. Pyle, Jon S., Lift and Drag Characteristics of the HL-10 Lifting Body During Subsonic Gliding Flight, NASA TN D-6263, March 1971.

13. Wind Tunnel Test of a 20% Scale Model of the Martin SV-5 Configuration Ninth Series, University of Maryland Wind Tunnel Report No. 424, College Park, Maryland, February 1965.

14. Wilson, Ronald J., Statistical Analysis of Landing Contact Conditions of the X-15 Airplane, NASA TN D-3801, January 1967.

15. Larson, Richard R., Statistical Analysis of Landing Contact Conditions for Three Lifting Body Research Vehicles, NASA TN D-6708, March 1972.

16. Schofield, B. Lyle, Richardson, David F.; and Hoag, Peter C., Major USAF, Terminal Area Energy Management, Approach and Landing Investigation for Maneuvering Reentry Vehicles Using F-111A and NB-52B Aircraft, FTC-TD-70-2, Air Force Flight Test Center, Edwards AFB, California, June 1970.

17. Herrington, Russell M., Major USAF, et al., Flight Test Engineering Handbook, AF-TR-6273, Air Force Flight Test Center, Edwards AFB, California, January 1966.

UNCLASSIFIED

Security Classification

DOCUMENT CONTROL DATA - R & D

(Security classification of title, body of abstract and indexing annotation must be entered when the overall report is classified)

1. ORIGINATING ACTIVITY *(Corporate author)* Air Force Flight Test Center Edwards AFB, California	2a. REPORT SECURITY CLASSIFICATION UNCLASSIFIED 2b. GROUP N/A

3. REPORT TITLE

Analysis of the Approach, Flare and Landing Characteristics of the X-24A Lifting Body

4. DESCRIPTIVE NOTES *(Type of report and inclusive dates)*

Final

5. AUTHOR(S) *(First name, middle initial, last name)*

David F. Richardson

6. REPORT DATE	7a. TOTAL NO. OF PAGES	7b. NO. OF REFS
July 1972	106	17

8a. CONTRACT OR GRANT NO. b. PROJECT NO. c. Project Directive 69-38 d.	9a. ORIGINATOR'S REPORT NUMBER(S) FTC-TD-71-9 9b. OTHER REPORT NO(S) *(Any other numbers that may be assigned this report)* N/A

10. DISTRIBUTION STATEMENT Distribution limited to U.S. Government agencies only (Test and Evaluation), April 1972. Other requests for this document must be referred to ASD (SDQR), Wright-Patterson AFB, Ohio.

11. SUPPLEMENTARY NOTES	12. SPONSORING MILITARY ACTIVITY
N/A	6510th Test Wing Edwards AFB, California

13. ABSTRACT The approach and flare were flown with clean configurations (landing gear up), having maximum lift-to-drag ratios (L/D)'s between 2.95 and 4.30. The landing configuration (gear down) had a maximum L/D of 2.65. The landing approach pattern was a 180-degree, unpowered, left-hand, circling approach followed by a short wings-level, high energy final approach at airspeeds ranging from 267 to 318 KCAS, terminating with a flare to near level flight near the ground, and a deceleration to landing. The landing gear was extended near completion of flare in close proximity to the ground. The landings were at airspeeds between 168 and 205 KCAS at sink rates of less than 5 feet per second and within 2,000 feet of the intended landing point. An effective speed brake function was generated on the X-24A by using the flap bias feature. This was essential to the accomplishment of accurate landings. Visibility and handling qualities of the X-24A in the final approach and landing configuration were excellent; however, lateral upsets in turbulence were disconcerting, especially near the ground. The trim change due to landing gear deployment was also somewhat objectionable. Differential braking and rudder/aileron deflection were sufficient for ground steering after touchdown for conditions of zero crosswind, but were inadequate for light to moderate crosswinds. Unpowered visual approach and landing were relatively easy for the pilots after extensive F-104A low L/D practice prior to the X-24A flights.

DD FORM 1 NOV 65 1473

UNCLASSIFIED

Security Classification

14 KEY WORDS	LINK A		LINK B		LINK C	
	ROLE	WT	ROLE	WT	ROLE	WT
X-24A lifting body approach flare landing final approach sink rate speed brake visibility handling qualities braking						